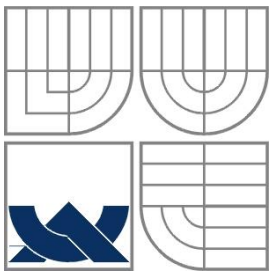

BRNO UNIVERSITY OF TECHNOLOGY
VYSOKÉ UČENÍ TECHNICKÉ V BRNĚ

FACULTY OF CIVIL ENGINEERING
DEPARTMENT OF BUILDING STRUCTURES

FAKULTA STAVEBNÍ
ÚSTAV POZEMNÍHO STAVITELSTVÍ

OPTIMIZING THE DESIGN OF MODERN LOW-ENERGY WOODEN HOUSES

OPTIMLAIZACE NÁVRHU MODERNICH NÍZKOENERGETICKÝCH DŘEVOSTAVEB

DOCTORAL THESIS
DISERTAČNÍ PRÁCE

AUTHOR
AUTOR PRÁCE
ING. EVA VAHALOVÁ

SUPERVISOR
VEDOUCÍ PRÁCE
ING. KAREL ŠUHAJDA, Ph.D.

BRNO 2016

Bibliography

VAHALOVÁ, Eva. *Optimizing the design of modern low-energy wooden houses*. Brno, 2016. 151 s., 0 s. app. Doctoral thesis. Brno University of Technology, Faculty of Civil Engineering, Department of Building Structures. Supervisor Ing. Karel Šuhajda, Ph.D.

Bibliografická citace VŠKP

Ing. Eva Vahalová *Optimalizace návrhu moderních nízkoenergetických dřevostaveb*. Brno, 2016. 151 s., 0 s. příl. Disertační práce. Vysoké učení technické v Brně, Fakulta stavební, Ústav pozemního stavitelství. Vedoucí práce Ing. Karel Šuhajda, Ph.D.

Declaration

I herewith declare that I have written the enclosed Doctoral Thesis "*Optimizing the design of modern low-energy houses*" by myself, and have referenced all sources used which led to the creation of this Doctoral Thesis.

Brno, 31st March 2016

…….

Ing. Eva Vahalová

Acknowledgements

First of all I would like to greatly acknowledge Brno University of Technology, Faculty of Civil Engineering, Department of Building Structures for the possibility to let me study my Ph.D. course and also allow me to use the ERASMUS programme to gain professional knowledge and technical experiences abroad. This would all not be possible without the support and human approach of my supervisor Ing. Karel Šuhajda, Ph.D.

Technical University of Denmark in Lyngby is greatly acknowledged for their materials, measuring equipment, laboratories and software, especially Ruut Hannele Peuhkuri who is greatly acknowledged for her supervising and technical contribution to this thesis. I would further like to acknowledge my colleagues and friends from the Passive House Institute in Darmstadt, Germany.

Last but not least, I would like to thank to husband Jan for taking care of our children during my work on this thesis.

Brno, 31st March 2016

…….

Ing. Eva Vahalová

Abstract in English

The design of joints of a timber wall on a monolithic foundation often carries the risk of defects, which are usually caused by inappropriately selected structural composition of details. Often the undesired absorption of water into the timber elements stored in the heel-level of construction occurs, inadequate treatment of thermal bridges in place contacting and subsequent internal condensation penetrating moisture and in the worst case, the growth of fungi and degradation of internal structural elements of the wall. Increased moisture incorporated materials as well as increased heat transmission of the wall results in a decrease of surface temperature and an increase in heat losses of the building. All of these factors can affect the quality of indoor environments, such as thermal comfort and indoor air quality, which in turn may adversely affect the welfare and health of people. Subsequent repairs then require considerable financial outlay.

The above-mentioned issues are discussed in previously published studies, for example that by Dalehaug (2013) [1], which documented sensitivity of unventilated, un-drained and vapour-retarding insulated walls of timber structures on damage due to moisture. Damage is often not visible on the surface of the wall, but it can be hidden within the wall or the junction of two components. For long-term durability of structural timber and maintaining the required quality of the internal environment, it is therefore necessary to perform a correct design and performance of the mentioned sensitive details with regard to possible thermal and moisture technical defects, which must be supplemented with good quality materials or suitable chemical treatments. The quality of the material and its chemical treatment has a significant effect on slowing the degradation of biological material and pests.

Requirements and recommendations for initial construction in wood moisture conditions vary in accordance to the laws of each country. However, the market reality of construction timber on site is often unresponsive. Traditionally, the impregnation is carried out using wood impregnates based on the liquid solvents that are used for the transport of biocide into the wood (Kjellow, 2010) [2]. However, during the last two decades, so-called Supercritical carbon dioxide has been investigated as a possible solvent for the impregnation of wood, due to its unique physical properties [3] and thus is considered as a possible solution against the biotic attack within the framework of this thesis.

The main aim of the thesis was focused on hygrothermal simulation of critical details of two prefabricated wooden buildings - especially connections of the perimeter wall to a monolithic foundation. The composition of the external walls of these selected buildings has quite different compositions and thus different potentials of drying integrated moisture from the components. Practical measurement of moisture weight-content was applied to the wooden bottom plate, which is in direct contact with the concrete slab structures, respectively, with the waterproofing layer. The influence of different design solutions on

hygrothermal characteristics of the wooden plate was examined with regards to the risk of mould growth, analysis of mass loss due to the decay fungi and with the aim to estimate the durability of the studied details of prefabricated wooden houses.

The subsequent research was focused on differences in physical and mechanical properties of natural spruce wood (Untreated, (-), A) and impregnated spruce (Treated, (+), B) using supercritical CO_2 and its possible impact on wood protection of mould growth. Samples of identical Untreated and Treated spruce were collected in the laboratory and subjected to thermal and hygrothermal experiments. The comparison of the resulting values of the individual experiments is presented. From these experiments required values needed for numerical calculations were obtained.

A survey of scientific literature presented in the opening chapters of the doctoral thesis provides basic information on the method of supercritical impregnation and composition of wood, with an emphasis on chemical and structural characteristics relevant to the treatment of wood and moisture transport. Thermal and hygrothermal behaviour of building materials, as well as a detailed description of studied compositions of the walls and foundation structures is also presented.

In conclusion, the summary of founded comparison on mechanical, thermal and hygrothermal properties of natural spruce wood (Untreated, (-), A) and impregnated spruce (Treated, (+), B) is presented. This impregnation treatment was chosen as a modern and possible solution of wood protection against microorganism growth. The mould growth analysis and its influence on the durability of wooden structures offer a view of the behaviour of the structures. Relevant findings and recommendations for the future praxis are mentioned. The conclusions of the experiments and simulations show, that the impregnation of wooden elements itself cannot be considered as the protection against mould growth, if there are not ensured optimal moisture conditions in the construction, or if the additional measures are not taken into account. The correct design in the planning stage, quality of the used materials, technical performance on the building site and lately user behaviour influence the reliability and durability of wooden structures.

Abstrakt v českém jazyce

Návrh konstrukčního spoje napojení (ukotvení) obvodové stěny montované dřevostavby na monolitický základ nese riziko vzniku vad, které jsou zpravidla způsobeny nevhodně zvolenou konstrukční skladbou daného detailu. Často dochází k nežádoucí absorpci vody do dřevěných prvků uložených v patě konstrukce, nedostatečnému ošetření tepelných mostů v místě styku a následné vnitřní kondenzaci pronikající vlhkosti, v horším případě pak k růstu hub a degradaci vnitřních konstrukčních prvků stěny. Zvýšená vlhkost zabudovaných materiálů a zvýšení prostupu tepla stěnou má za následek snížení povrchových teplot a zvýšení tepelných ztrát budovy. Všechny tyto faktory mohou ovlivnit kvalitu vnitřního prostředí, jako jsou tepelný komfort a kvalita vnitřního vzduchu, což v důsledku může mít nežádoucí vliv na pohodu a zdraví osob. Následné opravy pak vyžadují nemalé finanční výdaje.

O výše zmíněných problémech pojednávají i publikované studie, např. Dalehaug (2013) [1], které dokumentují citlivost nevětraných, neodvodněných (neodvlhčených) a paro-nepropustně izolovaných stěn dřevostavby na poškození z důvodu vlhkosti. Poškození často není vidět na povrchu stěny, ale bývá skryto uvnitř stěny nebo na spojích dvou konstrukčních prvků. Pro dlouhodobou životnost konstrukčního dřeva a udržení požadované kvality vnitřního prostředí je tedy nezbytné správné navržení a provedení zmíněných citlivých detailů s ohledem na možné tepelně a vlhkostně technické vady, které musí být zároveň doplněné správnou kvalitou použitého materiálu, případně jeho vhodným chemickým ošetřením. Kvalita materiálu a jeho chemické ošetření má významný vliv na zpomalení degradace materiálu a působení biologických škůdců.

Požadavky a doporučení pro počáteční vlhkostní podmínky konstrukčního dřeva se liší v souladu s právními předpisy každé země. Nicméně, realita na trhu se stavebním řezivem, potažmo na staveništi, těmto standardům často neodpovídá. Tradičně se impregnace dřeva provádí použitím impregnantů na bázi kapalných rozpouštědel, které slouží k přepravě biocidů do dřeva (Kjellow, 2010) [2]. Nicméně v průběhu posledních dvou desetiletí byl zkoumán jako možné rozpouštědlo pro impregnaci dřeva tzv. superkritický oxid uhličitý, kvůli jeho jedinečným fyzikálním vlastnostem [3], a tudíž se považuje za možné řešení proti biotickému napadení v rámci této práce.

Hlavní cíle disertační práce byl zaměřen na tepelně-vlhkostní simulace kritického detailu dvou realizovaných montovaných dřevostaveb – zejména napojení obvodové stěny na monolitický základ. Tyto vybrané budovy mají zcela odlišné složení vnějších stěn a tím i rozdílný potenciál vysychání konstrukční a zabudované vlhkosti dřeva. Praktická měření hmotnostní vlhkosti dřeva byla aplikována na hlavní základový trám, který je v přímém kontaktu s konstrukcí betonové desky, respektive s hydroizolační vrstvou. Byl zkoumán vliv odlišných konstrukčních řešení na tepelně-vlhkostní charakteristiky tohoto trámu,

s ohledem na rizika růstu plísní a hmotnostní ztrátou dřeva v důsledku růstu hub s cílem odhadnout trvanlivost takto provedených detailů montovaných dřevostaveb.

Následná část výzkumu byla zaměřena na porovnání rozdílů ve fyzikálních a mechanických vlastnostech přírodního (neimpregnovaného, ozn. A, (-)) smrkového dřeva a dřeva impregnovaného metodou superkritického CO_2 (ozn. B, (+)). Vzorky impregnovaného a neimpregnovaného identického smrkového dřeva byly shromážděny v laboratoři a podrobeny tepelně-vlhkostním experimentům. Z těchto experimentů byly získány potřebné údaje pro numerické simulace. Průběžné porovnání výsledných hodnot jednotlivých experimentů a jejich potenciální vliv na vlastnosti základového trámu dřevěné stěny jsou taktéž prezentovány.

Průzkum odborné literatury v úvodních kapitolách prezentované disertační práce čtenáři poskytne základní informace o metodě superkritické impregnace a složení dřeva, s důrazem na chemické a strukturní znaky relevantní pro impregnaci dřeva a transport vlhkosti. Tepelně-vlhkostní chování stavebních materiálů, stejně jako detailní popis simulačních programů a skladeb stěn a základových konstrukcí experimentálních dřevostaveb jsou rovněž uvedeny.

V závěru práce jsou shrnuty poznatky z provedených experimentů, tedy porovnání mechanických a tepelně-vlhkostních vlastností přírodního (neimpregnovaného, ozn. A, (-)) smrkového dřeva a dřeva impregnovaného metodou superkritického CO_2 (ozn. B, (+)). Tato metoda impregnace byla zvolena jako moderní možné řešení ochrany dřeva proti růstu mikroorganismů. Analýza růstu plísní a jejich vlivu na trvanlivost dřevěných konstrukcí nabízí pohled na chování jednotlivých konstrukčních řešení dřevostaveb a nastiňuje praktická doporučení pro budoucí praxi. Ze závěrů provedených experimentů a simulací vyplývá, že impregnace dřevěných prvků sama o sobě nemůže být považována za dostatečnou ochranu proti růstu mikroorganismů, pokud nejsou zajištěny optimální vlhkostní poměry v konstrukci, případně pokud nejsou přijata doplňková opatření. Správný návrh konstrukce ve fázi plánování, kvalita materiálu a technické provedení na staveništi a v neposlední řadě chování uživatelů ovlivňují spolehlivost a životnost dřevěných konstrukcí.

Key words

Treated spruce, impregnated spruce using supercritical CO_2, Untreated, non-impregnated spruce, hygrothermal performance, wooden building, mould and decay development methods, mould growth index, Viitanen's model, thermal and hygrothermal numerical calculations

Klíčová slova

Ošetřený smrk metodou superkritického CO_2, neošetřený-neimpregnovaný smrk, tepelně-vlhkostní posouzení, dřevostavba, metoda rozvoje růstu plísní, index růstu plísní, Viitanenův model, tepelně-vlhkostní numerické simulace

TABLE OF CONTENTS

INTRODUCTION

Wood is a hygroscopic material, meaning its condition depends on its moisture content. From an indoor microclimatic point of view, this property of wood is considered an advantage, but with regards to the actual construction of buildings and the dimensional stability of wood-based elements, the sensitivity to the moisture state can often be challenging. The combination of temperature and humidity in the environment in which the timber is located results in a certain moisture content of the wood, which does not necessarily depend on the tree species [5].

Since the timber continuously exchanges moisture with the surrounding environment, the moisture content of the timber can increase to a high level when the humidity of the environment is also high. If the wood is kept in a humid environment condition for more than a few weeks in a year, there will be a risk of infection and subsequent degradation of the wooden components by wood-destroying microorganisms. In terms of reliability of the construction, the increased moisture content of the wooden elements will also cause the expected increase of deformation of these elements over the value proved in static calculations.

Requirements and recommendations for initial moisture conditions of structural wood vary according to the legislation of each country, e.g. in Norway it is allowed to use a wood with 20 weight-% moisture content (MC), in Denmark, Germany, Austria and the Czech Republic 18 weight-% MC is allowed [6]. However, the on-site reality is often something else, and it is not unusual to see timber constructions soaking in rain as was documented at building sites in the Czech Republic and Denmark (Figure 1).

Figure 1: Total view of the wooden buildings on the building site in the weather conditions, which indicates the increscent of moisture content of the wood. Photos © Karel Šuhajda (left), Ruut Peuhkuri (right)

On-site measurements in the case in Denmark also showed that MC of the wood, specifically the bottom plate that is in direct contact with waterproofing layer (“murpap”) on the concrete screed, could reach the value over 35 weight-% (Figure 2). Connected wood-based materials (OSBs) of the wall systems are also affected.

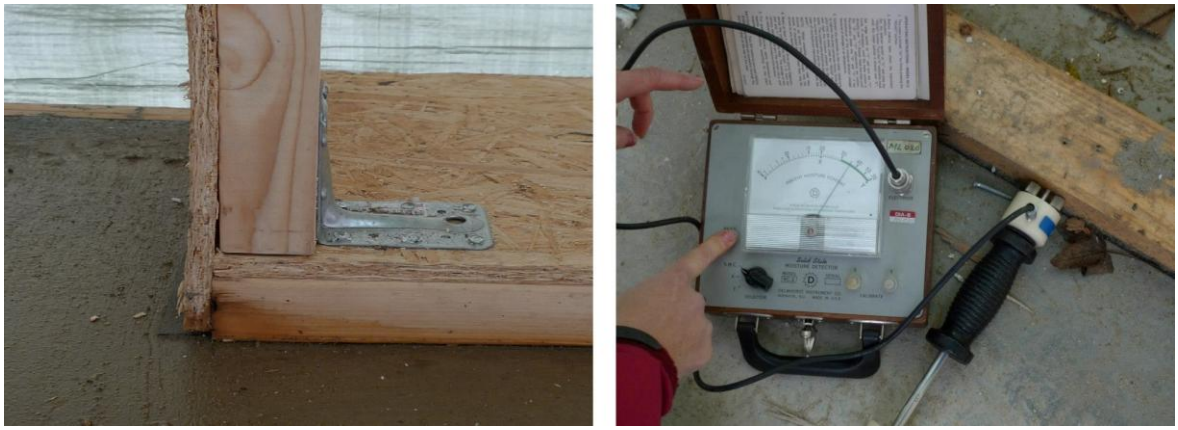

Figure 2: The wooden post with OSB soaked with water (left); Measurement of the MC of the bottom plate at a building site (CS2) in Denmark. The average MC was determined at 35 weight-% (right), Photos © Ruut Peuhkuri

Although high initial moisture content should never be accepted, it is still of interest to see how quickly excessive moisture can be dried from a critical construction element, respective of the critical connection detail of the wall to the monolithic base.

For the mould growth analysis, two well-insulated timber structures were chosen, which are quite different with regards to their possibility to dry out “built-in” moisture from the peripheral wooden wall and have therefore slightly different thermal properties. These two solutions are commonly used in newly built low-energy buildings in the Czech Republic and Denmark.

Traditionally, the impregnation is carried out using wood impregnates based on the liquid solvents that are used for the transport of biocide into the wood [2]. However, during the last two decades, the wood treatment process based on supercritical carbon dioxide as a carrier for the organic fungicide has been investigated as a possible solvent for wood impregnation. CO_2 gas combines physical properties (viscosity and surface tension) with liquid (density). High density of CO_2 supports its effectiveness as a solvent, while its low viscosity and low surface tension allows it to penetrate the material quickly and efficiently. The combination of these properties, with high level of diffusivity (conductivity) and the possibility of accurate adjustment of solubility using pressure and temperature changes, makes this impregnation

method very attractive. It was also found that through this method the impregnation is possible to significantly reduce the problems concerning environmental protection during the chemical treatment of wood [4]. Kjellow in his dissertation (2010), dealing with the retention of biocides and supercritical impregnation of wood against biological attack, concluded that "*the method of supercritical impregnation can store in the wood sufficient amount of biocide in order to slow the biodegradation of structural timber to an acceptable level*" [2].

This special impregnation treatment of wood itself cannot be considered as a solution against microorganism growth, if there are not ensured optimal moisture conditions in the construction.

The correct design of technical solutions of the critical details, as well as the practical performance on the building site and user behaviour are the most motivating factor for the life-time and durability of wooden structures.

1. BASIC THEORETICAL BACKGROUND

1.1 Wood anatomy and biology

1.1.1 Structure of softwood timber

Wood is a heterogeneous, hygroscopic, cellular and anisotropic material. It is composed of cells, and the cell walls are composed of micro-fibrils of cellulose (40 % – 50 %) and hemicellulose (15 % – 25 %) impregnated with lignin (15 % – 30 %) [7]. As a natural product, it has a wide variation in properties depending on factors including but not limited to wood type, growth conditions, wood dimensions and cross sectional shape, and post-growth treatment.

This Thesis focuses on a representative of temperate softwoods: Norway spruce (Picea abies). Its wood is yellowish to brownish yellow in colour with contents of resin canal. They are difficult to distinguish with the naked eye, can be seen on longitudinal sections as short lines or the cross-section as small bright dots in a summer wood. The wood is shiny and is characterized by the presence of mature timber. [9, 26]

Norway spruce has often visible and marked differences between latewood (darker) and earlywood (lighter), which gives a typical pattern of annual rings as shown in Figure 3. Greater decomposition of latewood defines better density together with strength. The latewood is about three times more dense than that of earlywood. When examined under a microscope, the cells of dense latewood are seen to be very thick-walled and with very small cell cavities, while those formed first in the season have thin walls and large cell cavities.

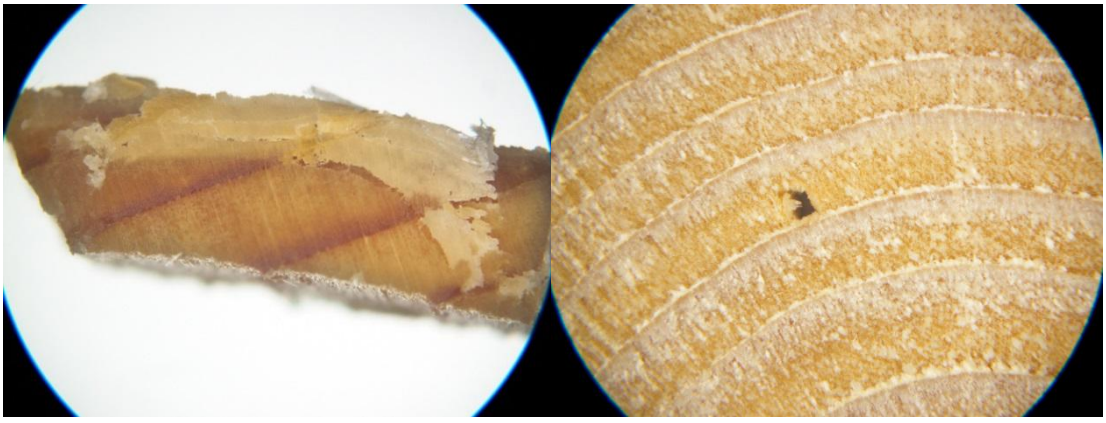

Figure 3: Total view on specimen of Norway spruce (left), A typical pattern – a visible difference between earlywood and latewood (right) [author]

It is average density when w = 0 % is ρ_0 = 420 kg·m^3 and so it belongs to the fourth class of durability - slightly durable wood (see Table 8 and Table 9). Spruce covers about 78.5 % of all timber harvesting in the Czech Republic. [12]

1.1.2 Structure at the macroscopic level

The trunk of the tree has three physical functions to perform: support the crown, conduct the mineral solutions absorbed by the roots upwards to the crown and store manufactured food (carbohydrates) until it is required. The entire cross-section of the trunk fulfils the function of support, conduction and storage and is restricted to the outer region of the trunk. This zone is known as sapwood, whereas the part in which the cells no longer fulfil these criteria is termed the heartwood. [9]

Seasonal growth of the tree forms the annual rings. In the early part of the season, so called earlywood, is a dominant function of thin-wall tracheids (about 2 μm) conduction, whereas thick-walled (up to 10 μm) and slightly longer (10 %) tracheids in the later part of the seasons have dominant factor support. The proportions and other terminology are shown on Figure 4.

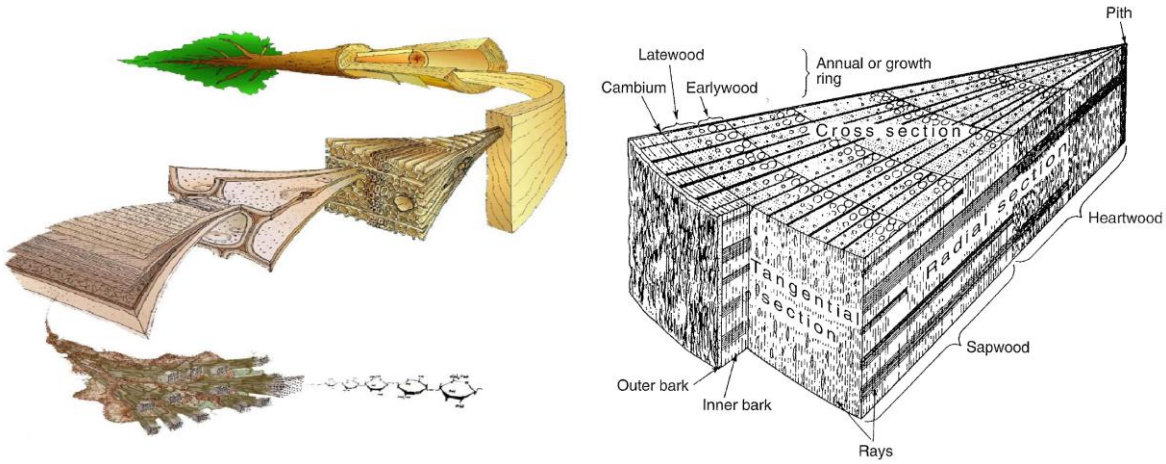

Figure 4: Schematic visualization of procedure "From Tree to cellulose chain" (left); Illustration of a wedge-shaped segment of sections of typical softwood with appropriate terminology (right) [8, 9]

1.1.3 Structure at the microscopic level

In normal cell walls, the cellulose micro fibrils are aggregated into thin lamellae which are, in turn, organized into layers as seen in Figure 5. The walls usually contain three layers of secondary origin. The outer envelope of the cell is termed the "primary wall" and consists of a loose network of micro fibrils with another material as well. This primary wall exists at the time the cell is formed in the cambium.

The secondary wall layers are designated as S1, S2 and S3, from the outside to the inner layer lining of the cell lumen. Within each layer, the micro fibrils are oriented more or less uniformly into a rather dense parallel array, as shown in Figure 5. Some species of wood will exhibit an additional layer over the S3 in the form of a rough or warty surface. [9]

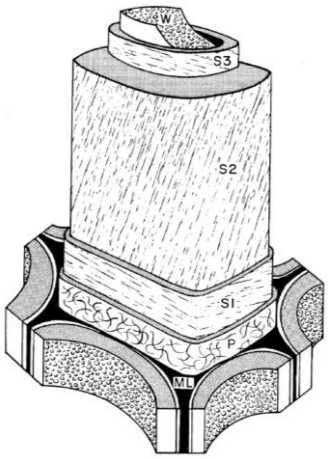

Figure 5: Organization of the wood cell wall (ML: middle lamella, P: primary wall, S1-3: outer, middle and inner layers of secondary wall, W: warty layer) [9]

The formation of long tracheids aligned in the longitudinal stem direction next to one another in each radial growth layer together with the differentiated growth within a season gives the typical pattern of annual rings in softwood concentric around the pith. This arrangement together with the properties of the tracheids and their connection gives the wood material three distinctive material directions in a cylindrical coordinate system, see Figure 6. Since there are different material properties in each direction, this material is called anisotropic, or more correctly cylindrical orthotropic with three main materials, see Figure 7.

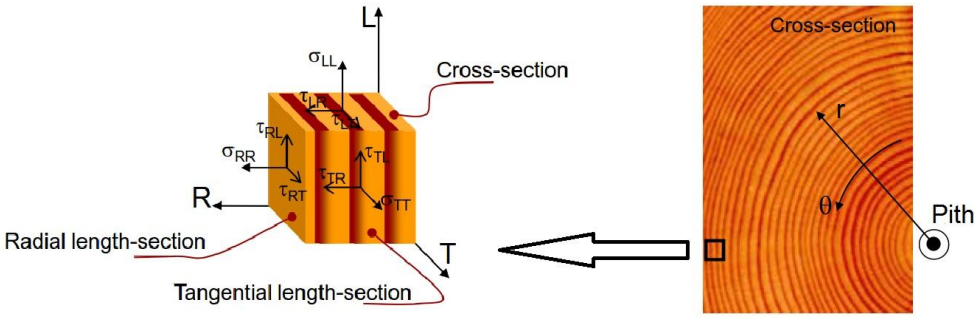

Figure 6: Anisotropic material with main material directions where each material direction is perpendicular to the other, an orthotropic material [author with 9]

Figure 7: Cross section (left); Tangential length-section (middle); Radial length-section (right) of Norway spruce [26]

1.2 Wood and water interaction

Wood exists in relation to its surrounding environment, the hygroscopic material able to receive or donate water, whether in liquid or gaseous state, and has the ability to change its moisture under ambient humidity. The ability to attract dry wood cell wall construction materials (cellulose and hemicellulose), liquids and gases follow from ontogeny elements of wood which were differentiated in a fully saturated aquatic environment.

Although wood may receive other fluids and gases, the water is most important in practical terms. A growing tree contains a large amount of water which is necessary for its existence. After felled water content in the wood, according to another application further reduces or increases. Due to the hygroscopicity of wood, it almost always contains water. In most cases, water in wood affects its properties and often causes its deterioration. With the change of water content in wood, come associated changes in physical and mechanical properties, resistance to fungi and insect attack, processes wood processing and other processes. [9]

1.2.1 Moisture movement in wood

In the living tree, the transport of water from the roots to leaves occurs through the tracheid lumens. Because of the limited length of the tracheid, water must move through numerous tracheids as it moves upwards in the tree. Water moves from one lumen to another through intercellular openings in the cell walls comprised of bordered pit-pairs, which appears as donut shaped apertures in the cell wall. [9]

The movement of moisture within hygroscopic capillary building materials is a combination of vapour and liquid flow which have complex integrations with temperature and humidity gradients and the properties of the material. Wood is a hygroscopic material so the volume and moisture content of wood constantly interacts with the surrounding climatic state, i.e. by varying air humidity and temperature. In these conditions moisture transport through the material occurs. Moisture transport in wood is present in wood below fiber

saturation point and includes three processes dependent on each other [9, 10] which are also illustrated on Figure 8:

1. Diffusion of vapour in the open porous system;
2. Sorption on all surfaces, resp. sorption of water to regain equilibrium between vapour water in pores and bound water in cell wall;
3. Diffusion of bound water in cell wall structure.

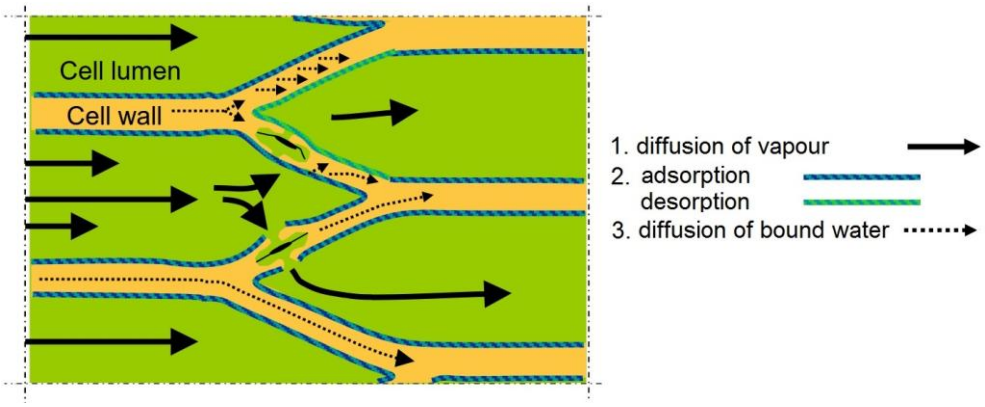

Figure 8: Transport of moisture in wood is a coupled diffusion phenomena [author with 9]

The fibre saturation point (FSP) is a theoretical defined moisture state, when no liquid water is present in the voids but the cell wall is still saturated.

The anatomic features of spruce that composes the porous structure are cell lumens of the tracheid cells, intercellular pits, rays and resin canals. These pores of wood have a range from 5-100 μm and one water vapour occupies a volume of 0.3 nm (0.0003 μm) [9]. This indicates that water vapour molecules can move freely in the wood voids without affecting a wood cell walls. The hydroxyl groups of the macromolecules in wood are to a large extent accessible to water molecules. There are four possible states for the water molecules:

1) to remain in vapour phrase;
2) to chemically bond with wood: 3) to break the bond;
4) to remain in this state.

The molecular kinetics of bonding and bond breaking between water molecules and wood is identified as the physic-chemical process of sorption and is described further on. As the amount of bound water changes in the cell walls, it effects (among others), the free shrinkage, mechano-sorption, modulus of elasticity and diffusion coefficients. The three forms of water are depicted in Figure 9 along with their association with free shrinkage. [9, 10]

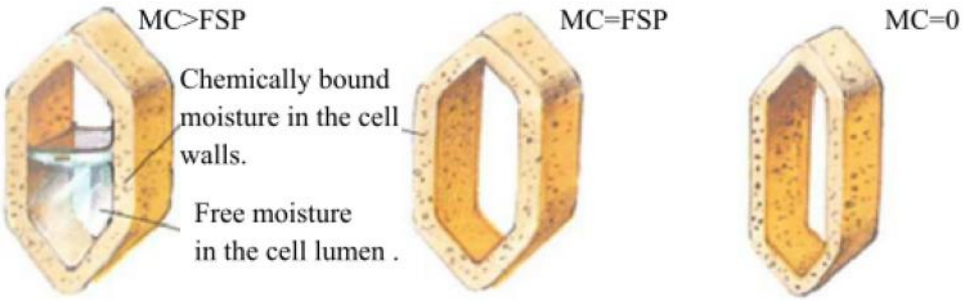

Figure 9: Different forms of moisture storage within wood and their relation to free shrinkage [10]

The value of humidity when reaching the saturation limit of the cell walls depends on the wood species and the temperature. It ranges from 23–36 %. For technical purposes a mean value of 30 % has been introduced. For practical purposes "technical (production) humidity" and "usable humidity" is used. Production humidity is called a wood moisture at the time of manufacturing of the product. Usable humidity means the humidity during the product use. It is necessary for the production moisture humidity to be equal or about 2 % smaller then usable humidity. Otherwise, it may cause adverse effects. From this perspective, the basic requirements for usable humidity were stated for building construction of 15-22 % of usable humidity. [9, 10]

Capillary elevation

Surface tension and capillary effects are closely linked and are a result of exposure of most cohesive forces of the molecules. For a liquid which wets the walls of the narrow capillaries, capillary elevation phenomenon occurs. Liquid molecules have higher attraction forces with the molecules of the capillary wall than between each other. This leads to the tendency to maximize the wetting surface under given conditions, thus the contact between the wall and the liquid. The liquid is in the vertical capillary pulled out by adhesive forces to such a height at which the total elevation force of the surface tension is in balance with the weight of liquid column. For a water-filled glass tube in air at standard laboratory conditions, $\gamma = 0.0728\ \mathrm{N \cdot m^{-1}}$ at 20 °C, $\theta = 0°$ (cos(0) = 1) (Figure 10). [11, 12]

In the simplest case, when the pores in the wood are considered as cylindrical capillaries of radius r and length equal to the length of the entire body. As a body is immersed in water, the liquid in each capillary is risen to certain height (Požgaj et al., 1993). If it is greater than 90 °C, as with mercury in a glass container, the liquid will be depressed rather then lifted. [12]

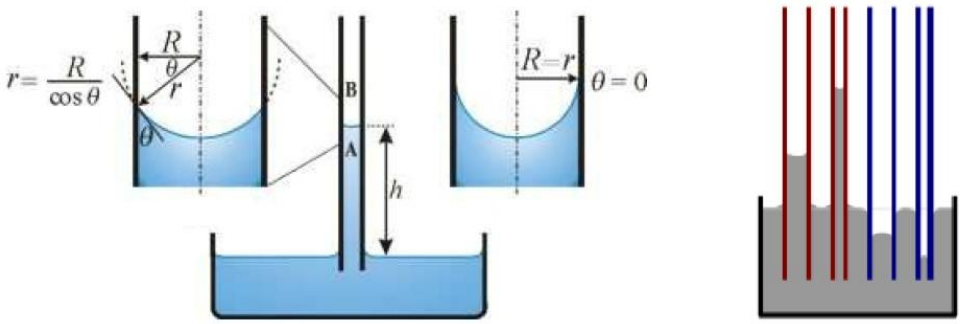

Figure 10: Capillary elevation with assigned liquid column „h“(left); Illustration of capillary rise and fall. Red=contact angle less than 90°; blue=contact angle greater than 90° (right), Level increases with decreasing diameter depending on surface energies [author with 12, 13]

To determine the height the liquid is lifted “h”, the following relationship is used:

$$h = \frac{2 \cdot \gamma \cdot \cos\theta}{\rho \cdot r \cdot g} \qquad [\mathrm{m}] \qquad (1.1)$$

where
- γ liquid-air surface tension [$N \cdot m^{-1}$];
- θ contact angle [°];
- ρ density of the liquid [$kg \cdot m^{-3}$];
- r radius of the capillary [m];
- g acceleration due to gravidity = 9.81[$m \cdot s^{-2}$].

Chemical potential of moisture

The chemical potential of the moisture “μ_u” is a thermodynamic potential of the water transport. Its gradient is the driving force of the main moisture transport process. It is defined as a partial enthalpy change “G” according to the amount of the moisture content “w” during the constant pressure, temperature and the quantities of other parts.

$$\mu_u = \left| \frac{\partial G}{\partial m_w} \right| p, T, m_i \neq m_w \qquad [\mathrm{J \cdot kg^{-1}}] \qquad (1.2)$$

where
- G free enthalpy [J];
- p pressure [Pa];
- T thermodynamic temperature [K];
- m_i mass of substance [kg];
- m_w mass of water [kg];

$m_i \neq m_w$ means, that the process occurs under constant masses all used components m_i, except of mass of water contained in substance m_w.

The importance of the chemical potential is that it is possible to determine the moisture content in the different position of the building substance or building construction and thus to estimate the sources of the moisture.

According to thermodynamics law the transport of the moisture leads from the position with the higher chemical potential towards the position with the lower chemical potential. On this base it is possible to specify the direction of the moisture (water) transport, which is used in praxis. [11]

Conductivity of moisture

The so-called transmission is the ability of the material to carry the moisture in the liquid state to the surface, where it evaporates or diffuses. This is actually the capillary movement of water in continuous water channels. Moisture transport is happening at a **moisture gradient** (i.e. the gradient of moisture at a temperature difference of 0 °C) or at a **temperature gradient** (during the moisture gradient). [11]

When the humidity gradient and zero temperature difference is used to calculate the density of the mass flow rate of liquid water transmission, Lykov's transmission law is used. The density of a mass flow of liquid water by transmission "$q_{mt,1}$" is then expressed through the following formula:

$$q_{mt,1} = -\kappa_m . \rho_s . \frac{du}{dx} \qquad [kg \cdot m^{-2} \cdot s^{-1}] \qquad (1.3)$$

where κ_m coefficient of moisture conductivity during the moisture gradient [$m^2 \cdot s^{-1}$];

ρ_s volumetric mass density of material in dried state [$kg \cdot m^{-3}$];

$\frac{du}{dx}$ moisture gradient [m^{-1}].

If the moisture gradient takes place also during the temperature gradient, then this density mass flow of liquid water by transmission "$q_{mt,2}$" is expressed by the formula:

$$q_{mt,2} = -\kappa_m . \rho_s . \kappa_t . \frac{dt}{dx} \qquad [kg \cdot m^{-2} \cdot s^{-1}] \qquad (1.4)$$

where κ_t coefficient of moisture conductivity during the temperature gradient [K^{-1}];

$\frac{dt}{dx}$ temperature gradient [s·m^{-1}].

In the building praxis, the moisture and temperature gradient takes place at the same time so the overall density mass flow of liquid eater by transmission "q_{mt}" is calculated as:

$$q_{mt} = q_{mt,1} + q_{mt,2} \qquad [kg \cdot m^{-2} \cdot s^{-1}] \qquad (1.5)$$

1.2.2 Permeability of liquids in wood

For the wood industry, the movement in wood has serious practical significance (e.g. during drying, wood penetration, plasticizing of wood, etc.).

The driving forces of such movements are influenced by a number of factors (humidity gradient, capillary pressure, osmotic pressure, water vapour diffusion, etc.). [11, 12]

Permeability is the volume flow of fluids through the material (wood) caused by the gradient (difference) of external pressures - static or capillary. This is collectively called hydrodynamic movement and in most of literature it is described by Darcy's law in integral formula:

$$\frac{V}{t} = c \cdot \frac{A \cdot \Delta p}{\eta \cdot L} \qquad [m^3 \cdot s^{-1}] \qquad (1.6)$$

where
- V volume of the extruded liquid [m^3];
- t time flow [s];
- c permeability coefficient [m^2·s^{-1}·Pa^{-1}];
- A area of flow [m^2];
- Δp pressure difference at the end of test specimen [Pa];
- η dynamic viscosity of the fluid [-];
- L length of element [m].

The permeability coefficient "c" informs the state of conduction in the wood structure. If we consider the dynamic viscosity of the liquid, the new coefficient of specific permeability "C" is used ($C = c \cdot \eta$) [m^2].

The movement speed of the liquid affects the kind of capillary flow (laminar, turbulent, non-linear). These types of flow determine the critical Reynolds and Nusselt numbers. Relatively frequently is used Reynolds number "Re", which is defined as:

$$\mathrm{Re} = \frac{2 \cdot \rho \cdot Q}{3.14 \cdot r \cdot \eta} \qquad [-] \qquad (1.7)$$

where Q volume flow [$m^3 \cdot s^{-1}$];
ρ density of the liquid [$kg \cdot m^{-3}$];
r radius of the capillary [m].

When Reynolds number Re > 2000, laminar movement turns to turbulent. Turbulent movement speed is not so usual in coniferous trees in which non-linear movement caused by thinner dimensions of cell walls is more important.

Darcy's law characterizes fluid flow in the capillaries of the wood where the following conditions are fulfilled (Kurjatko, Reinprecht, 1993) [11, 12]:

- liquid flow is viscous and laminar
- the liquid is incompressible and homogeneous
- capillary or capillary systems are homogeneous over the entire length, which is the condition of independence of coefficient C (c) of length L
- between the liquid and the surface of the capillary are no interactions

For the scientific proposes of wood permeability is sometimes used also Poiseullo law (Sian, 1984), expressed with the formula:

$$\frac{V}{t} = \frac{\pi \cdot r^4 \cdot N \cdot \Delta p}{8 \cdot \eta \cdot L} \qquad [m^3 \cdot s^{-1}] \qquad (1.8)$$

where V volume of the extruded liquid [m^3];
t time flow [s];
r radius of the capillary [m];
N number of capillary in area unit [-];
Δp pressure difference at the end of the test specimen [Pa];
η dynamic viscosity of the fluid [-];
L length of element [m].

Permeability of wood for fluids is highly dependent on the type and thus anatomical wood structure, anatomical directions, dimensions of anatomical elements, structure and thinner dimensions of the cell walls, the permeability of the anatomical elements due to deposition of various materials (resins, ethyl formation etc.), density, moisture wood and previous drying processes

(Matovič, 1993). The movement of the liquid water above the hygroscopicity limit during the drying process causes the formation of considerable capillary forces. These can cause deflection of the closure blanks or margarine and the torus in the colons of conductive elements and causes the closure of conducting paths. **Colon aspiration** contributes to the reduction of permeability. [11, 12]

For conifers, wherein the permeability of the wood is affected by thinner dimensions of cell walls, there is a noticeable effect of layer W, whose presence might cause the low permeability to increase. The specific permeability coefficient "C" in the longitudinal direction of the wood is in the range 10^{-10} to 10^{-4} m^2, and in the cross direction in the range of 10^{-12} to 10^{-10} m^2 (Horáček, 1998). [11, 12]

1.2.3 Water interaction on physical properties of wood

The basic characteristics of moisture on building materials, which have been tested in laboratories for many years, are the porosity, water absorption, capillarity and the equilibrium moisture state. [11]

Porosity

Porosity of the substance is expressed as a pore volume fraction of closed cavities, and the whole volume of the dried solid. This is the total perceptual amount of the free space of the substance, which is not filled by solid particles.

To determine the porosity "p", the following relationship is used:

$$p = \left(\frac{V_v}{V_s} \right) \cdot 100 \qquad [\ \%\ ] \qquad (1.9)$$

where V_v volume of void space [m^3];
V_s volume of solids [m^3].

The porous building material structure is comprised of a wide range of radius of pores, starting from the smallest water molecules up to pores of macroscopic sizes. According to Dubinin, the pores are divided by size into three groups [11]:

- 1^{st} group - macroscopic pores on the effective radius > $2 \cdot 10^{-7}$ m;
- 2^{nd} group - transient pores on the effective radius $2 \cdot 10^{-7}$ – $1.5 \cdot 10^{-9}$ m;
- 3^{rd} group - microscopic pores on the effective radius < $1.5 \cdot 10^{-9}$ m.

Water absorption

Absorbency is the ability of wood, due to its porous structures to absorb water (or other substances) in a liquid form. Water absorption is characterized by weight moisture expressing the relative amount of water that can be absorbed by tested dried building materials, when immersed into water for a certain period of time and under pre-determined conditions. According to absorption, we can determine the total amount of so-called open pores and frost resistance of the building substance.

To determine the mass absorption, resp. moisture content, "NV" the following relationship is used. The result is given within an accuracy range of 1.0 %:

$$NV \equiv \left(\frac{w_w - w_d}{w_d} \right) \cdot 100 \qquad [\%] \qquad (1.10)$$

The volumetric absorption is recalculated from the following equation:

$$NV_v \equiv \frac{NV . \rho_d}{\rho_w} \qquad [\%] \qquad (1.11)$$

where
- w_w mass of a sample before drying [kg];
- w_d mass of a sample after drying [kg];
- ρ_d volumetric mass density of dried sample [kg·m^{-3}];
- ρ_w volumetric mass density of the water [kg·m^{-3}].

In addition to the normalized method, the following water absorptions can be defined:

- under the cold conditions NV;
- under the cold conditions with the forced submersion NV_f;
- under boiling on the water surface NV_{ws};
- under boiling with the forced submersion $NV_{ws,f}$;

Wood is fully soaked, when it has a maximum amount of bound water (on the hydroscopicity level) and the largest possible amount of free water. There is an absorbency rule, whereby the density of the wood increases, the lower its ability to absorb water. It follows that the absorbability depends mainly on the volume of the pores in the wood. [12]

Theoretically the maximal moisture "w_{max}" can be calculated by the formula:

$$w_{max} = MH + \left(\frac{1530 - \rho_0}{1530 \cdot \rho_0} \right) \cdot 100 \qquad [\%] \qquad (1.12)$$

where MH moisture at the hydroscopicity level, average for wood is determined 30 % [%];
1530 density of wood substance ρ_s [kg·m^{-3}];
ρ_0 density of absolutely dry sample [kg·m^{-3}].

For wood moisture on the hygroscopicity level and density of the wood substances used in formula (1.12) the average values often do not correspond to reality. For various reasons, all cavities in the wood do not need to be filled with water (e.g. because of presence of resins etc.). Maximal moisture content of some wood types is expressed in Table 1.

Table 1: Maximal moisture content of some wood types (by UgoleCS1975) [12]

Wood type	Moisture [%]	Wood type	Moisture [%]
Larch	123	Hornbeam	96
Pine	178	Oak	119
Spruce	203	Birch	131
Fir	250	Poplar	198

Critical moisture content

Critical moisture level represents the maximal tolerable amount of moisture in building materials in building praxis. After exceeding critical moisture content the changes in building substance are crucial that it changes its mechanical and physical properties (strength, volume, thermal conductivity, chemical properties and so on). Usage of the materials with the above level content of critical moisture is unwanted in building praxis, inappropriate, and in many cases dangerous. [11]

The value of critical moisture content is described in respective standards, usually as a value of maximal usable weight-moisture content of building substances. The typical requirements for usable weight-moisture content of wood products is mentioned in Table 2.

Table 2: Standard requirements of moisture content for wooden products [author with 15]

Product	Maximal weight-moisture content [%]
Building construction	15-22 %
Building components (windows, door etc.)	12-15 %
Furniture in slightly heated rooms	10-22 %
Furniture in rooms with central heating	8-22 %
Veneer, plywood	5-7 %
Musical instruments	5-7 %

Hydrophobization

Water absorption of building materials is affected by hydrophobization and hygroscopicity.

Hydrophobization is a change of physic-chemical properties of treated materials, which at the interface of the solid and gaseous environment rapidly increases the contact angle for water (Kettle, 2008).

According to the contact angle value of water with the surface are recognized as:

a) $\Theta < 90°$ - the solid surface is wetted;
b) $\Theta > 90°$ - the solid surface is not wetted.

Thanks to its large surface tension and a small wetting angle, the water easily penetrates into the pores of building materials (similarly as into the glass capillary). However, if we increase the contact angle of water (e.g. with a thin layer of wax or oil), water does not wet the glass surface and penetration of the glass capillary is more difficult or does not occur at all – see Figure 11.

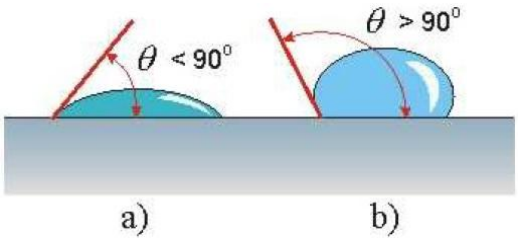

Figure 11: The contact angle of the water on a solid surface [12]

Hydrophobization (resp. waterproofing) therefore consists of forming a thin layer of hydrophobic material on the inner surface of the pores. This layer may be very thin (about the size of only a few molecules), that is virtually invisible to the eye and not decreasing the diameter of pores. Nevertheless, it is able to significantly suppress the penetration of liquid water into the pore. It is clear that the pore penetration through gases (including the water vapour) remains. [11, 12]

Besides reducing the risk of frost damage, decreasing the rate of chemical reactions taking place in an aqueous environment and improving the thermal insulating properties of a porous material, the hydrophobic treatment affects its ability to stain.

The level of the hydrophobization "H_v" indicates how many times the absorption of hydrophobic matter is decreased in comparison with the initial state and can be calculated as:

$$H_v = \frac{NV_{ws}}{NV_{ws,h}} \qquad [m^3] \qquad (1.13)$$

where NV_{ws} absorption due to the boiling on the water surface of the non-hydrophobic matter [%];
$NV_{ws,h}$ absorption due to the boiling on the water surface of the hydrophobic matter [%].

Equilibrium moisture state

This state is characterized by a certain temperature and humidity that correspond to a wood moisture value (equilibrium moisture content). The rate of evaporation of water from the timber depends on the following factors (Brumovský Council, 1991):

When water affects the porous building material both by absorption of moisture from the ambient air and the accumulation of moisture at the contact of the two phases due to intermolecular forces, the common name, sorption, is used. It is the common expression for absorption, adsorption and sometimes also for chemisorption.

Adsorption is caused due to van der Waals forces, which attract the molecules of liquids and gases. During adsorption, the condensed component in the gas and liquid phase on the surface of solid materials diffuses into the interior of the solid phase therefore forming a solid solution. During chemisorption, chemical forces are applied, which have a much stronger bond than physical. [11, 12]

Equilibrium states occur at a constant temperature and are characterized by the sorption isotherm. An equation for isotherms was defined by H. Freudlich and I. Langmuir:

$$a_d = \frac{c_1 . p}{1 + c_2 . p} \quad [m^3] \qquad (1.14)$$

where a_d amount of absorbed gas [m^3];
$p_{ws,h}$ pressure of gas [Pa];
c_1, c_2 constants [-].

In construction practice, the most important absorbent is water vapour. If the partial pressure of water vapour is lower in the body than in the ambient air, the body receives water vapour from the air. This process is called **sorption**. However, if the partial pressure of water vapour in the body is higher than in the ambient air, water vapour releases the body. This process is called **desorption**. [11, 12]

A balance between the moisture of the body and the moisture of the ambient air during the steady temperature and humidity states is called

equilibrium moisture state. This is characterized by the zero increment of moisture and temperature conditions in the time under the conditions:

$$\left|\frac{\partial w}{\partial r}\right|_{\tau\to\infty} \to 0 \left|\frac{\partial T}{\partial \tau}\right|_{\tau\to\infty} \to 0 \qquad (1.15)$$

Because this condition is practically impossible to fulfil, the equilibrium moisture state is expressed by relation:

$$w_{mc} = f(\varphi) \qquad \text{for = constant} \qquad (1.16)$$

where
- w_{mc} mass equilibrium moisture content [%];
- w water (moisture) content [-], [%];
- T temperature of ambient air [°C];
- τ time [s];
- φ relative humidity of air [-], [%].

The equilibrium moisture content of the air depends on the temperature, relative humidity and atmospheric pressure of the air. During the constant atmospheric pressure the equilibrium moisture content depends on the temperature and the relative humidity of the ambient air.

The correction curve between the moisture of the building material and the relative humidity of air at a constant temperature is called the isotherm moisture equilibrium. Its typical shape is shown on Figure 12. The moisture equilibrium of wood is history dependent.

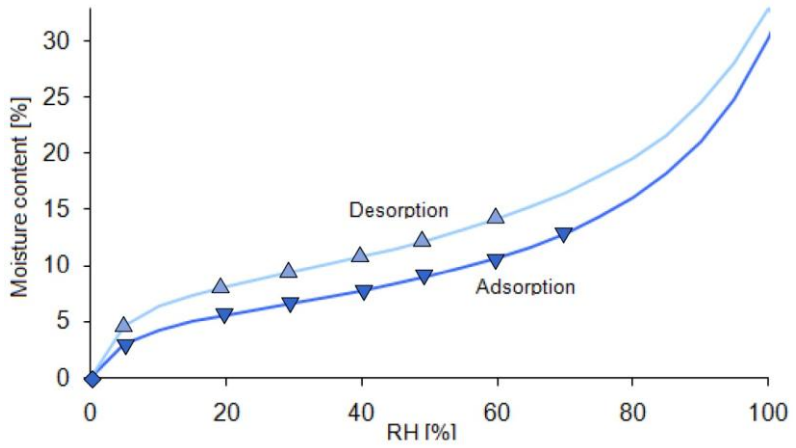

Figure 12: Typical shape of adsorption and desorption isotherm (moisture states in equilibrium) [author with 9]

The curve contains two branches. When we reach the equilibrium state by humidification process, we get adsorption isotherm. The opposite equilibrium state is reached by the drying process, we get the desorption isotherm. For

adsorption and desorption isotherms the zipper theory applies, which is expressed by Figure 13.

Maximal equilibrium (sorption) moisture is when φ = 1 and is called hygroscopic moisture. At the same temperature, the desorption curve is always higher than the adsorption curve. The difference between these two branches is called **hysteresis**.

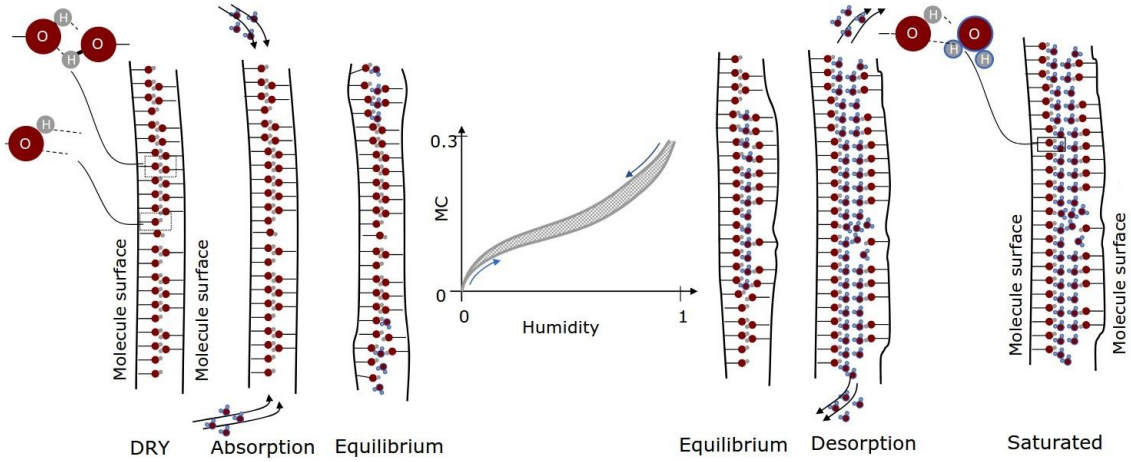

Figure 13: Absorption and desorption zipper theory [author with 9]

The sorption isotherms of certain selected construction materials are shown in Figure 14.

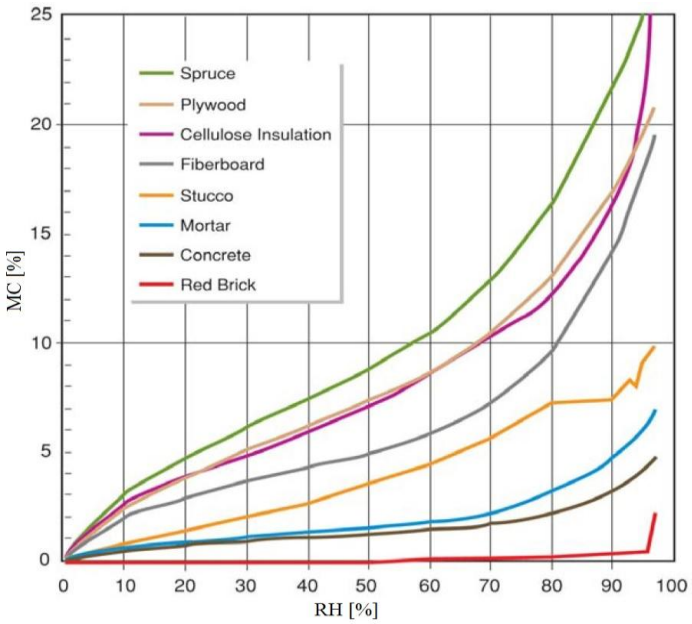

Figure 14: Sorption isotherms for some buildings materials [14]

With increasing temperature the equilibrium moisture in both arms decreases. As the material dries, the water content in the pores drops and the adsorbed water will try to leave the surface of the pores. However, the strength of the bond between water molecules that make up the adsorbed

layers results in tension forces as drying progresses. It is these internal tension forces that cause drying shrinkage stresses and the consequent cracking in wood. [14]

Nevertheless the building materials may have higher moisture than the hygroscopic moisture, and thus we distinguish:

• the equilibrium state of the substance in contact with the water vapour;
• the equilibrium state in the direct contact of the substance with water.

1.2.4 Water interaction on mechanical properties of wood

The mechanical properties of wood depend on its ability to resist the effects of external mechanical forces. These features include: flexibility, strength, hardness and toughness of wood. [15]

External mechanical forces can act in the following manner:

- statically (smoothly and slowly growing strength);
- impulsively (force acts immediately on the full amount);
- oscillating (alternating force changes the direction and size);
- permanently (force acts for a long time).

The mechanical phenomenon creep is fundamental for structures that last for long period of time. A solid material such as wood deforms as a function of time and at a constant load. Creep of a wood is influenced by a number of variables. The density of the wood is the main factor showing its stiffness [16]. The wood becomes stiffer as the density increases. There are some factors to be considered such as:

- the grain angle has a major effect on bending strength [17];
- the load carrying capacity is stronger when the wood is loaded parallel to the grain direction, but drops drastically as the angle gets closer to the level of 45°, and it gets reduced when the angle reaches to the level of 90° which is the weakest level [18].

There are several facts which influence the mechanical properties of wood. They can be divided into three groups [9, 15]:

1. The regularity in structure in micro- and macroscopic levels, such as cell wall structure and size, cell shape, cell orientation, cell bonds and spatial arrangement;
2. External interfaces, such as moisture state and moisture changes, time rate and time duration;
3. Irregularities in wood structures, such as knots, grain angle, reaction wood and other phenomena that cause irregularities in the regular cell arrangement.

A strong hypothesis is that nature has made wood optimize its mechanical properties to withstand natural excitation and natural competition. Tensile and compressive strength in longitudinal direction is totally dominating. This enables the tree to withstand large bending that arises from horizontal load, wind load, or eccentricity of vertical loads.

Stiffness is the parameter governing the stability capacity. Large stiffness properties in a longitudinal direction enable the tree to compete for sunlight by growing tall.

The clear wood has in a longitudinal direction a tensile strength f_t in the range of 80-120 MPa and compressive strength f_c is in the range of 30-60 MPa. The compressive failure is more ductile compared to the tensile failure. Stiffness, respectively modulus of elasticity E_{LL} of clear wood in a longitudinal direction is in the range of 12-17 GPa. [9] Group stiffness of selected tree species is shown in Table 3.

Table 3: Group stiffness of selected tree species [9]

Group	**Stiffness** [MPa]	**Examples**
soft	<40	spruce, fir, pine, poplar, linden
medium stiff	≥40	ash, elm, oak, walnut
stiff	≥80	hornbeam, acacia, yew

1.2.5 Consequences of changes in moisture content of wood

Properties of wood greatly vary with moisture changes in the range of the saturation point of the cell walls to 0 %. The most important changes from the perspective of all forms of mechanical processing and use of finished products are shape changes, such as: shrinkage, swelling, warping, cracking, stagnation and hardening of wood. Closer look is fixed on shrinkage and swelling.

- **Shrinking**

Shrinking of the wood is a process which reduces the size and volume of the timber during evaporation of bound water (from moisture decrease below the fiber saturation point). During the evaporation of free water, the dimensions and volume of the timber do not change. Shrinking is divided into two categories: linear and volumetric. **Linear shrinkage** is characterized by reducing dimensions in one of the three basic directions - tangential, radial, and longitudinal. On the other hand during the **volume shrinkage,** the volume will decrease. For scientific purposes and in practice total shrinkage (linear and volume) is important, corresponding to the change of humidity above the fiber saturation point to 0 %. Values of total shrinkage are very different in fundamental ways and vary even for individual trees species. The most

significant is the shrinkage in the tangential direction (3–6 %), whilst in the longitudinal direction it is the least significant (it is almost negligible, averaging about 0.3 %) – see Figure 15. The volumetric shrinkage is about 12-15 %. The values relate to the most widely used species. [9, 15]

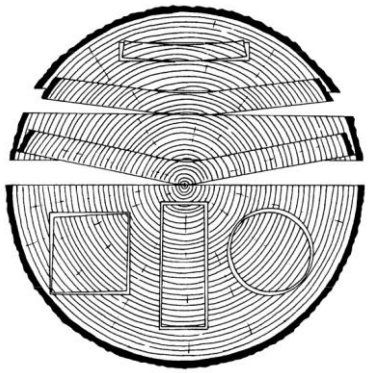

Figure 15: Shrinkage in cross-grain direction [9]

The explanation for the difference in shrinkage behavior for radial and tangential direction of wood is based on divergence in three anatomic related structures, such as arrangement of early and late wood; orientation of rays and the position of bordered pits.

Practical implementation of sorption isotherm to shrinkage of typical wood is shown on Figure 16.

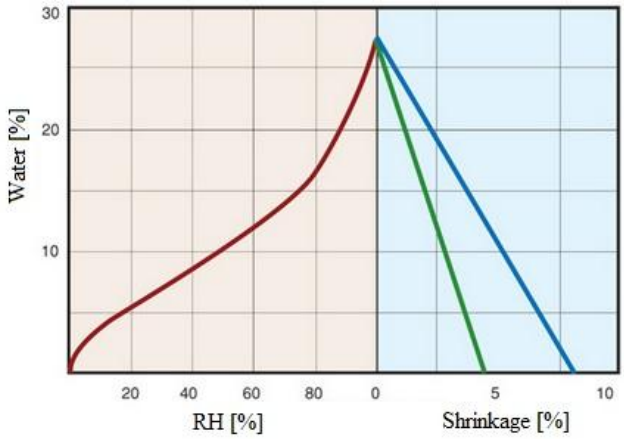

Figure 16: Moisture content versus RH and shrinkage versus MC of a typical wood [14]

- **Swelling**

Swelling of wood is the opposite of shrinkage. It occurs when the wood is moistened (receiving water that is stored in the cell membranes) and consists of increasing the dimensions of the wood, which means the ambient air humidity is greater than the moisture content of wood. The storyline follows the same regularities as shrinkage. Runs from 0 % of water to the fibre saturation limit of the cell walls. Linear values swelling in three basic directions are almost the same as the linear shrinkage. [9, 15]

1.3 Wood impregnation methods

To protect wood from biological degradation, chemical preservatives are applied to the wood by non-pressure, pressure or special treatment methods (such as acetylation, heat treatment, furfurylisation, injection or bandaging).

The reason of adding wood preservatives is to obtain long-term effectiveness for wood products, thus sequestering carbon. Penetration and retention of a chemical will depend on the wood species and the amount of heartwood and sapwood. Heartwood is generally more difficult to treat respective impregnate.

The degree of protection of a particular preservative and treatment process depends on 4 basic requirements: toxicity, permanence, retention, and depth of penetration into the wood. Toxicity refers to how effective a chemical is against a biological organism, such as decay, fungi, insects and marine borers. Permanence refers to the resistance of the preservative to leaching, volatilization, and breakdown. Retention specifies the amount of preservative that must be impregnated into a specific volume of wood to meet standards and ensure that the product will be effective against numerous biological agents. Figure 17 shows penetration of chemicals in:

a) surface treatment, where the liquid solvent stays at the surface of the impregnated element (advantage is that already existing structures are possible);
b) pressure treatment are the chemicals transported by pressure about 12-13 bar deeper into the wood structure, only the heartwood is not fully impregnated;
c) vacuum treatment has a higher concentration of chemicals on the surface and may be used for larger specimens than for pressure treatments. [9, 19]

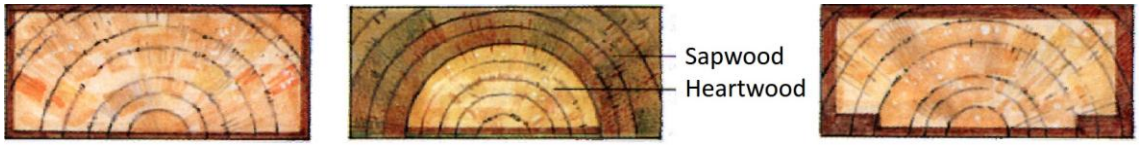

Figure 17: Penetration of chemicals in a) surface treatment; b) pressure treatment; c) vacuum treatment [author with 9]

Wood preservatives can be divided into two general classes: Oil-type, such as creostate and petroleum solutions of pentachlorphenol, and waterborne salts that are applied a water solutions, such as chemicals that are used for pressure treatment CCA, CC, CCB, CCP (CC = chromated copper, A = arsenate, B = borate, P = phosphorate), corper and boron. For vacuum impregnation Pentachlorophenol is often used. The effectiveness of each

penetration can vary greatly depending on its chemical composition, retention, depth of penetration, and ultimately the exposure conditions of the final product.

Chemical preservatives are used only where it is unavoidable to protect wood, and which realistically feasible ways of physical or structural protection are less effective or cannot be used. [9, 19]

Method of application of the protective agent is chosen according to CSN 49 0615 and depends on the risk class, type of protective agent, moisture content and type of wood. When choosing the method of application it is necessary to give priority to the one that least impacts the environment. [20]

- Risk class 1: Method of application preservative is arbitrary if there is no limitation in the test certificate for the device (vacuum-pressure impregnation, vacuum impregnation, impregnation coating, spraying, immersing and soaking etc.);
- Risk class 2: Method of application of the protective composition is the same as in Risk class 1;
- Risk class 3: Method of application of protective agent will depend on the range of timber (logs, sawn wood, glued elements, etc.). In most cases, it is recommended to use a vacuum-pressure impregnation or long-term immersing (for several days);
  To protect the wooden elements, which are freely exposed to the weather impregnation may be used, such as coating and spraying, if these elements are regularly checked and the cracks are additionally treated, or when these components are treated with topcoat (regularly refreshed) protecting wood surfaces against cracking.
- Risk class 4: Only vacuum and over pressurized impregnation methods are applicable

1.3.1 Non-pressure (surface) technology

Traditionally, wood impregnation is carried out using liquid solvents for transport of biocides into wood. Typical surface technologies can be divided according to the application of fungicides, such as coating and spraying or immersing and soaking.

Using the liquid impregnations has some unwanted technical and environmental issues, such as avoiding exposure of workers and the environment to treatment solutions. Many low permeability wood species provide a substantial resistance to the flow of fluids which makes it difficult or impossible to impregnate such species with liquid solvents [2]. After liquid impregnation the wood is wet and will need additional time to dry.

1.3.2 Pressure technology

The use of supercritical carbon dioxide as a solvent provides a potential solution to the limitations of the liquid impregnation processes and has proven capable of significantly reducing problems related to the environment during wood impregnation. Because of its low viscosity and surface tension, supercritical CO_2 can penetrate the refractory species otherwise considered non-treatable. Furthermore, since CO_2 at atmospheric pressures is a gas at temperatures above -78.5 °C, below this temperature it exists as a solid, the treated wood is dry and can be used immediately after impregnation. The exposure of workers to treatment solutions is greatly reduced, if not eliminated, since the treatment solution only exists at pressures above the critical point of CO_2, i.e. in closed loop systems. Similarly, the exposure of the environment to run off of excess treatment fluid is eliminated because as already mentioned, the wood is dry after treatment.

Like other gases CO_2 enters a supercritical state beyond a certain point (31 °C, 72.8 bar). In this state, the carbon dioxide has the ability to dissolve the fungicide and due to the low surface tension and gas like diffusivity, it has the capacity to penetrate the micro capillary network in wood. These properties combined with the capacity to act as a strong solvent, enables the supercritical CO_2 to penetrate the entire wood matrix. The process is schematically shown in Figure 18. [4, 21]

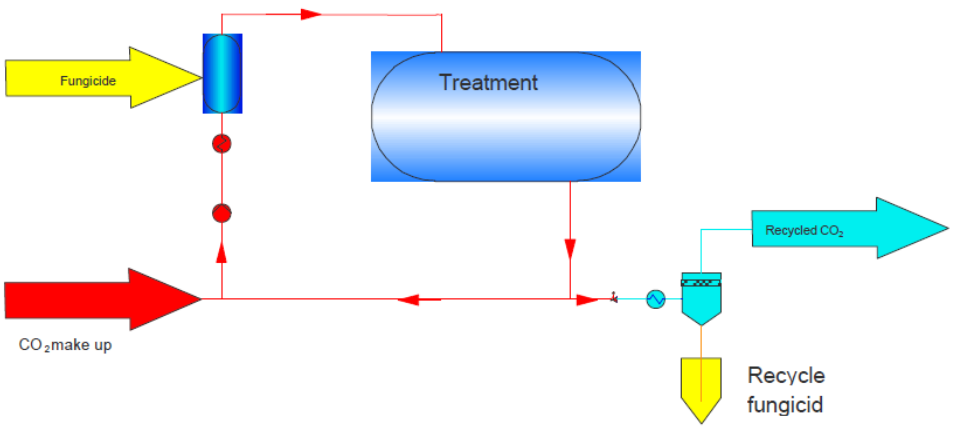

Figure 18: Schematic visualization of the supercritical wood treatment process [4]

The fungicides penetrate both the sapwood and heartwood, and distribution can be obtained in both the longitudinal and also in the radial direction of the wood. An example of a Scanning Electron Microscopy photo along with an elemental analysis mapping of the fungicide distribution in the cross section is shown in Figure 19. [4, 21]

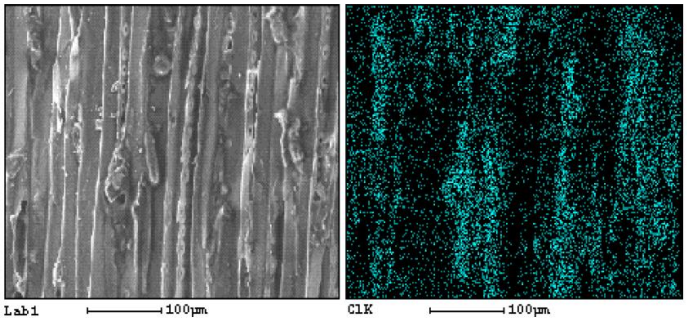

Figure 19: SEM photo (left) and fungicide mapping (right) of a wood cross section [4]

The pressure impregnation process is illustrated in Figure 20 and can be divided into three steps: a pressurization phase (A-B), an impregnation phase (B-C) and a depressurization phase (C-D). [2, 4, 9, 21]

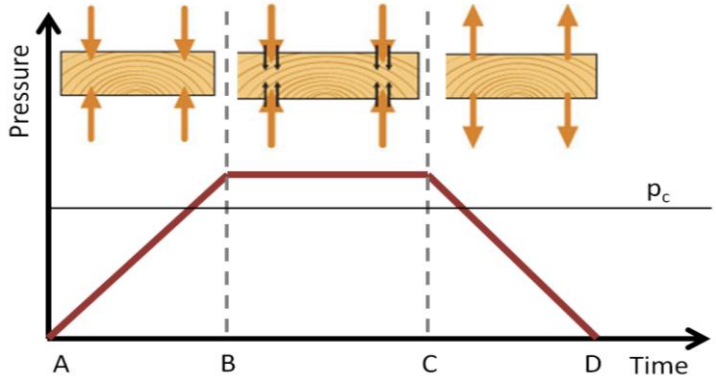

Figure 20: Main steps in the supercritical wood impregnation cycle [2, 4, 21]

A-B: The dry wood is impregnated in packages as they are received from sawmill. The wood is forwarded to the impregnation vessel. CO_2 and wood preservatives are added to the vessel and the pressure is increased. After pressurization, the treatment vessel achieves a "critical" pressure of approx. 150 bar and a temperature of 40-60 °C and the CO_2 - now supercritical - carries the wood preservatives into the wood.

B-C: The wood is impregnated to the core and remains dry for the entire duration of the process.

C-D: The pressure returns to normal and the process is completed. The wood, still as dry as before the process began, is now impregnated to the core and can be used immediately. Excess CO_2 and wood preservatives are collected and recycled. [4, 21]

1.3.3 Vacuum and vacuum-pressurized technology

Impregnation technologies use different pressures inside and outside the timber. A combination of under-pressure in the timber, and over-pressure in

the air and temperature etc. will achieve the maximum penetration of the wood preservative in a relatively short time. Receiving and penetration depth of preservatives are defined in standards, ranging from 3 mm to several centimetres.

This method depends upon MC and species type and is used to impregnate wood with moisture content to 30-40 %. For wooden materials with moisture content from 60 to 100 % cyclic and pulsatile waveforms of vacuum-pressure processes are used. [24]

1.4 Heat transfer in building materials

The heat transmission in the building materials and structures depends on the materials and geometry of the structure and can take place as radiation, convection and conduction.

1.4.1 Thermal bridge and thermal bonds

The thermal bridge is a place in the structure, which leads to higher heat flows due to 2- or 3- dimensional effects. The locally increased heat flow is reflected by a lower surface temperature of the structure from the interior side.

Thermal bridges can be:

- Structural – connections of two structures, e.g. foundation and wall, wall and window, pipe penetrations;
- Geometric - geometric design changes, e.g. a corner wall, wall endings;
- Systematic - many places with poorer thermal properties regularly repeated, e.g. clips, rafters between insulation in roof;
- Convective - there is a transfer of energy flow through the insulation, e.g. leaks in the roof structure. [31]

The influence of thermal bridges must be taken into account when calculating the heat transfer coefficient (U-value) and, together with the thermal constraints when calculating heat losses of the building.

1.4.2 Heat transfer coefficient

The construction of heated buildings in areas with designed relative humidity $\varphi_i \leq 60$ % of indoor air have to meet the requirement for heat transfer coefficient U-value [32]:

$$U \leq U_N \qquad [\mathrm{W \cdot m^{-2} \cdot K^{-1}}] \qquad (1.17)$$

where U_N required heat transfer coefficient [$\mathrm{W \cdot m^{-2} \cdot K^{-1}}$].

For the construction of heated buildings with a relative humidity of indoor air $\varphi_i \geq 60$ % the required heat transfer coefficient value U_N is set as the lower value of relations [33] and the conditions for increased humidity environments:

$$U_{\omega,N} = \frac{0.6 \cdot (\theta_{ai} - \theta_{\omega})}{R_{si} \cdot (\theta_{ai} - \theta_e)} \qquad [\mathrm{W \cdot m^{-2} \cdot K^{-1}}] \qquad (1.18)$$

where θ_{ω} dew point according to CSN 730540-3 [°C];
R_{si} heat transfer resistance [$\mathrm{m^2 \cdot K \cdot W^{-1}}$].

For opaque structures is R_{si} = 0.25 $\mathrm{m^2 \cdot K \cdot W^{-1}}$ and for transparent components R_{si} = 0.13 $\mathrm{m^2 \cdot K \cdot W^{-1}}$.

If the condition of equation (1.17) cannot be fulfilled, then it is necessary to ensure an impeccable function of the structures during the surface condensation and to avoid adverse effects of the condensate on connected construction, respectively ensuring a safe removal of the condensate for maintaining required value of heat transfer coefficient U_N.

U-value of insulated timber structures depends on the addition of insulation thickness and its thermal conductivity (λ_{iso}), and also of the percentage of wood. Wood insulates fairly well as the two-dimensional (2D) effects at the transition between timber and insulation is therefore small. U-values of the composite wood constructions can be determined with a good accuracy by use of λ-value which is weighted by the ratio of timber and insulation in the entire thickness of the skeleton and includes the wooden frame (Andersen 2008). Expression of the total thermal conductivity of the composite wooden wall for one section can be expressed as [34]:

$$\lambda_{wall} = \frac{L_{wood} \cdot \lambda_{wood} + (L_{wall} - L_{wood}) \cdot \lambda_{iso}}{L_{wall}} \qquad [\mathrm{W \cdot m^{-1} \cdot K^{-1}}] \qquad (1.19)$$

where L_{wood} length of the wood used in the wall [m];
λ_{wood} thermal conductivity of used wood [$\mathrm{W \cdot m^{-1} \cdot K^{-1}}$];
L_{wall} length of the composite wall for one section [m];
λ_{ISO} thermal conductivity of insulation [$\mathrm{W \cdot m^{-1} \cdot K^{-1}}$].

Heat heterogeneity of mutual contact of two or more kinds of structures is called a thermal bond. It is a special case of thermal bridge, which is different because it applies to the whole building envelope, perceived as an envelope structure system with mutual thermal bonds.

The thermal bond is classified as an interface between two or more structures (e.g. structural connection of opaque envelope with foundation or

with non-bearing wall etc.), where the heat flow in the structure is significantly changed by their interactions. The effect of thermal bonds is not included in the calculation or measurement of the heat resistance R or heat transfer coefficient U of each structure. It is considered when calculating the specific heat transmission losses "HT" and specific heat demand "ev", etc. In the terms of evaluating heterogeneity of the structure, the thermal bond can be classified as **linear** - with matching cuts in one direction or **point** – non-identical cuts in any direction. [35]

From the prevention of surface condensation point of view and mould growth it is necessary for thermal bridges and thermal bonds to meet the requirement to provide the lowest internal surface temperature.

1.4.3 Linear and point thermal transmittance

Linear thermal transmittance is a quantity that characterizes the thermal properties of two-dimensional thermal bridges and bonds. It expresses the amount of heat in Watts, which extends at a unit temperature difference per unit length of the thermal bridge. It is, therefore, something like the equivalent of the heat transfer coefficient of flat structures. [32]

The linear thermal transmittance "ψ" and point thermal transmittance "χ" of thermal bonds between structures must meet the condition:

$$\psi \le \psi_N \qquad [\mathrm{W \cdot m^{-1} \cdot K^{-1}}] \qquad (1.20)$$

$$\chi \le \chi_N \qquad [\mathrm{W \cdot K^{-1}}] \qquad (1.21)$$

where ψ_N required value of linear thermal transmittance [$\mathrm{W \cdot m^{-1} \cdot K^{-1}}$];
χ_N required value of point thermal transmittance [$\mathrm{W \cdot K^{-1}}$].

Required and recommended standard values for linear and point thermal transmittance are mentioned in [32].

For the experimental numerical calculation described in Chapter 9.1 and in order to evaluate the thermal bridge effect correctly it was necessary to use numerical transient calculations and to include a large volume of the soil underlying the building model – 20 m x 20 m [36]. The thermal transmittance of the wall/floor connection "$\psi_{connection}$" was the calculated as:

$$\psi_{connection} = \frac{q_{total} - q_{wall} - q_{floor}}{\Delta T} \qquad [\mathrm{W \cdot m^{-1} \cdot K^{-1}}] \qquad (1.22)$$

where q_{total} 2D heat flow through section for transient mean external temperatures (Heat2) [$\mathrm{W \cdot m^{-1}}$];

q_{wall} 1D heat flow through the adjacent wall segments for transient mean external temperatures [W·m^{-1}];
q_{floor} 1D heat flow through the floor slab [W·m^{-1}];
ΔT mean temperature difference between inside and outside air for heating season [K], see Equation (9.2).

$$q_{wall/\,floor} = U_{wall/\,floor} \cdot L_{wall/\,floor} \cdot \Delta T \quad [\mathrm{W \cdot m^{-1}}] \tag{1.23}$$

where $U_{wall/floor}$ thermal transmittance of the wall or floor [W·m^{-2}·K^{-1}];
$L_{wall/floor}$ length of the modelled wall (floor) [m];
ΔT temperature difference between inside and outside air pertaining to a mean external temperatures in every month [K], see Equation (9.2).

1.4.4 Minimal surface temperature of the construction

In winter, buildings in areas with designed relative humidity $\varphi_i \leq 60$ % of indoor air have to meet the requirement for minimal surface temperature according to the following relationship. [32] Meeting this, the requirement of the relation mitigates the risk of mould growth in the building:

$$f_{Rsi} \geq f_{Rsi,N} \quad [-] \tag{1.24}$$

where $f_{Rsi,N}$ required value of minimal surface temperature on the internal side [-], which is settled from:

$$f_{Rsi,N} = f_{Rsi,cr} \quad [-] \tag{1.25}$$

where $f_{Rsi,cr}$ critical factor of minimal surface temperature on the internal side [-].

Wherein the internal air with designed relative humidity φ reached critical inner surface moisture on the internal surface $\varphi_{si,cr}$ and is determined from the relationship:

$$f_{Rsi,N} = f_{Rsi,cr} = 1 - \frac{237.3 + 2.1 \cdot \theta_{ai}}{\theta_{ai} - \theta_{ex}} \cdot \frac{1}{1.1 - 17.269 / \ln(\varphi_{i,r} / \varphi_{si,cr})} \quad [-] \tag{1.26}$$

where θ_{ai} designed temperature of indoor air [°C];
θ_{ex} designed temperature of environment connected to the external side of construction in winter phase [°C] (as a designed temperature of soil θ_{gr} for construction connected to soil);
$\varphi_{i,r}$ relative humidity of indoor [%].

The obligation to fulfil the minimal temperature factor $f_{Rsi,cr}$ in the construction of the inner surface of the object is regulated through legislation of the Czech Republic. The respective values of the minimal temperature factor of surface and appropriative temperature are mentioned in [32].

1.5 Moisture transfer in building materials

There are two transport forms of moisture in building materials: vapour and liquid transfer. These transfers are driven by water vapour pressure or capillary pressure gradients. The vapour transfer can be divided into convection, diffusion and advection. For the purposes of this thesis the focus will be mostly on water vapour diffusion within the building materials. The liquid capillary transfer (sorption) is shortly mentioned in Chapter 1.2.1.

1.5.1 Water vapour diffusion

The water vapour diffusion occurs due to the difference of partial pressure of water vapour in structures, soils and in the air between the external environment and inside of the building. Gas or vapour diffuses any porous material, when the pores (spaces intermolecular) are greater than the mean free path of thermal transfer of gas or vapour molecules. The mean free path of molecules of H_2O is $2.78 \cdot 10^{-10}$ m. In building construction materials micro and macro capillaries are found. [11]

With a macro capillary of dimension $d >> 10^{-7}$ m capillary condensation does not occur, because free path of molecules of water vapour is smaller than the pore diameter of the substance. The water vapour moves by diffusion laws.

In micro capillary dimensions $d << 10^{-7}$ m capillary condensation occurs, because free path of molecules of water vapour is equal or larger than the pore diameter of the substance and movement of water vapour occurs by law effusion. [11]

The transport mechanism can be seen in Figure 21. **Diffusing water vapour** moves from a place of higher partial pressure (higher water concentration, the higher temperature) to the point of lower partial pressure. With low outdoor temperatures (winter), the main direction of diffusion is from the inside out, but with high outside temperatures (summer), the reverse diffusion occurs (outside to inside).

Individual absorbed water molecules are immobile due to the high adhesion to the pore walls. With the formation of a absorb films the liquid water becomes increasingly more flexible. There is a transfer from the region of higher film thickness (higher RH) for lower film thickness range (lower humidity) instead. This process is also called **surface diffusion**. The surface

diffusion is already effective in cellulose at 30 % RH and at sandstones at about 60 % RH. Effective means that the water transport is by surface diffusion of a similar magnitude, such as the water vapour diffusion.

Because the pores are not completely filled in this area, surface diffusion always occurs simultaneously to vapour diffusion.

In the right side figure the surface diffusion takes place counter-vapour diffusion current. Thus, it is possible that moisture which has passed through vapour diffusion in winter inside the wall structure in liquid form back towards the space is transported back. Thus, the maximum occurring moisture is reduced, for example, in the old plaster level. [57]

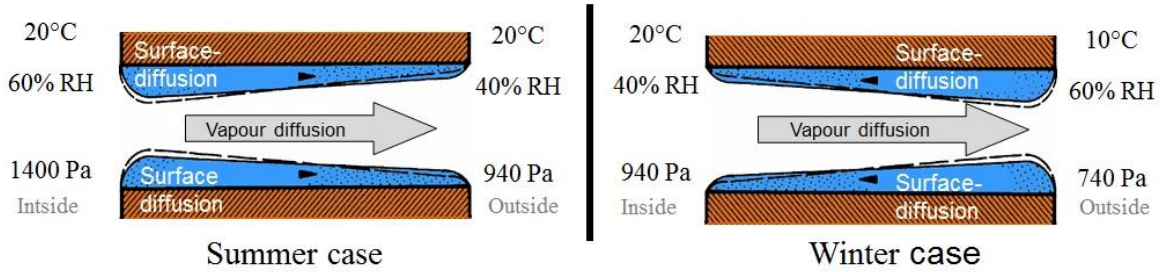

Figure 21: Surface diffusion: Water transport in thin films or layers of molecules in the direction of lower water concentrations [author with 57]

Under certain temperature and pressure conditions, water vapour in a substance or structure condensates. Water vapour cannot concentrate freely in the air, but only up to a partial pressure of saturated water vapour (i.e. exponentially decreases thermodynamic temperature).

The highest risk of water vapour concentration occurs in cold weather, when the peripheral wall carries a large temperature difference between the interior of the house and the outside environment, and the inside of the high partial pressure of water vapour outside is very low. Any condensation which accumulates mostly in insulation or insulating walls is then always unwelcome. Only small amounts of condensate can be tolerated, which is in the spring and summer safely removed.

This condensation of water vapour is more dangerous in more layered construction, such as a wooden wall with a relatively vapour tight layer on the external side, because the condensate does not have the possibility to evaporate and so it may lead to the degradation of the construction in the middle of the wall and have fatal consequences to the building. For homogeneous one layer construction, the condensation effect is practically negligible. [37]

There are two standard technical solutions of more wooden layered construction:

a) “Diffusion closed”, using vapour- and air- retarding foils positioned on the interior side to protect the exterior walls by penetrating of diffusion or convection of the vapour (Case study 1 in Chapter 4.1);
b) “Diffusion opened”, i.e. "breathing" design criteria designed so that any condensation to occur only in extreme conditions (frost), and only a very small extent (Case study 2 in Chapter 4.2).

Description of water vapour diffusion flow rate through the structure is analogous to the description of the heat flow by conduction. The density of the water vapour diffusion flow describes Fick’s law (analogous to Fourier law for heat flux density by conduction) in the general shape (in the x-direction):

$$g(x) = -\delta \frac{dp(x)}{dx} \qquad [\mathrm{kg \cdot m^{-2} \cdot s^{-1}}] \qquad (1.27)$$

where δ water vapour permeability of material, respectively its pores system [$\mathrm{kg \cdot m^{-1} \cdot s^{-1} \cdot Pa^{-1}}$];
$dp(x)/dx$ gradient of partial water vapour pressure in the air in the construction in the x-direction [$\mathrm{Pa \cdot m^{-1}}$].

For the density of the water vapour flow rate “g” of one homogenous layer from homogeneous material in a steady state can be then stated:

$$g = \delta \cdot \frac{\Delta p}{d} = \delta \cdot \frac{p_1 - p_2}{d} \qquad [\mathrm{kg \cdot m^{-2} \cdot s^{-1}}] \qquad (1.28)$$

where δ water vapour permeability of material, respectively its pores system [$\mathrm{kg \cdot m^{-1} \cdot s^{-1} \cdot Pa^{-1}}$];
p_1, p_2 partial water vapour pressures of air of outside and inside surface of the construction [Pa];
d thickness of the material [m].

The water vapour resistance permeability “δ” is defined by equation:

$$\delta = \frac{\delta_a}{\mu} \qquad [\mathrm{kg \cdot m^{-1} \cdot s^{-1} \cdot Pa^{-1}}] \qquad (1.29)$$

where δ_a water vapour permeability of stagnant air [$\mathrm{kg \cdot m^{-1} \cdot s^{-1} \cdot Pa^{-1}}$], for general conditions $\delta_a = 1.9 \cdot 10^{-10}$ $\mathrm{kg \cdot m^{-1} \cdot s^{-1} \cdot Pa^{-1}}$;
μ water vapour resistance factor [-].

The water vapour permeability of air and the material may be assumed to vary equally with the barometric pressure. The factor μ can therefore be considered independent of barometric pressure. When calculation the density of water vapour flow rate "g" will be for homogeneous material calculated as:

$$g = \frac{\delta_a}{\mu} \cdot \frac{p_i - p_e}{d} \qquad [\mathrm{kg \cdot m^{-2} \cdot s^{-1}}] \qquad (1.30)$$

To complete the analogy with heat conduction can be to Equation (1.30) introduced a diffusion resistance in the form:

$$Z_p = \frac{\mu \cdot d}{\delta_a} \qquad [\mathrm{m \cdot s^{-1}}] \qquad (1.31)$$

And then the density of water vapour flow rate "g" will be written as:

$$g = \frac{p_i - p_e}{Z_p} \qquad [\mathrm{kg \cdot m^{-2} \cdot s^{-1}}] \qquad (1.32)$$

where
- δ_a water vapour permeability of stagnant air [$\mathrm{kg \cdot m^{-1} \cdot s^{-1} \cdot Pa^{-1}}$], for general conditions $\delta_a = 1.9 \cdot 10^{-10}$ $\mathrm{kg \cdot m^{-1} \cdot s^{-1} \cdot Pa^{-1}}$;
- μ water vapour resistance factor [-];
- p_i partial water vapour pressures of inside air [Pa];
- p_e partial water vapour pressures of outside air [Pa];
- d thickness of the material [m].

Equation (1.32) also applies to composition structures in the steady state, when Z_p represents the overall diffusion resistance of the material layers (analogous to the overall thermal resistance $R_{si}+R+R_{se}$).

The dimensionless water vapour resistance factor μ [-] is the material characteristic specified by manufacturers. It says how many times is the water vapour permeability "δ" of material smaller than the water vapour permeability of stagnant air "δ_a". Water vapour resistance factors and diffusion resistance layer thickness of 0.1 m for some materials are in Table 4.

Table 4: Water vapour resistance factor and diffusion for some materials [37]

Material	**Water vapour resistance factor**	**Diffusion resistance of the layer**
	μ [-]	$Z_p \cdot 10^{-9}$ [m·s^{-1}]
Wood - flow perpendicular to grain	157	83
Wood - flow parallel to the grain	4.5	2.4
EPS	30	16
Fiber insulation	2	1.1
Concrete	20	11

The water vapour permeability values can be changed to **diffusion coefficients** "D" by equation by Siau [44].

$$D = \frac{\delta \cdot p_{sat}}{G_w \cdot \rho_w} \frac{\partial H_{Rh}}{\partial MC} \qquad [\mathrm{m \cdot s^{-2}}] \qquad (1.33)$$

where
- ∂H_{Rh} difference in relative humidity across the specimen;
- ∂MC difference in moisture content across the specimen;
- δ water vapour resistance permeability [$\mathrm{kg \cdot m^{-1} \cdot s^{-1} \cdot Pa^{-1}}$];
- P_{sat} saturated vapour pressure 2584.1634 Pa. Equation (7.6).

The **water vapour diffusion-equivalent air layer thickness** "s_d" is given by either:

$$s_d = \mu \cdot d \qquad [\mathrm{m}] \qquad (1.34a)$$

$$s_d = \delta_a \cdot Z \qquad [\mathrm{m}] \qquad (1.34b)$$

Since the definition of the s_d-value contains the thickness Δd of the layer, the s_d-value is a property of the given layer, not of the material itself. Two layers made from the same material but with different thicknesses will have different s_d-values, but in both cases the material will have the same μ-value. In particular, the s_d-value is used to characterize vapour retarders ($s_d \geq 10$ m), vapour barriers ($s_d \geq 1000$ m) and surface coatings (mineral paints: $s_d \sim 0.04$ m, oil paints: $s_d = 1.0$ to 2.6 m), where it can be difficult to determine their thickness properly. [59]

Systematically repeating non-homogeneous elements in the material layer can be introduced into the calculation by using the equivalent water vapour resistance permeability δ_{ekv} (analogy to λ_{ekv}), respective of its equivalent water vapour resistance factor μ_{ekv}. [38, 39]

The water vapour resistance permeability is settled as a weighted average of water vapour resistance permeability through the surface representation of the various materials in a characteristic arc design:

$$\delta_{ekv} = \frac{A_1 \cdot \delta_1 + A_2 \cdot \delta_2}{A_1 + A_2} \qquad [\mathrm{kg \cdot m^{-2} \cdot s^{-1}\ Pa^{-1}}] \qquad (1.35)$$

If we add Equation (1.29) to Equation (1.35), we get the equivalent resistance factor of non-homogeneous material layers as:

$$\mu_{ekv} = \frac{A_1 + A_2}{\frac{A_1}{\mu_1} + \frac{A_2}{\mu_2}}, \text{ resp. } \mu_{ekv} = \frac{\sum_i A_i}{\sum_i \frac{A_i}{\mu_i}} \qquad [-] \qquad (1.36)$$

For foil vapour barrier we enter their properties after incorporation into the construction, i.e. we reduce the nominal factor of diffusion resistance of the material to 10× to 100× by the realization quality. Substantial quality joints are e.g. overlaps, adhesive sealants and taped, but also the treatment of penetrations.

Previous calculations by Equations (1.36) can be used to calculate the equivalent resistance factor of perforated OSB. One possibility is drilling boards in regular grids. [38, 39]

The moisture transport properties for isothermal water vapour transport are usually determined with steady-state cup measurements. The principle of the measurement, performed in detail and described in Chapter 7.3, is to expose a sample with a given thickness d to a water vapour pressure gradient Δp. This gradient is often provided by a saturated salt solution in a cup with a known RH and a humidity controlled climate chamber outside the cup. [40]

1.5.2 Condensation

Condensation means the precipitation of water vapour on the surface or between some layers in the body. Air at given temperature can always hold only a certain amount of vapour. If the partial pressure of water vapour reaches a certain maximum value of $P_{v,sat}$, the air is saturated with water vapour and so reaches the dew point. Table 5 mentions maximum amount of water in the air for certain air temperatures.

Table 5: Dew point: the air fully saturated by water vapour at certain temperature [11]

Air temperature	[°C]	-20	-10	0	10	20	30
Max. amount of water vapour in the air	[g·m^{-3}]	0.9	2.2	4.8	9.4	17.3	30.3

If the saturated air is fed by more water vapour, then the condensation is formed, respectively the precipitation of water vapour in the water occurs. This can be performed as fog, water droplets or hoarfrost. In all cases, the phenomena is called surface condensation of water vapour. It can then be stated that condensation occurs when the surface temperature is lower than the dew point. The ratio of the partial water vapour pressure P_v and the partial pressure of saturated water vapour $P_{v,sat}$ is referred to as relative humidity:

$$\varphi = \left(\frac{p_v}{p_{v,sat}} \right) \cdot 100 \qquad [\%] \qquad (1.37)$$

where P_v partial water vapour pressure [Pa];
$P_{v,sat}$ partial pressure of saturated water vapour [Pa].

The water content in the air is expressed either by relative humidity [%] or by absolute humidity [$g \cdot m^{-3}$]. The percentage of water vapour saturation of the air is a function of temperature (Figure 22). Relative humidity of the air is therefore for particular value $P_{v,sat}$ (with the same tension) at different air temperature different (

Table 6). It is visible that colder air can absorb less moisture.

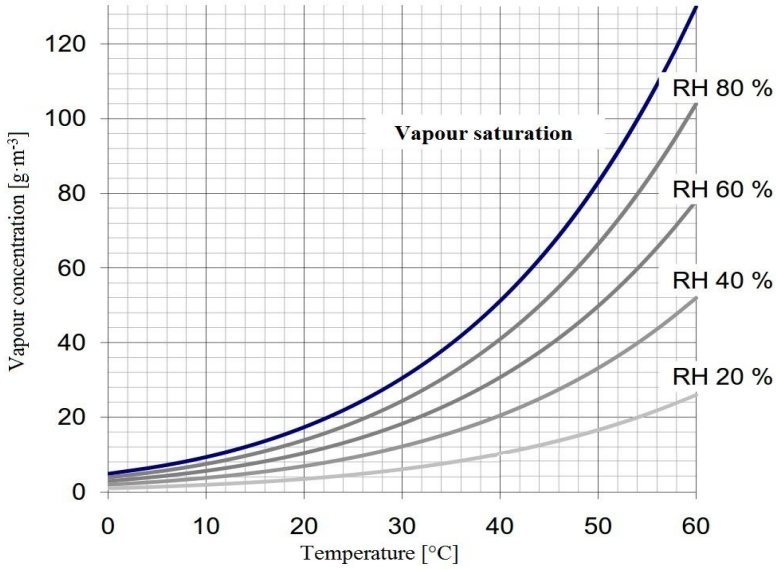

Figure 22: Vapour concentration in the air for certain temperatures [author with 30]

Table 6: Table amount of the water vapour in the air at different RH [author with 11]

RH of air	**Amount of water vapour in air [$g \cdot m^{-3}$] for air temperatures [°C]**					
φ [%]	**-20**	**-10**	**0**	**10**	**20**	**30**
30	0.3	0.7	1.4	2.8	5.2	9
40	0.35	0.9	1.9	3.8	6.9	12
50	0.45	1.1	2.4	4.7	8.7	15
60	0.54	1.3	2.9	5.6	10	18
70	0.63	1.5	3.4	6.6	12	21

The capillary condensation takes place in the pores, whose radius is greater than $0.5 \cdot 10^{-6}$ mm, since the radius of a water molecule is 10^{-7} mm. In the smaller pores no water vapour diffusion occurs. For the curved surfaces with a radius less than 10^{-4} mm the condensation occurs much sooner than the surface condensation is formed. For construction practice, this means that for the same humidity, temperature conditions and with the same pore volume two of the same substances will differ from each other by internal moisture content, if they have pores of different radius.

1.5.3 Standard requirements

Moisture transfer within the construction is defined by a technical standard CSN 730540. For the construction in which the condensed water vapour inside the structure in $kg \cdot m^{-2} \cdot year^{-1}$, could compromise its required function, the condensation must not even happen ($M_{c,a} = 0$). Threats to the desired function usually significantly shortens the expected life structure, such as:

- lowering of the internal surface temperature of the structure leading to formation of mould;
- the volume change and a significant increase in weight of the structure outside of the reserve static calculations;
- increase the weight of the material to a level of humidity causes its degradation.

The conditions for the application of wood and/or wood-based materials in building construction must be respected. Whenever the conditions for the use of standardized mass equilibrium moisture content of wood or wood-based material exceed the value of 18 %, the desired function of the structure is compromised. [39]

In building construction with allowed limited condensation of water vapour inside the construction, there may not be in annual balance condensation and evaporation of water vapour left over any amount of condensed water vapour, which would permanently increase the moisture of the structure. The annual quantity of condensed water vapour within the structure in $kg \cdot m^{-2} \cdot year^{-1}$ must be lower than the annual amount of water vapour inside the structure in $kg \cdot m^{-2} \cdot year^{-1}$, written also as $M_{c,a} < M_{ev,a}$.

The amount of condensed water has to meet the requirement:

- in one layered roof and peripheral walls made of materials of high diffusion resistance in the exterior side $M_{c,a} \leq 0.1\ kg \cdot m^{-2} \cdot year^{-1}$;
- in other construction one from the lower values $M_{c,a} \leq 0.5\ kg \cdot m^{-2} \cdot year^{-1}$ or 0.5 % of area weight of material.

The wood and/or wood-based materials implemented in the structures must be designed with suitable structural measures to protect the organic materials from the adverse effects of moisture and a long-lasting protection of these materials at least for the 2nd class of risk. [39]

1.6 Biological degradation models and wood durability

The development of mould and decay on wood and the influence of environmental factors on wood durability has been studied e.g. by Viitanen & Co (1996) [60], Carll & Co (1999) [64], Sedlbauer (2001) [61], Leicester & Co (2003) [62], Brischke (2008) [63] and some of this work has been formulated as an empirical model for durability.

In this dissertation the main focus was on the biological degradation model on wood, experimentally studied and formulated by Viitanen & co.

The found relationship between the wood mass loss due to wood decay fungi and the temperature and relative humidity conditions the studied wood samples were exposed to, was updated by Viitanen and his team [25] to an empirical numerical model for wood decay development.

The model is based on laboratory experiments on pine sapwood and can be used for post-processing hygrothermal building physics simulations. Furthermore, the model „*is applied to the ERA-40 reanalysis data, based on six-hour weather observations in Europe, to estimate wood decay in different parts of Europe*," Viitanen in [25]. This method enables use of measured or modelled moisture or humidity levels of the material environment (microclimate) over a long period to estimate the decay risk.

There are some important factors for development of organisms in a porous organic material, such as temperature, availability of nutrients, time and most important factor water activity.

The other effects, such as coating and treatment of modified wood were not included in the experimental data. A future need for modification of the model for other materials and treatment was identified and should be done by studying the decay resistance and experimentally finding the corresponding relationships. [25]

For wood products and other species of wood, the critical factors may be different from those of untreated sapwood. The resistance of heartwood against decay is higher than that of sapwood as the coatings protect the wood against water, high humidity and micro-organisms.

For mould development, the ambient critical RH level of the microclimate is between 80–95 % - as shown in Figure 23 (left). [25]

For most decay fungi development, the optimum wood moisture condition is around 25 to 30 weight-% (Viitanen 1996). This means that for decay to develop in untreated pine sapwood, the ambient relative humidity of air (microclimate humidity conditions), should stay above RH 95-99 % for weeks

or even months, depending on the temperature, as shown in Figure 23 (right). [25, 27]

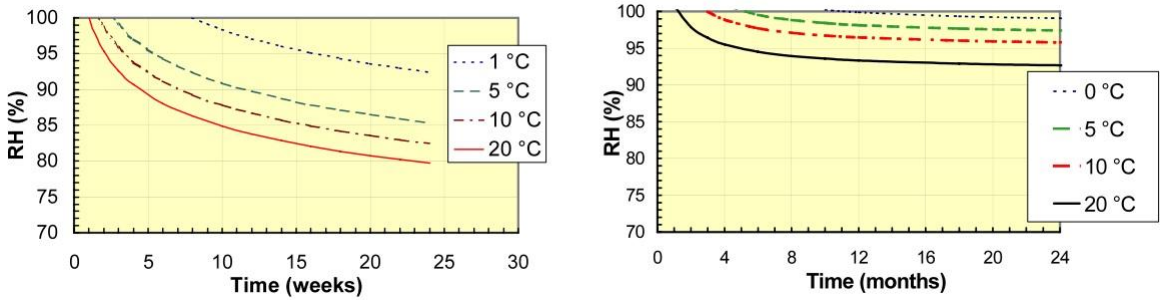

Figure 23: RH of the ambient air and temperature isopleths as a function of time for start of mould growth (left) and of decay development (right) in untreated pine sapwood, according to Viitanen (1997) [author with 25]

1.6.1 Mould development method - mould growth index – VTT model

The mould index (Hukka and Viitanen 1999), for calculating the development of mould growth is defined in

Table 7 and depends on the extent of the growth and if the growth can be detected using microscopy or visually. On the building materials different mould species can grow, therefore this mould index is based on the growth activity of different, but typical, mould species. [49, 60]

Table 7: Mould growth index for the experiments and modelling (Viitanen and Ritschkoff 1991) [60]

Index	Growth rate	Description
0	No growth	Spores not activated
1	Small amounts of mould on surface (microscope)	Initial stages of growth
2	< 10 % coverage of mould on surface (microscope)	Initial stages of growth
3	10-30 % coverage mould on surface(visual)	New spores produced
4	30-70 % coverage mould on surface (visual)	Moderate growth
5	> 70 % coverage mould on surface (visual)	Plenty of growth
6	Very heavy and tight growth	Coverage around 100 %

The equation (1.38) solves the mould growth index „M“ as a function of time (weeks), relative humidity, temperature, wood species and the surface quality from the drying process. These parameters and the model itself is described more detailed in (Hukka and Viitanen 1999) and (Viitanen et al. 2000). [49, 60]

$$\frac{dM}{dt} = \frac{1}{7 \cdot \exp(-0.68 \ln T - 13.9 \ln RH + 0.14W - 0.33SQ + 66.02)} \cdot k_1 k_2 \quad [-] \tag{1.38}$$

where t time [weeks];
T temperature of air [°C];
RH relative humidity of air [%];
W the wood species (0 = pine and 1 = spruce);
SQ surface quality from the drying process;
k_1, k_2 coefficients expressing the delay in early and late stages of growth.

1.6.2 Decay development method

For mould and decay development a different dose response exists. Figure 24 shows the development of decay in pine sapwood as mass loss of the wood occurs in an accelerated test under a constant, worst case scenario of high humidity conditions at different temperatures.

In nature, the humidity and temperature conditions vary, so the laboratory experiments at constant conditions are not very useful, but can be informative and predict the worst behaviour. Development of decay is evaluated using mass loss value caused by the fungus in untreated pine sapwood. The curves are fit to the mean values of laboratory test data (Viitanen 1996). [25, 27]

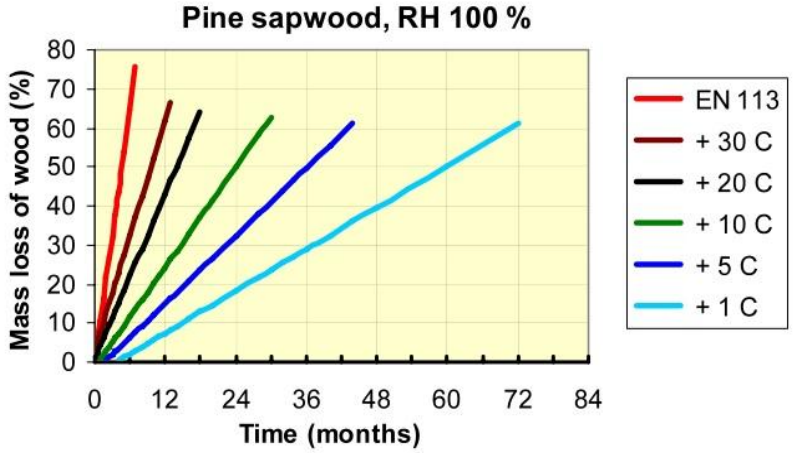

Figure 24: Development of decay of Pine sapwood in accelerated decay test (EN113:1997) and at 100 % RH of ambient air at different temperatures [25]

The evaluation of decay development in the model is based on the mass loss caused by the decay fungus on a sample with a given volume. The wood decay model, developed for untreated pieces of pine sapwood under constant conditions, provides a general picture of the effect of the humidity, temperature and exposed time on the start progress of decay. [25]

Based on the experimental data on different moisture and temperature levels (an example is shown in Figure 24) the following regression equation for mass loss of the original mass „ML“ in [%] was developed for the decay growth of brown rot in pine wood under constant conditions:

$$ML(RH,T,t) = -42.9t - 2.3T - 0.035RH + 0.14T \cdot t + 0.024T \cdot RH + 0.45RH \cdot t \quad [\%] \qquad (1.39)$$

where t time [months];
T air temperature [°C];
RH relative humidity of air [%].

This growth model applies only when T ≥ 0 °C and when RH ≥ 95 %. Outside these conditions the mass loss process is stopped. [25]

1.6.3 Environment and natural durability of wood

To assess and determine the risk of infestation of a particular timber structure built in a certain environment by decaying fungi and for a qualified estimation of its service life, the following two critical factors must be known:

a) the natural durability of wood against decaying fungi; and
b) the parameters of the environment in which the wood will be built, i.e. to determine the risk class.

Knowledge and evaluation of these fundamental factors for specific conditions then allows the assessment of the need for any additional protection of timber construction and the best protection method.

The natural durability of wood is owed to its resistance to infestation by wood decaying organisms. The natural resistance of certain selected coniferous trees for the Central European region to wood-destroying fungi is mentioned in Table 8. Individual species are tested using the methods described in the relevant European standards and the results are compared with the results of reference trees (Table 9). [20]

Table 8: The natural resistance of certain selected coniferous trees of Central European region to wood-destroying fungi [author with 20]

Wood species			**Resistance class according to EN 350-1, 2**	**Possible durability in risk class 4 (EN 335-1, 2) [Year]**
English name	**Czech name**	**Botanical name**		
Eastern white pine	Borovice vejmutovka	Pinus strobus	4*)	6-10*)
European silver fir	Jedle	Abies alba	4*)	6-10*)
Norway spruce	Smrk ztepilý	Picea abies	4*)	6-10*)
Sitka spruce	Smrk sitka	Picea sitchenzis	5*)	3-6*)
European larch	Modřín	Larix decidua	3*)	10-15*)

Note: *) The data apply to the heartwood; sapwood is classed resistance class 5 (durability of less than 6 years).

Table 9: Natural resistance against wood-destroying fungi - determined on the basis of results of Field tests conducted in accordance with EN 252 [author with 20]

Resistance class according to EN 350-1, 2		**Average life test specimens found according to EN 252**	
No.	**Classification**	**Expressed as a multiple lifetime of reference specimens** *)	**During the average lifetime Reference specimens 5 years**
1	Very durable	More than 5x	More than 25 years
2	Durable	3.0 – 5.0x	(15-25) years
3	Middle durable	2.0 – 3.0x	(10-15) years
4	Little durable	1.2-2.0x	(6-10) years
5	Not durable	Less than 1.2x	Less than 6 years

Note: *) x = average service life of reference objects in a specific region, eg. tests carried out in VZL Březnice, the service life was defined as: reference specimens of beech wood 2 ÷ 4 years and reference specimens of Scots pine sapwood 4 to 6 years

Individual risk classes by wood biotic pests are defined and parameters are established against an international classification system to European standards EN 335-1, 2, 3; these are of course also valid in the Czech Republic. Principles of classification and the main parameters are listed in Table 10. The experience of laboratories in the Czech Republic is that the effect of decaying fungi causes the most damages to wood built-in risk class 2nd (humid, closed and not air-conditioned space in the interiors of buildings). [20]

Table 10: Definition of risk classes of wood biotic pests - classification according to EN 335-1, 2, 3 [author with 20]

Class of risk	**Characteristic effects and conditions**	**Environments and examples of use**	**Biotic pests** *)
0	MC always < 10 %	Air-conditioned interiors with RH ≥ 60 % (residential rooms)	none
1	MC 10 % - 20 %	Not air-conditioned dry interiors (attics, rafters)	I
2	MC sometimes > 20 %	Not air-conditioned interiors with RH ≥ 80% (basements, laundry)	F_B, I, P, B
3	MC often > 20 % + weathering	Exteriors, without contact with ground (exterior cladding and structures)	F_B, I, P, B
4	MC always > 20 % + weathering and contact with ground	Timber built into the ground and/or water (even partially) (columns, sleepers, cold. tower)	F_A, F_B, I, P, B
5	MC always > 20 % + effect of sea water	Timber built into the sea water (even partially) (boats, equipment ports)	Sea pests, F_A, F_B

Note: *) meaning of symbols:

I wood-destroying insects
F Ascomycetes fungi (soft rot)
F Basidiomycetes fungi (brown and white rot)
B wood staining fungi (blue stain)
P moulds

2. SPECIFICATION AND GOALS OF THE DISSERTATION

This thesis deals with the correct design of build in wooden elements used in the wooden structures and the prediction of biotic attack to the wood with increased humidity in order to ensure the long durability of timber structures. The expansion of theoretical and experimental knowledge is focused on the effects of supercritical carbon dioxide impregnation, as a possible prevention of biotic attack and its comparison with non impregnated wood. This issue is very broad, includes areas concerning the anatomic structure and history of the wooden elements and interactions with humid environments. Important part plays the moisture transport theory and its application in building practice.

2.1 Specification of the issue

The dissertation generally summarizes the influence of design on wall to floor junction with increased moisture content of wooden bottom plate to irreversible damage to wooden structures and analysing the possible impregnation as prevention against mould growth on wood. The results obtained from author's laboratory and on site experiments concerning the comparison of natural and carbon dioxide impregnated spruce were used for numerical calculations of simulated wall/floor junction.

Chapter 1 outlines the broad theoretical shot of three disciplines: wood anatomy, impregnation effect on the structure of wood and on heat and moisture transfer in building materials, especially in wood and wooden structures. Attention is also paid on wood durability and biological degradation models, practically implemented in Chapter 9.2.

The dissertation topic combines all disciplines in the application of knowledge to 2D numerical calculations and thus tries to interconnect the simulation theory with predicted praxis. The important parts of the fundamental knowledge are the initial moisture conditions of wood which differ in the laboratory and on the building site and are thus hardly provable by numerical calculations.

Chapter 4 provides an introduction, respectively describing the technical solution of two modern wooden structures, used as case studies of the thesis. Their wall/floor structures have been used for the mould growth analysis and analysis of mass loss due to the decay fungi in Chapter 9.2.

From Chapter 5 to Chapter 8 the author's experiments within the framework of this thesis tried to verify and compare the effects of supercritical carbon dioxide impregnation on the selected mechanical, thermal and hygrothermal properties of wood.

In Chapter 9.1 the relevant results obtained from above mentioned experiments were theoretically used in numerical calculation of the thermal transmittance coefficient (Ψ) of chosen wall/floor junction. The non-impregnated and supercritical carbon dioxide impregnated spruce were used as a bottom plate wood with dried and conditioned initial conditions (0 weight-% and 35 weight-%).

In Chapter 9.2 on site measurements of moisture content of the bottom plate were applied on the bottom plate of two new build timber structures (Chapter 4) in order to analyse by Viitanen's model the mould growth and mass loss due to the decay fungi and so to predict the behaviour of the wood with increased initial moisture content.

2.2 Goals of the dissertation

The dissertation is a complex experimental and theoretical analysis of the carbon dioxide impregnation issue in comparison with non-impregnated timber elements with increased initial moisture content and its potential impact on the heat losses of the building. Presented impregnation was chosen as a newest impregnation method to protect wood against biotic attack and thus, not itself, could be a solution of limited protection of build in wooden elements with increased moisture content.

The theoretical knowledge was applied to an analysis of mould growth prediction and an analysis of mass loss due to the decay of two timber structures with slightly different ability to dry out the moisture within the wooden elements.

The final recommendations are based on these findings and analysis both from the laboratory experiments and numerical calculations. The following are goals of the dissertation:

2.2.1 Determination of differences in anatomic structure between impregnated and non-impregnated spruce

- to gain further knowledge on the behaviour of moisture transport in spruce;
- to find possible differences in anatomic structure between non-impregnated and supercritical carbon dioxide impregnated spruce;

- to find the possible damage of the anatomic structure thanks to a high pressure involved during the supercritical carbon dioxide impregnation.

2.2.2 Determination of thermal and hygrothermal differences between impregnated and non-impregnated spruce

- to find the differences in behaviour of the non-impregnated and supercritical carbon dioxide impregnated spruce in Hot, Room and Cold conditions;
- to set the graph of sorption isotherms;
- to set the water vapour permeability coefficient;
- to determine the thermal conductivity of the non-impregnated and supercritical carbon dioxide impregnated spruce with increased moisture content from 0 to 35 weight-%. The obtained results were applied on thermal calculation of wall to floor junction to see the differences in linear thermal transmittance (goal 2.2.4).

2.2.3 Determination of mechanical differences between impregnated and non-impregnated spruce

- to find the differences in the creep properties in longitudinal direction for bending and shearing.

2.2.4 Influence of moisture content on heat losses

- the measured thermal conductivity data obtained from laboratory experiments (goal 2.2.2) were used in numerical simulations to find out and compare how much can increased initial moisture content in the non-impregnated and impregnated wood effect the heat losses of modelled details of the connection of outer wooden walls on monolithic foundations.

2.2.5 Influence of construction design on moisture damage

- to optimize two well-insulated wooden structures with increased initial moisture content of the wooden plate for comparison on irreversible moisture damage;
- to use Viitanen model (VTT) to analyse the risk the mould growth and mass loss due to the decay fungi of wooden material to predict the future behaviour of wooden walls;

- to specify the technical solution to protect the wooden elements against moisture damage and eventually consequential mould growth in timber structures.

2.3 Resources to achieve the goals of the dissertation

To meet the targets of dissertation the laboratories, instrumental equipment and software of the Department of Civil Engineering, Section of building physic and services and Section for Construction Materials at "Technical University of Denmark", Lyngby was primarily used, within an external stay for one year. This stay was financially supported by Brno University of Technology, Faculty of Civil Engineering, Department of building structures and EU funded ERASMUS programme.

The materials required to perform all presented experiments on spruce were acquired from the company Superwood® Denmark who is specialized in carbon dioxide impregnation.

Finally, to attain the dissertation goals, two real wooden objects, built in different potentials to dry out "built in" moisture were used. The owners of these structures have provided the design documentation and photographs of the construction process needed for numerical calculations and simulations of selected details.

3. METHODS USED IN DISSERTATION

For the processing of the dissertation and data analysis several basic methods were chosen, such as the theoretical, practical and the combination of both. Already during the planning of individual research steps the analogy method was applied. The analogy is based on already published scientific publications and studies, supported by results obtained from the presented experiments and compared with previously measured data itself.

3.1 Theoretical methods

3.1.1 Literature study

Theoretical knowledge was obtained mainly from scientific papers and conference proceedings and also within the course materials of "Wood science and technology" and "Heat and mass transfer in buildings" completed during the external stay in "Technical University of Denmark in Lyngby (DTU). Information on the solved issue was constantly supplemented through updates available on the internet and deepened by available forum discussions.

3.1.2 Experts' consultations

Theoretical knowledge, experimental processes and practical findings were regularly discussed with the professors and experts on solved issues at DTU in Lyngby, Denmark. The procedure, results and findings related to the treatment process as well as wood impregnation were consulted with a Danish company Superwood® dealing with supercritical carbon dioxide impregnation.

Another information source was professional discussions with participants at relevant conferences.

3.1.3 Numerical calculations

One important part of the solution of the dissertation became a numerical calculation. In Chapter 9.1 this method was used to perform the heat transfer investigation in one and two dimensional (1D and 2D) commercial software Heat 2, version 8.1 (Blomberg et al. 2000) [48] to calculate the heat loss from the building to the ground. In Chapter 9.2 a study on the hygrothermal condition of the two constructions is mentioned. This investigation and the coupled heat and moisture calculations were performed with the 2D hygrothermal simulation tool Delphin version 5.6.8 [51] to acquire the

data needed for modelling of the mould growth risk and mass loss due to the decay fungi of two wooden buildings. The description of the models and simulation programmes are clearly described in the aforementioned chapters.

3.2 Experimental methods

3.2.1 Laboratory methods

All laboratory experiments were conducted at the Department of Civil Engineering, Section of building physic and services and Section for Construction Materials at "Technical University of Denmark" in Lyngby.

In the laboratory experiments the following data were collected and calculated:

- Microscopic structure of non-impregnated and supercritical carbon dioxide impregnated spruce.
- The water content at the beginning and at the end of the experiments – the gravimetric method.
- Thermal conductivity of non-impregnated and supercritical carbon dioxide impregnated spruce during dry and increased initial moisture content of spruce.
- Initial and final mass gain for monitoring of capillary suction of non-impregnated and supercritical carbon dioxide impregnated spruce in Hot, Room and Cold conditions.
- Initial and final mass gain for determination of hydroscopic sorption properties of non-impregnated and supercritical carbon dioxide impregnated spruce.
- Initial and final mass gain for determination of water vapour transmission properties of non-impregnated and supercritical carbon dioxide impregnated spruce.
- Failure load of the Stenhøj machine for determination of bending and shearing of non-impregnated and supercritical carbon dioxide impregnated spruce.

3.2.2 Equipment used

The general list of equipment used in experiments mentioned in the dissertation is listed here. Nevertheless, the materials and equipment for each experiment are described in the associated chapters.

- low-vacuum electron imagine microscope FEI Quanta 200;
- portable device for measurement of heat transfer properties of materials Isomet, a surface probe with range 0.04 - 0.3 $W \cdot m^{-1} \cdot K^{-1}$, the accuracy

for the thermal conductivity around 5-10 %, the volume heat capacity 15 % and the temperature 1 °C;
- hygrometer;
- analytical balance, for weighing the specimens to an accuracy of ±0.1 % of the mass of the specimen;
- calliper, for measuring dimensions of the test specimens;
- water tank with thermometer and constant temperature 30 °C;
- device for keeping the test specimen in position, pins;
- timer;
- weighing cups which do not absorb water and with tight-fitting lids;
- balance, capable of weighing to an accuracy of ± 0.01 % of the mass of the test specimen;
- drying oven, in accordance with EN ISO 12570;
- desiccators, capable maintaining the relative humidity with ±2 % RH;
- constant temperature, constant humidity chamber, capable of being maintained within ±3 % RH around the set point RH and ±0.5 K around the set point T;
- suitable sensors and a logging system to continuously record the T, RH and the barometric pressure within test chamber
- bending machine Stenhøj for determining the failure load;
- test set up for creeping test;
- deflection meter; sealant.

3.2.3 Experimental measurements on site

For the increased initial moisture content of wood on site measured values were used, during the construction of the wooden building built to passive house standard in Denmark (Introduction, Figure 2). This value was settled to 35 weight-% and served as a base for numerical calculations of modelled wall to floor junction of two wooden structures and followed by calculation of Viitanen model for prediction of mould growth and decay risk of wooden buildings (Chapter 9.2).

3.3 Comparative methods

The comparative method was used for both the experiments in the laboratory and numerical calculations. The results from the laboratory experiments were compared with each other and with the standard values, generally used in the simulations' software. The results from the numerical calculations using a decay risk models were compared with the standard values of these models to come to final conclusions.

4. CASE STUDIES: WALL SYSTEMS OF WOODEN BUILDINGS

This chapter is an introduction for two wooden structures, which have been used for the mould growth analysis and analysis of mass loss due to the decay fungi in Chapter 9.2.

The first and most important practical detail in timber construction is to connect the peripheral wall to the foundation structure. To build a foundation with limited heat loss depends mainly on isolating the foundation construction to non-freezing depth and the desired height of the finished floor in the first floor. The solution of timber construction corner of exterior walls and floors creates a three-dimensional thermal bridges effect which offers an effort to be constantly optimized.

Performing footing parts, which provides a protection against splash water, in combination with the composition floor is always seen in its entirety on the resulting surface temperature of the walls in the inner corner of the room. Thermography surveys show the colder corners of the room and at installation of transparent components from interior due to lack of circulation of warm air (Figure 25).

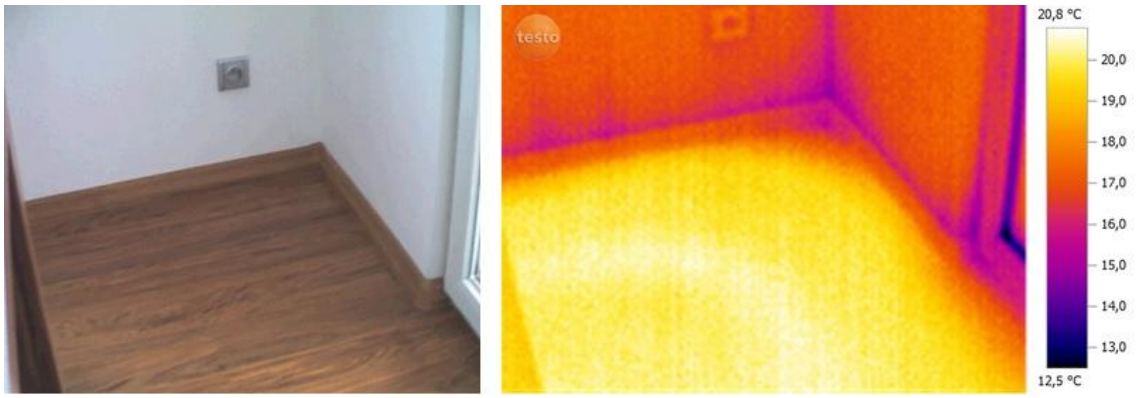

Figure 25: A corner of outer wall in a basement (left); thermograph picture with temperature field of the same corner (right) [28, 56]

The floor construction on the first floor should be according to the Czech regulations of at least 0.15 m above the highest point of the landscaped terrain or patios on the ground. The height of the floor construction with regards to minimum required thermal resistance of the floor structure on the ground is about 120 to 140 mm above the base plate. Therefore, the standard solution in wooden structures is to choose the height of the connection of the outer wall on the underside structure of the building at a minimum height of 300 mm above the adjacent modified terrain [56]

4.1 Diffusion closed peripheral wall

Diffusion closed structural systems are based in placing the vapour barrier on the peripheral structures from the interior side, which prevents the entry of water vapour into the wooden structure.

An example of a diffusion closed peripheral wall is a wooden building built in the Czech Republic (Figure 26), further named as Case study 1 (CS1).

Figure 26: View of a wooden building with a diffusion closed system of the wall built in the Czech Republic; mounted OSB (bottom right) and EPS (left) on the outer wall. Airtight layer from the internal side is secured by a vapour barrier on an aluminium base (top right). Photos © Karel Šuhajda

Table 11 and 12 show the compositions of the floor and wall structure with respective calculations of U-values. The schematic composition of both structures is shown in Figure 27.

Table 11: U-value for floor construction of diffusion closed Case study 1 (original stage)

CS1 Floor	d [m]	λ [$W \cdot m^{-1} \cdot K^{-1}$]	R [$m^2 \cdot K \cdot W^{-1}$]
$R_{internal}$	-	-	0.17
Wooden floor	0.01	0.13	0.078
2x OSB	0.03	0.13	0.23
Mineral wool	0.120	0.04	3.00
Concrete slab	0.150	2.1	0.071
Stone	0.100	2.43	0.041
Σd=	0.410	ΣR=	3.58
		U=1/ΣR=	0.28 $W \cdot m^{-2} \cdot K^{-1}$

Table 12: U-value for wall construction of diffusion closed Case study 1(original stage)

CS1 wall	d [m]	λ [$W \cdot m^{-1} \cdot K^{-1}$]	R [$m^2 \cdot K \cdot W^{-1}$]
$R_{internal}$	-	-	0.13
Gypsum board	0.013	0.2	0.065
Mineral wool	0.04	0.056	0.714
Post, MW	0.15	0.047	3.19
OSB	0.015	0.13	0.115
EPS	0.10	0.04	2.500
Plaster	0.003	0.700	0.004
$R_{external}$	-	-	0.04
Σd=	0.321	ΣR=	6.74
		U=1/ΣR=	0.15 $W \cdot m^{-2} \cdot K^{-1}$

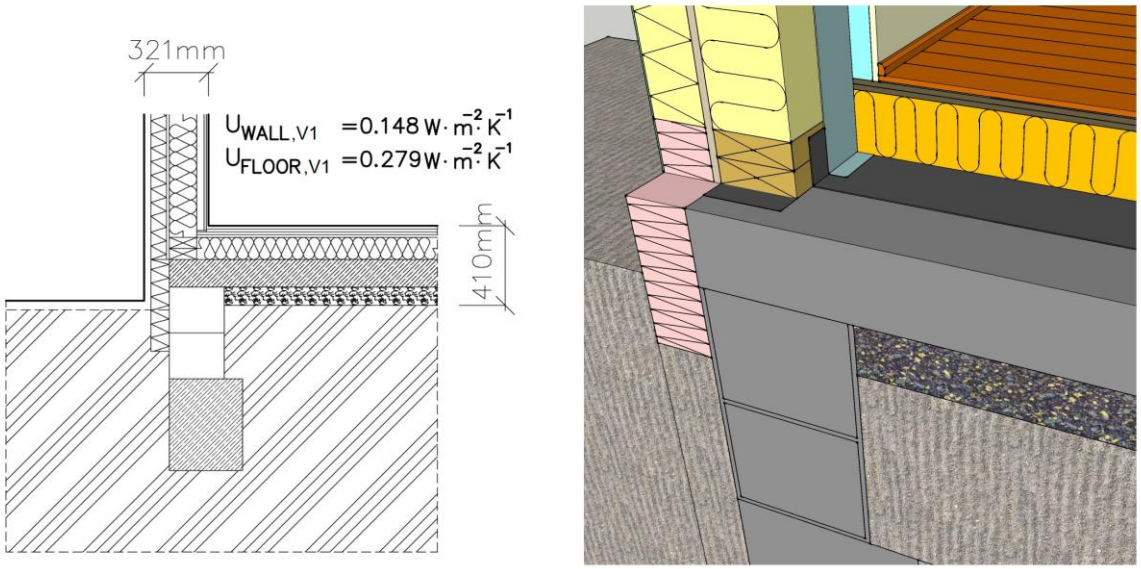

Figure 27: The wall and floor construction of diffusion closed wooden structure [author]

Damages of such sealed walls arise by missing or damaged thermal insulation in composition of the wall or not correctly mounted vapour barriers, which have to be tight, without gaps or interruptions and joints must be sealed with special tape that will guarantee the long-term and airtight seal. Barriers should be protected against damage (e.g. by front walls), especially in the case of ducts penetrating the walls.

To ensure better ventilation facades and thus the removal of moisture, it is necessary to ensure the best possible diffusion, i.e. water vapours. For these purposes, special diffusion permeable polystyrene were developed, which are called breathable. Among breathable polystyrene include expanded polystyrene boards EPS, which are adapted with transverse perforations (holes). From the perspective of security and the possible formation of condensation, it is therefore safer to diffuse the structure which allows for the passage of moisture already during the design techniques.

The temperature field and the process of isotherms in the diffusion closed Case study 1 in wall/floor junction detail at the end of 10th simulated year are shown in vertical section in Figure 28.

The dew point should occur at the outer side of the facade in the insulating material which ensures a sufficient layer of insulation.

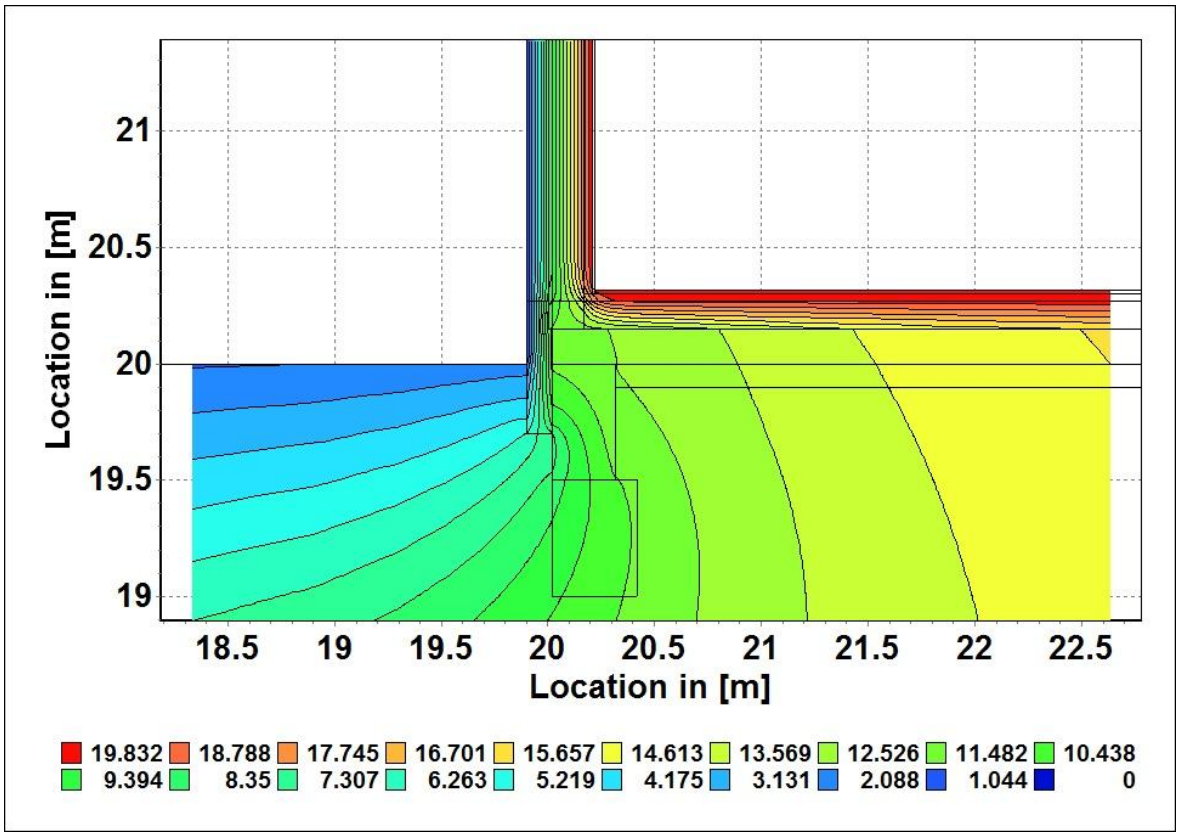

Figure 28: Temperature field and the process of isotherms in diffusion closed Case study 1 in wall to floor junction detail[author with 51]

4.2 Diffusion opened peripheral wall

For diffusion opened systems infiltration of air and water vapour materials through the composite wall is desirable. An important part of developing diffusion opened walls are the wood fiber insulation boards based on wood. They are applied from the outside as an external insulation structure together with a rendering system or ventilated wood panelling, which ensures easy removal of moisture in a gaseous state from the chamber wall so that condensation does not form. This layer must also meet strict criteria on the tightness of the whole structure.

As an example of diffusion opened peripheral wall is a wooden building built in Denmark (Figure 29), further named as Case study 2.

Figure 29: View of a wooden building with a diffusion opened system of the wall built in Denmark; the wooden posts to frame the outer wall (top left). The vapour retarding layers – OSB and gypsum board, on the ceiling is wooden render for mounting suspended ceiling to ensure the space for ventilation ducts (top right). The fiber insulation board mounted form the external side with the grid of wooden horizontal posts to hold the vertical wooden cladding (bottom left). The formwork for casting the concrete with XPS at the external side (bottom right). Photos © Ruut Peuhkuri

Table 13 and 14 show the compositions of the wall and floor structure with respective calculations of U-values. The schematic composition of both structures is shown in Figure 30.

Table 13: U-value for floor construction of diffusion opened Case study 2 (original stage)

CS2 floor	d [m]	λ [$W \cdot m^{-1} \cdot K^{-1}$]	R [$m^2 \cdot K \cdot W^{-1}$]
$R_{internal}$	-	-	0.17
Wooden floor	0.015	0.13	0.115
Concrete screed	0.100	2.1	0.048
EPS	0.265	0.031	8.549
Σd=	0.380	ΣR=	8.88
		U=1/ΣR=	0.11 $W \cdot m^{-2} \cdot K^{-1}$

Table 14: U-value for wall construction of diffusion opened Case study 2 (original stage)

CS2 wall	d [m]	λ [$W \cdot m^{-1} \cdot K^{-1}$]	R [$m^2 \cdot K \cdot W^{-1}$]
$R_{internal}$	-	-	0.13
Gypsum board	0.013	0.2	0.065
OSB	0.012	0.13	0.09
Post, cellulose	0.36	0.048	7.5
Wood fireboard	0.01	0.05	0.2
Air gap	0.025	-	-
Cladding	0.025	-	-
$R_{external=internal}$	-	-	0.13
Σd=	0.395	ΣR=	8.12
		U=1/ΣR=	0.12 $W \cdot m^{-2} \cdot K^{-1}$

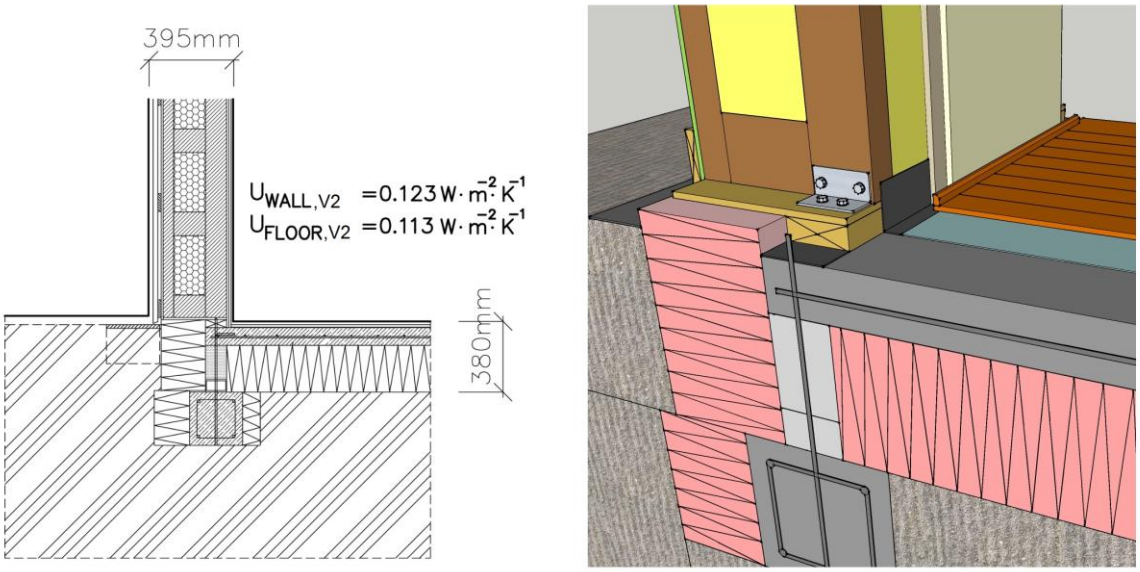

Figure 30: The wall and floor construction of diffusion opened wooden structure [author]

Even if the moisture gets into the structure due to decreasing diffusion resistance of construction the moisture has the possibility to evaporate. It is also important that the plaster or external layer on the facade system insulator should minimize vapour resistance.

By substituting polystyrene for insulation or mineral fibreboard the timber construction reaches better acoustic properties in comparison with polystyrene, due to the higher weight and smaller modulus of elasticity. Also due to higher specific heat capacity of materials that replace polystyrene, the interior temperatures during the hot summer months are lower.

The temperature field and the process of isotherms in the diffusion opened Case study 2 in wall/floor junction detail at the end of 10th simulated year are shown in vertical section in Figure 31.

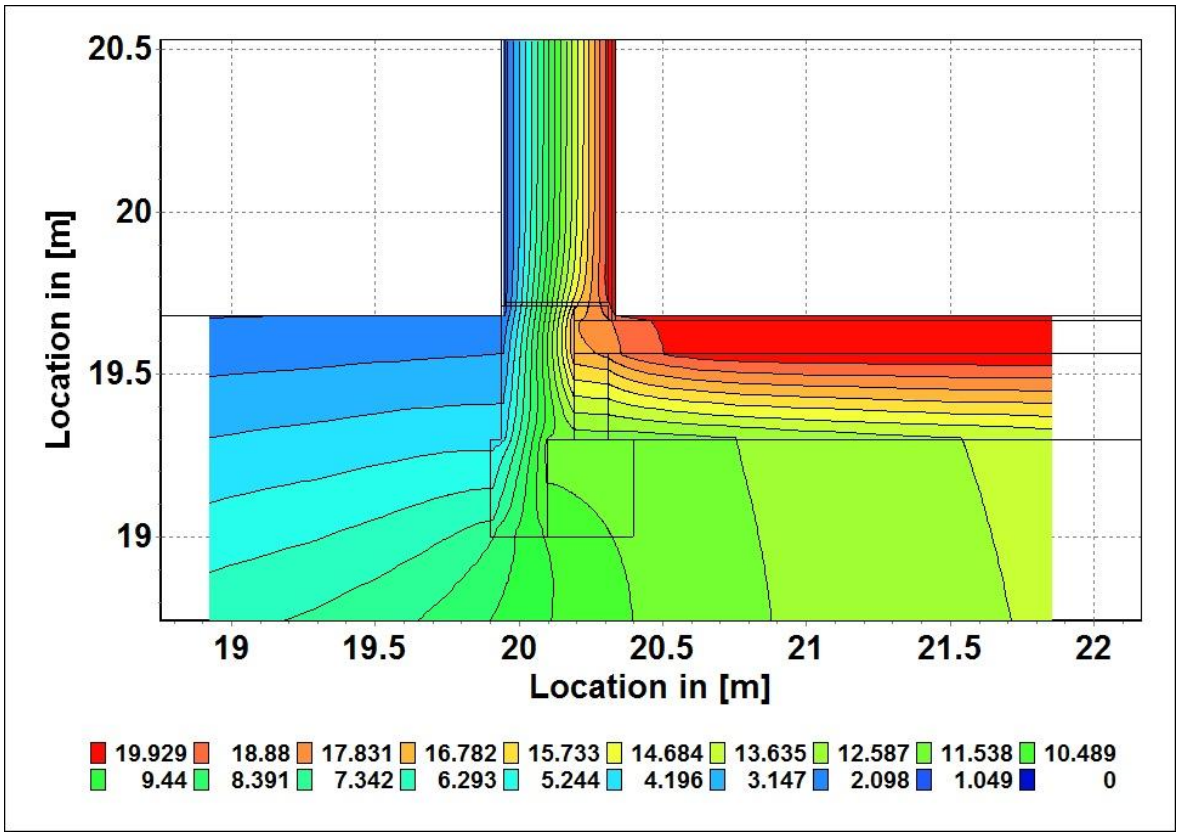

Figure 31: Temperature field with the process of isotherms in diffusion opened Case study 2 in wall to floor junction detail [author with 51]

5. MICROSCOPIC ANALYSIS ON STRUCTURE OF SPRUCE

5.1 Comparison of anatomic structure

The following analysis of the microscopic structure of spruce is based on the author's experiments within the framework of this thesis. The presented results describe the differences in anatomic structure between Untreated and Treated spruce.

5.1.1 Materials

Small matched controlled samples of untreated and treated Norway spruce (Picea Abies) were collected in the laboratory. They were cut in wet conditions and then re-dried at 105 °C in order to get the most possible sharp cut. The specimens were then placed into low-vacuum electron imagine microscope FEI Quanta 200 for the wooden anatomic investigations.

5.1.2 Methods

The anatomic investigations were performed on low-vacuum electron imagine microscope FEI Quanta 200 at Technical University of Denmark in Lyngby (Figure 32).

Two detections: LTD and dual BSD with internal pressure of 130 Pa were used to get the clearest possible results.

The distance size was settled according to the desired outcome view, such as:

- 1 mm for Scanning Electron Microscopy image of radial surface of longitudinal tracheids in with visible transition of earlywood and late wood in both untreated and Treated Norway spruce samples (Figure 33);
- 50 μm for Scanning Electron Microscopy image of earlywood (Figure 34) and latewood (Figure 35) - the axial surface of a single longitudinal tracheid in both untreated and Treated Norway spruce samples and detailed SEM image of bordered pits in the radial cell walls of longitudinal tracheids in both untreated and Treated Norway spruce samples (Figure 37);
- 200 μm for Scanning Electron Microscopy image showing bordered pits in the radial cell walls of longitudinal tracheids in both untreated and Treated Norway spruce samples (Figure 36).

Figure 32: Microscope FEI Quanta 200 (left), inside chamber of the microscope FEI Quanta 200 with a spruce sample prepared for investigations (right) [author]

5.1.3 Results

Scanning Electron Microscopy (SEM) pictures in radial direction (Figure 33, Figure 34 and Figure 35) and longitudinal direction (Figure 36 and Figure 37) of untreated and treated Norway spruce samples.

A visible difference between earlywood and latewood is formatting a typical pattern of annual rings (Figure 33). The earlywood thin-wall tracheids (Figure 33) have the function of conduct nutrients, whereas the latewood thick-walled tracheids (Figure 35) have the function of support the whole plant.

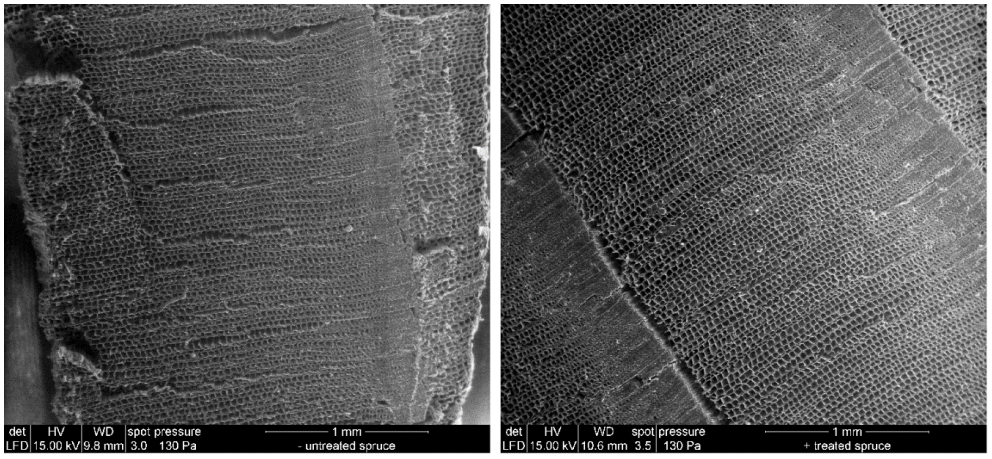

Figure 33: SEM image of radial surface of longitudinal tracheids of Norway spruce. untreated (left) and treated (right), with visible transition of earlywood and latewood [author]

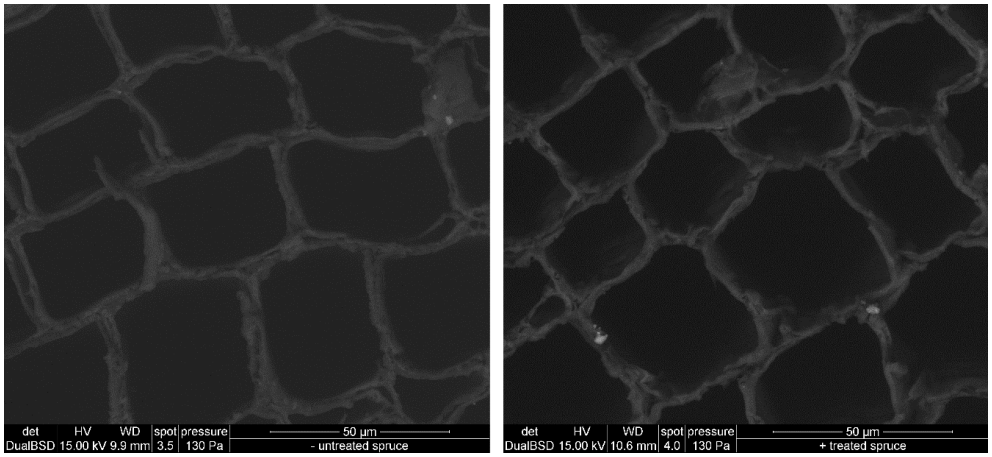

Figure 34: SEM image of earlywood (the axial surface of a single longitudinal tracheid) of untreated Norway spruce (left) and treated Norway spruce (right) [author]

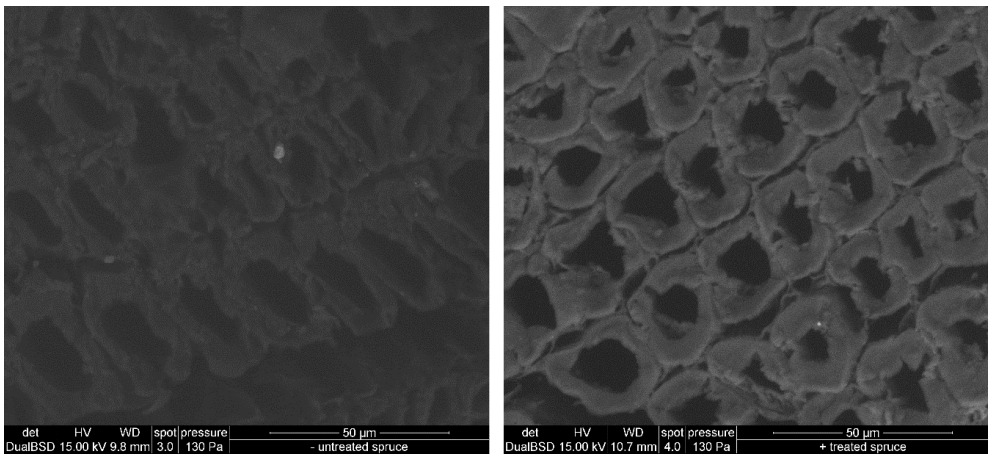

Figure 35: SEM image of latewood (the axial surface of a single longitudinal tracheid) of untreated Norway spruce (left) and treated Norway spruce (right) [author]

Figure 36 and 37 show the cavities, bordered pits in the lignified cell walls of xylem conduits (tracheids) that are essential components in the water-transport system.

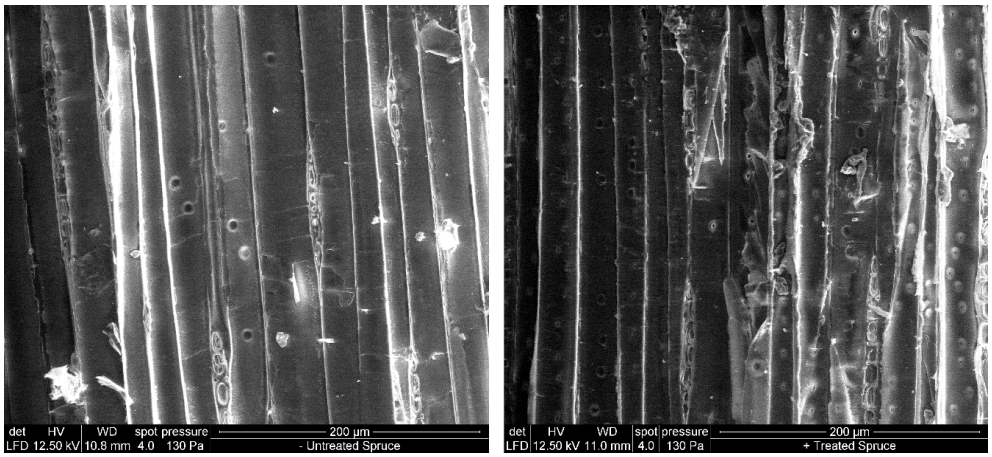

Figure 36: SEM image showing bordered pits in the radial cell walls of longitudinal tracheids in untreated Norway spruce (left) and treated Norway spruce (right)

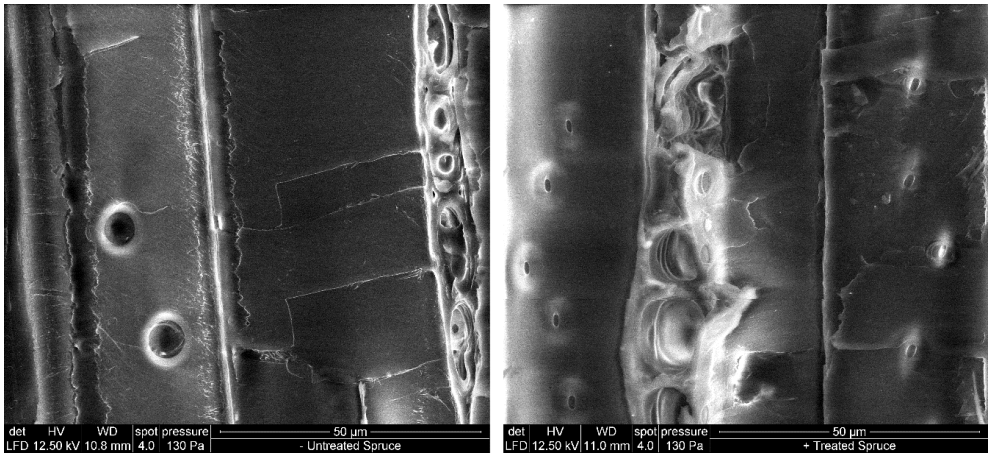

Figure 37: Detailed SEM image of bordered pits in the radial cell walls of longitudinal tracheids in untreated Norway spruce (left) and treated Norway spruce (right)

5.1.4 Conclusions and discussions

As Kjellow already mentioned in his Dissertation (2010) "*the supercritical impregnation procedure is theoretically simple, it is difficult to control in practical use*. *Because of the relatively high pressures involved during the treatment, there is a risk of developing excessive pressure gradients in the wood that can cause fatal aftermaths to the structure*." [2].

This statement was also confirmed by Scanning Electron Microscopy pictures results. In radial direction, there is a visible difference in the shape of the cell wall of Treated spruce (Figure 34 and 35). The cell walls look to be slightly damaged; a high-pressure during the impregnation process could explain it. In the longitudinal direction there are not any visible perceptible differences in the anatomic structure (Figure 36).

The question remains: do these structure differences in the radial section have a fatal influence to thermal and hygrothermal behaviour of spruce and then later on in the timber structure itself. Several such experiments comparing the Untreated and Treated spruce samples were performed within this dissertation.

6. THERMAL EXPERIMENTS ON SPRUCE

6.1 Determination of thermal conductivity

The following chapter is based on the author's experiments within the framework of this thesis. The presented results determined and specified the differences in thermal conductivity between dry and conditioned Untreated and Treated spruce.

The obtained results were used for numerical calculations in Chapter 9.1 Influence of using treated wood on thermal properties and heat losses in basements of wooden buildings.

This issue and results were presented at the conference and published in [54].

6.1.1 Materials

Norway spruce (Picea abies) boards of Untreated (A) and Treated (B) samples were collected in laboratory with average moisture contents of about 10 weight-%, measured with a hygrometer for wood. The wood treatment process of the treated samples in this study was based on supercritical carbon dioxide as a carrier for organic fungicide. After the treatment, the wood should be protected against biological decay and mould growth [2, 3].

The dimensions of all 12 test samples were about 300 x 300 x 32 mm. The annual ring growth was from 1.5–2.5 mm. The density of the dry material was for untreated (A) samples of 370 $kg \cdot m^{-3}$ and for treated (B) samples of 470 $kg \cdot m^{-3}$. The samples were purchased from standard distribution of both type of lumber. [54]

Experiments were performed on 3 conditioned samples of each kind of material in three series of tests with 0 %, 40 % and 80 % of RH, which corresponds to approx. 0 %, 10 % and 20 % of weight moisture content of the wood (see also Figure 16). The first three A and three B samples were conditioned at 80 % RH with a temperature of 20 °C in a small climate chamber (with dimensions of 500 x 1100 x 500 mm) until they reached equilibrium state (Figure 38). [54]

Another three samples of both A and B were conditioned in room conditions with 40 % RH and T of 18 °C. After the determination of the thermal properties of moist samples all samples were dried in the oven at T of 105 °C until they reached equilibrium state – and the thermal properties were measured again. The MC was determined by direct weighing in each of three conditions such as 0 %, 40 % and 80 % of RH.

Figure 38: Climate chamber with 80 % RH and T 20 °C [author]

6.1.2 Methods

Thus conditioned samples were measured on a portable device (Isomet) that estimates the thermal properties of the materials, more specifically, the thermal conductivity, the thermal diffusivity, the volume heat capacity and the temperature. The principle is based on the heat flow impulses by means of detecting electrical heating. The analyser was used with a surface probe with range 0.04-0.3 $W \cdot m^{-1} \cdot K^{-1}$. The accuracy is for the λ around 5-10 %, the volume heat capacity 15 % and the temperature 1 °C.

The measurement was taken in 5 parts of each sample to get average values for the homogeneous material as shown in Figure 39. [54]

Figure 39: Designation of areas on the A-untreated sample at 40 % RH, T = 18 °C and Isomet device for determining thermal properties placed above the sample (left); Measuring the RH and detecting the electrical heating in a plastic bag which reached the equilibrium state at 80 % RH and T = 18 °C (right). In both cases the thermal properties were measured perpendicular to the grain [54]

Dried and moist samples were measured in two layer plastic bags to prevent evaporating or exposure of the sample to moisture. RH and T were recorded consistently in the plastic bag during the measurement.

6.1.3 Results

The average values of the density ρ_{mat}, the thermal conductivity λ_{mat} and the volume heat capacity $c_{p,mat}$ for A-untreated and B-treated spruce samples in all three conditions, perpendicular to the grain are expressed in Table 15.

Table 15: Average values of the measured properties, 3 replicates for each. [54]

	ρ_{mat} [kg.m^{-3}]	λ_{mat} [W·m^{-1}·K^{-1}]	$c_{p,mat}$ [MJ·m^{-3}·K^{-1}]
A80	368	0.110	0.541
A0	345	0.089	0.380
A40	385	0.103	0.477
A0	369	0.091	0.356
B80	496	0.133	0.520
B0	477	0.110	0.465
B40	497	0.125	0.614
B0	476	0.106	0.490

The λ of B-treated spruce increased about 21 % and 24 % for A- untreated spruce when in equilibrium with 80 % RH compared to the dry reference value (MC = 0 %). As for the equilibrium in 40% RH compared to the dry reference value, the λ of B-treated wood samples increased 18 % and A-untreated samples increased 13 %. This increase of λ is clearly described in Figure 40. [54]

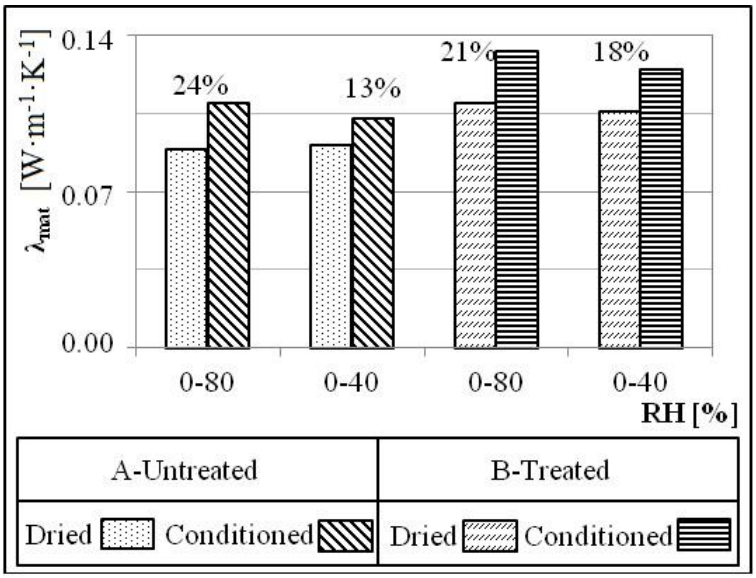

Figure 40: Increase of thermal conductivity of A-untreated and B-treated wood samples in three conditions such as 0 %, 40 % and 80 % RH [54]

6.1.4 Conclusion and discussions

The thermal conductivity of B-treated spruce samples increased to 21 % and 24 % (both approximate values) of A-untreated spruce when in equilibrium with 80 % RH compared to the dry reference value (MC = 0 %). The thermal conductivity of B-treated and A-untreated wood samples was increased, respectively, 18 % and 13 % higher than the equilibrium situation having 40 % RH compared to the dry reference value. So the influence of moisture is clearly affected by this thermal property.

The higher density of B-treated spruce samples could be a part of the explanation. These observations are confirmed in the literature e.g. according to (Koch 1950) [58] the standard increase of thermal conductivity in dependency of moisture content and dry density similar to the present study is around 33 %.

Nevertheless, the thermal behaviour seems to be the same for both types of Untreated and Treated spruce and was measured under 0.14 $W \cdot m^{-1} \cdot K^{-1}$. This corresponds to the standard values of thermal conductivity of spruce perpendicular to the grain $\lambda_{\perp}$ = 0.12-0.18 $W \cdot m^{-1} \cdot K^{-1}$ at T 25 °C and w = 12 %. [54]

7. HYGROTHERMAL EXPERIMENTS ON SPRUCE

7.1 Monitoring of capillary suction in three different conditions

The following monitoring of capillary suction in three different conditions of spruce is based on the author's experiments within the framework of this thesis. The presented results describe the differences in capillary suction between Untreated and Treated spruce.

The experiments were performed according to [41]. This issue and results were presented at the conference and published in [53].

7.1.1 Materials

For each series of experiments 8 small, randomly selected specimen samples were used – A-Untreated spruce and B-Treated spruce. They were cut into rectangular shapes with dimensions of about 15 x 15 x 35 mm (W x H x L) with constant cross sections to ensure one dimensional water flow. In order to ensure that the longitudinal surfaces were free from irregularities, they were painted with clear varnish.

The specimens were studied at three different temperature conditions: cold, room and hot. The numbering in each condition is shown in Table 16.

Table 16: Naming the specimens in various conditions [53]

Cold condition T ~ 5 °C		**Room condition T ~ 19 °C , RH ~ 45 %**		**Hot condition T ~ 30 °C**	
Untreated spruce	Treated spruce	Untreated spruce	Treated spruce	Untreated spruce	Treated spruce
AF1-8	BF1-8	AR1-8	BR1-8	AH1-8	BH1-8

The test apparatus used for testing in each condition include:

a) balance, for weighing a test specimens to an accuracy of ±0.1 % of the mass of the specimen;

b) calliper, for measuring dimensions of the test specimens

c) water tank with thermometer (room condition); water tank with thermometer and constant temperature 30 °C (hot conditions); water tank in fridge with thermometer and constant temperature 5 °C (cold conditions);

d) device for keeping the test specimen in position, pins;

e) timer.

7.1.2 Method

The following procedure was applied to each specimen in each condition.

1) All test specimens were stored in a room with a constant temperature and relative humidity and used when the mass of each specimen was stabilized;
2) Test specimens were weighed with an accuracy of ±0.1 % of its mass to determine the initial mass m_i;
3) The tank was filled with distilled water and conditioned to the test temperature (Figure 41 shows the samples settled in room conditions, Figure 42 shows the water tank in hot conditions and Figure 43 shows the water tank placed in the fridge for the experiment in cold conditions). The specimens in the tank were placed to ensure the water level was kept constant during the test at (5±2) mm above the highest point on the base of the specimen;
4) The timer was started as the specimen was immersed in the water;
5) After approximately 5 min specimens were removed from water, the surface was blotted with a damp cloth and then the specimens were weighed with an accuracy of ±0.1 % of its mass;
6) The continuous procedure of immersion, removal, surface drying and weighing was done to give a series of masses m_t at times t.

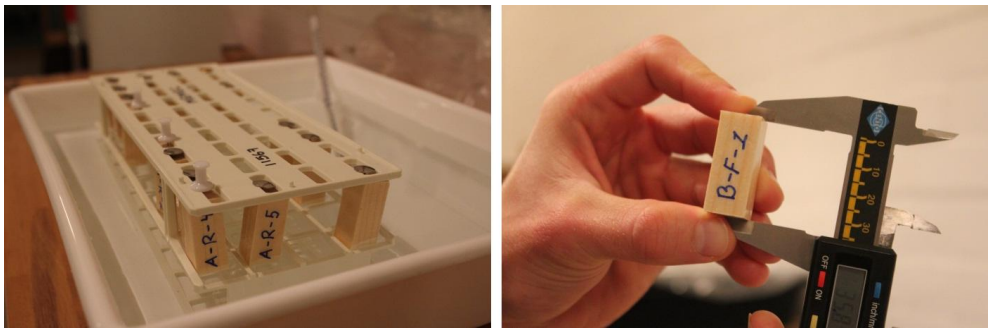

Figure 41: Test settled in room conditions (left); Measuring of initial dimensions (right) [53]

Figure 42: Water tank for test with hot condition (left); Equipment for measuring physical properties (right) [53]

Figure 43: Water tanks in the fridge ready for the test (left); Oven for re-drying the specimens (right) [53]

7.1.3 Results

The average weight, area, volume and density of all specimens, which represent the whole material, are shown in Table 17.

Table 17: Physical properties of specimens in different conditions [53]

	Weight		**Area**		**Volume**		**Density**	
	Initial	**End**	**Initial**	**End**	**Initial**	**End**	**Initial**	**End**
	g		**cm^2**		**cm^3**		**g·cm^{-3}**	
AR	3.62	4,.90	2.38	5.41	8.396	8.412	0.431	0.581
AH	3.46	4.82	2.31	2.38	8.218	8.479	0.420	0.569
AF	3.30	5.15	2.30	2.38	8.127	8.420	0.406	0.611
BR	3.95	6.24	2.23	5.32	7.972	8.001	0.496	0.780
BH	3.53	6.27	2.26	2.40	8.108	8.627	0.436	0.727
BF	3.58	7.15	2.24	2.40	8.040	8.646	0.445	0.827

The difference between the mass at each weighing and the starting mass per area was calculated:

$$\Delta m_t = \frac{(m_t - m_i)}{A} \qquad [\text{g}\cdot\text{cm}^{-2}] \qquad (7.1)$$

where Δm_t mass gain per face area after time t [g·cm^{-2}];
m_t mass of specimen after time t [g];
m_i initial mass of specimen [g];
A initial face area [m^2].

When the change in mass is plotted against the square root of the weighing times $\sqrt{t}$ we get the following graphs shown in Figure 44, Figure 45 and Figure 46 according to the test conditions.

After a period of stabilization, a straight line could be drawn through the values of Δm_t against $\sqrt{t}$. Each of the lines has its own equation. This line was then extended back to zero line where it cut the vertical axis at $\Delta m'_0$.

The water absorption coefficient "W_w" was then calculated:

$$W_w = \frac{\Delta m'_{tf} - \Delta m'_0}{\sqrt{t_f}} \qquad [g \cdot cm^{-2} \cdot h^{-0.5}] \qquad (7.2)$$

where $\Delta m'_{tf}$ value of Δm on the straight line at time t_f [$g \cdot cm^{-2}$];
t_f duration of the test [h].

There is an increase in mass of the materials over a time in room (T ~19 °C, RH ~ 45 %), hot (T ~ 30 °C) and cold (T ~ 5 °C) conditions. To allow for a simpler comparison between results, the graphs have been presented using the same time range.

Mass gain of specimen over time in Room conditions on Figure 44 shows sharp increases for both samples, but the mass increase of sample BR-Treated spruce is more obvious. The readings of both sample kinds are nearly linear, illustrating the tread lines.

Mass gain of specimen over time in Hot conditions on Figure 45 shows a sharp increase in the first time period, but the reading then slowly falls. This may be caused due to a mistake of the experiment; the water from the tank evaporated and several samples were not properly immersed.

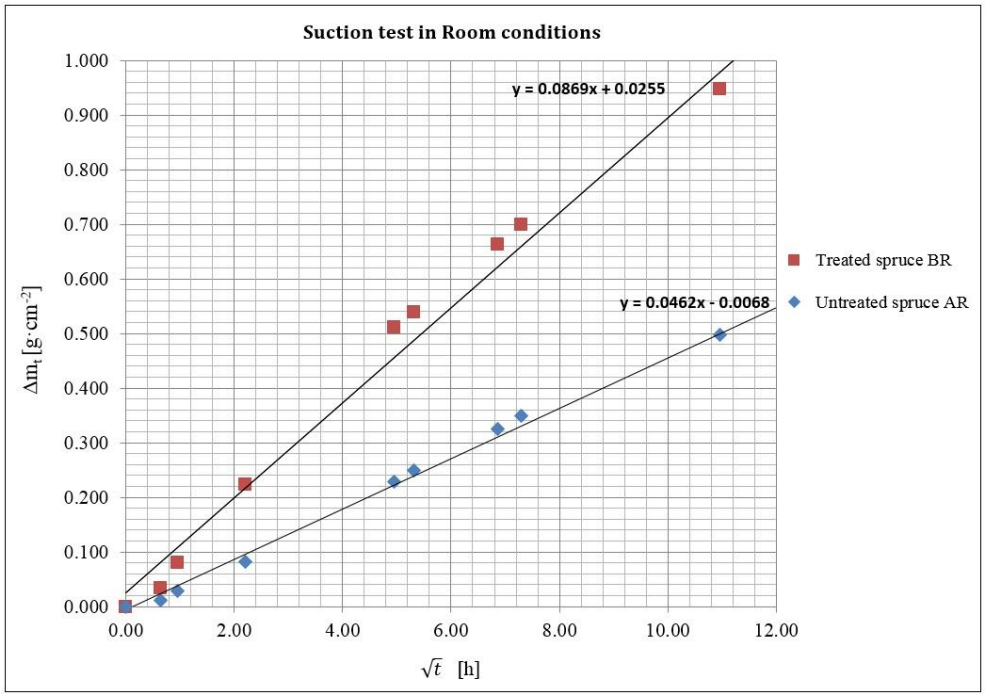

Figure 44: Mass gain of specimen over time in Room conditions [53]

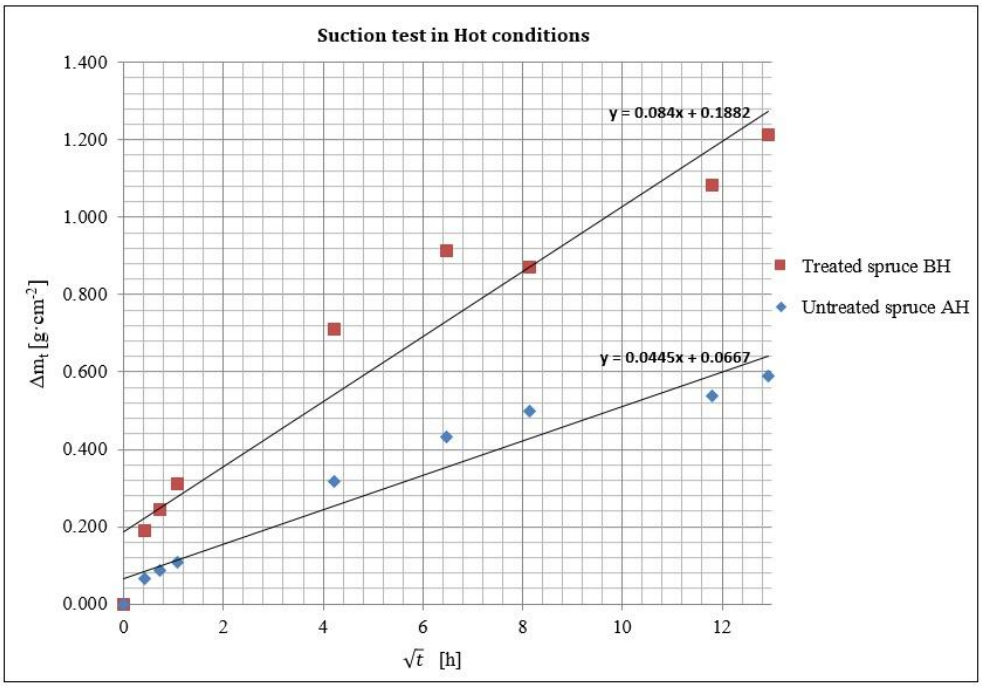

Figure 45: Mass gain of specimen over time in Hot conditions [53]

Mass gain of the specimen over time in Cold conditions in Figure 46 shows sharp and regular increases of both samples and again the mass increase of sample BF – Treated spruce is more obvious.

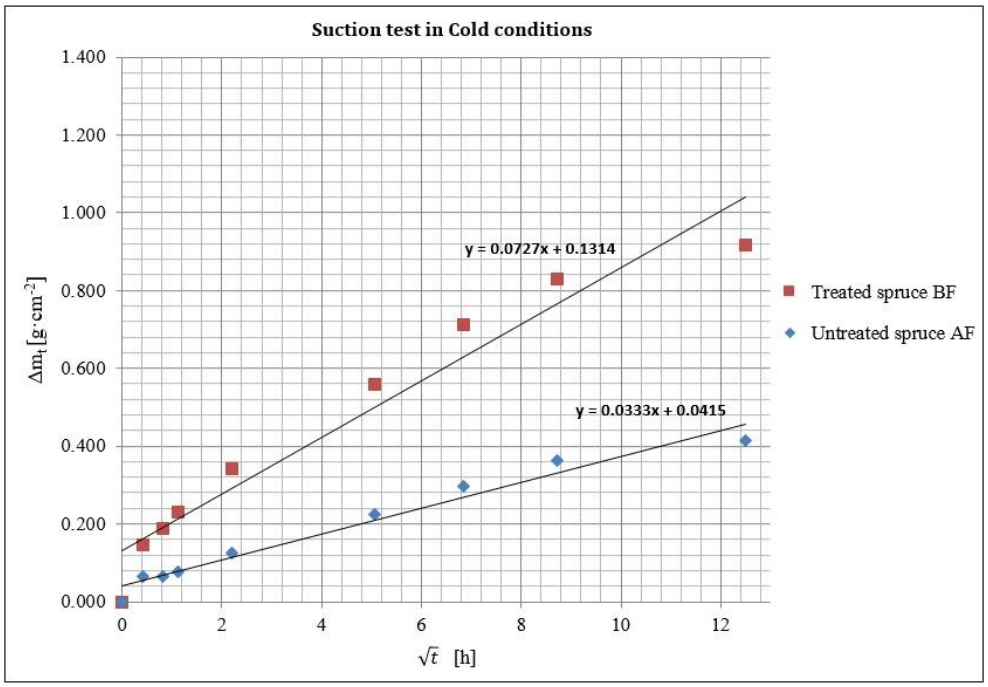

Figure 46: Mass gain of the specimen over time in Cold conditions [53]

Figure 47 shows the comparison of mass gain in Room, Hot and Cold conditions. It is clear that Treated spruce – B sample has higher mass increase Δm_t over time than untreated samples, regardless of the conditions to

which the samples were subjected. The highest increase of the mass Δm_t over time was for sample BH – Treated spruce immersed in water with temperature about 30 °C. Still, if there is a comparison of a material without a specific condition, Treated spruce (B) has nearly twice the mass gain than untreated spruce in the same amount of time.

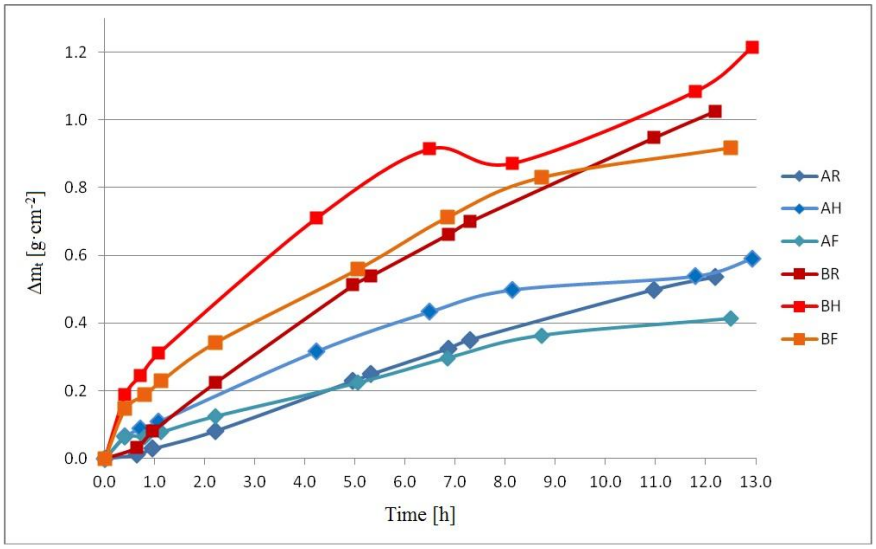

Figure 47: Comparison of mass gain in various conditions over time [53]

Looking at the water absorption coefficient W_w in Figure 48, the highest value is again BH – Treated spruce in Hot conditions, 0.0840 $g \cdot cm^{-2} \cdot h^{-0.5}$ and then BR – Treated spruce in Room conditions, 0.0833 $g \cdot cm^{-2} \cdot h^{-0.5}$. The sample with the poorest absorption coefficient W_w was AF – Untreated spruce in cold conditions, 0.033 $g \cdot cm^{-2} \cdot h^{-0.5}$.

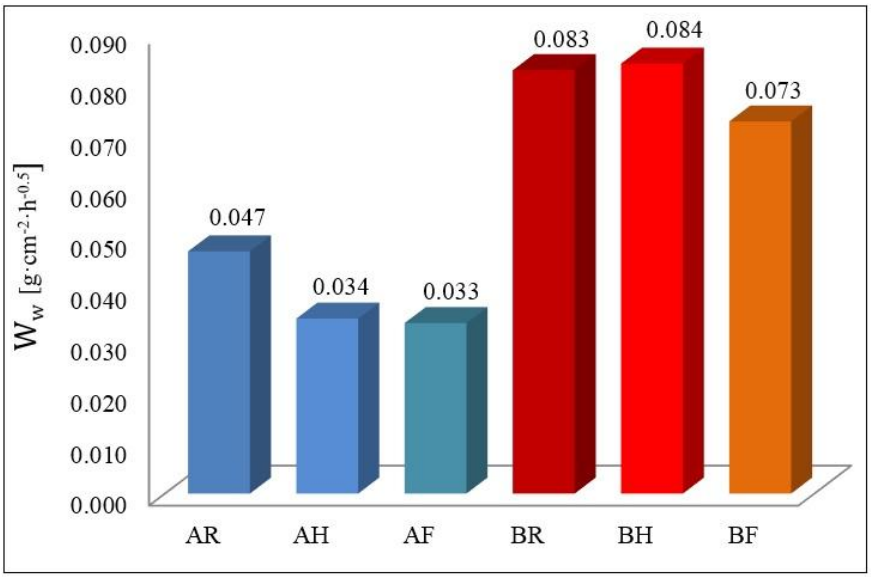

Figure 48: Total overview of water absorption coefficient W_w of A- untreated and B-treated spruce samples in Room, Hot and Cold conditions [53]

7.1.4 Conclusions and discussions

A – Untreated spruce: results show that Untreated spruce has about the same water absorption coefficient W_w in Room and Hot water conditions. The lowest value was shown for AF – Untreated spruce in Cold conditions.

B – Treated spruce: results show that the highest water absorption coefficient W_w is in Hot water conditions, but is also similar in Room conditions. The average difference of these water temperatures is about 10 °C.

As the experiments show, the Treated spruce (B-samples) has a higher value of mass gain Δm_t over time and also a higher water absorption coefficient W_w than Untreated spruce (A-samples). Out of the three test conditions, the Hot water condition, with a temperature around 30 °C had a higher influence on the water absorption and an increase of mass gain for both Untreated and Treated samples. The difference of W_w of Untreated and Treated spruce in Hot water conditions is about 56 %.

The liquid water did not appear on the top surface of the specimen in any condition. Removing the samples from the device proved to be a problematic part of the experiment, as it was very likely that the samples would be contaminated by grease from human fingers. In order to prevent this, the gloves should be used to ensure clean samples at all times.

The experiment results were quite unexpected, because in the same conditions, the treated samples had nearly twice higher mass gains Δm_t and water absorption coefficients W_w. An explanation for this phenomenon could be a difference in density of the material together with differences of slow and fast grown wood, from which the samples came.

Nevertheless, the water absorption of wood is an extremely variable property, which accounts for the huge natural variation. To draw a conclusion of this basic property, the work would need to be performed with matched controls for treated materials and a very high number of samples (800 samples instead of 8 samples) must be used. The treated material came from a very small number of boards - even as few as one or two - and no matching controls were cut from the boards before the CO_2 impregnation treatment. The higher water absorption coefficient that was measured for the B-samples could very likely be due to the fact that the water absorption coefficient W_w in these boards was naturally higher - even without treatment - than the non-treated boards.

7.2 Determination of sorption isotherms by desiccators' method

The following determination of sorption isotherms of spruce is based on the author's experiments within the framework of this thesis. The presented results describe the adsorption curves of Untreated and Treated spruce.

The experiment was performed according to [42]. For determination of the sorption curve desiccators' method was used.

7.2.1 Materials

The wood samples were collected in a laboratory and cut in approximate dimensions of 14 x 22.5 x 35 mm. The annual ring growth was between 1.5-2.5 mm. The density of the matched controlled dry material for untreated (-) samples was 435 $kg \cdot m^{-3}$ and for treated (+) samples 450 $kg \cdot m^{-3}$. Five pieces of A and five pieces of B samples represented the material in each of seven climate conditions to get the most appropriative behaviour of the material. In Figure 49 the total number of the samples which were put into the desiccators is shown. The series "A" had to be replaced with the series "H", because of unexpected behaviour during the conditioning in the chamber.

Preparation of saturated solutions

Seven test atmospheres were selected in the humidity range. The specific climate conditions for each series needed to be prepared by saturated solutions (Table 18). A mixture of distilled water and the quantity of substance necessary to produce a saturated solution was heated to the given temperature (where the excess of substance is just dissolved) and it then cooled slowly to room temperature, with continuous stirring. Reagent grade chemicals were used for preparation. Samples used in each environment are shown in Table 18.

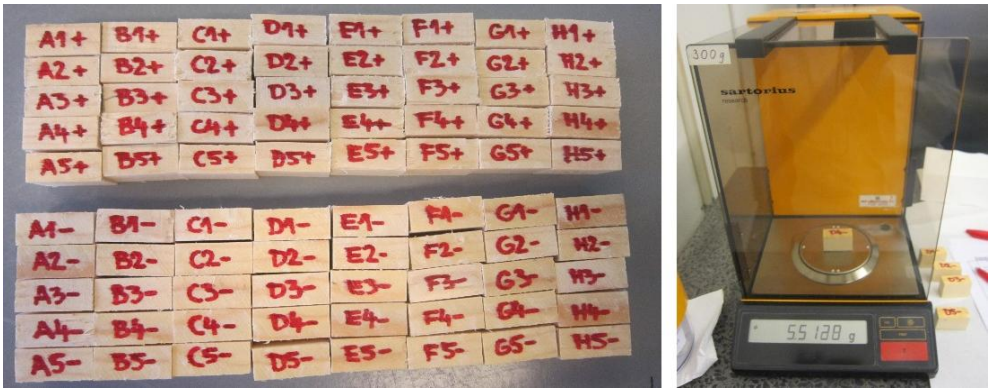

Figure 49: Wood samples of treated (+) and untreated (-) spruce (left); Weighing the sample on the weigh (right) [photos author]

Table 18: Mixture of distilled water and the quantity of substance necessary to produce a saturated solution for desiccators' method; Relative air humidity above saturated solution in equilibrium

Sample		Element	Salt	RH at T 20 °C	Water of crystallisation[1)]	Solubility	
						at T of water [°C]	g per 100ml of distilled water
H ±	1	LiCl	Lithium chloride	11,31 ± 0,31	0 · H_2O	95	130
B ±	2	$MgCl_2$	Magnesium chloride	33,07 ± 0,18	6 · H_2O	100	367
C ±	3	NaBr	Sodium Bromide	59,14 ± 0,44	0 · H_2O	100	121
D ±	4	NaCl	Sodium chloride	75,47 ± 0,14		100	39.12
E ±	5	KCl	Potassium chloride	85,11 ± 0,29		100	56.7
F ±	6	KNO_3	Potassium Nitrate	94,62 ± 0,66		100	247
G ±	7	K_2SO_4	Potassium Sulphate	97,59 ± 0,53		100	24.1

[1)] Molecule of crystal water per molecule of salt

7.2.2 Method

For this experiment desiccators' method was used. The test apparatus is drawn in a vertical section in Figure 50, in the horizontal section in Figure 51 and shall include:

- weighing cups which do not absorb water and with tight-fitting lids;
- balance, capable of weighing to an accuracy of ± 0.01 % of the mass of the test specimen;
- drying oven, in accordance with EN ISO 12570;
- desiccators, capable of maintaining RH within ±2 %;
- constant-temperature chamber, capable of maintaining the specified test temperature to an accuracy of ±0.5 K

The specimen was dried to constant mass. Whilst maintaining a constant temperature, the specimen was placed consecutively in a series of the test environments - desiccators, with relative humidity increasing in stages. They were then left for about three months, being periodically weighted, until they reached equilibrium with the respective environment. Constant mass was reached when the change of mass between three consecutive weightings, each made at least 24 h apart, was less than 0.1 % to the total mass. After establishing the moisture content at each relative humidity the adsorption curve could be drawn.

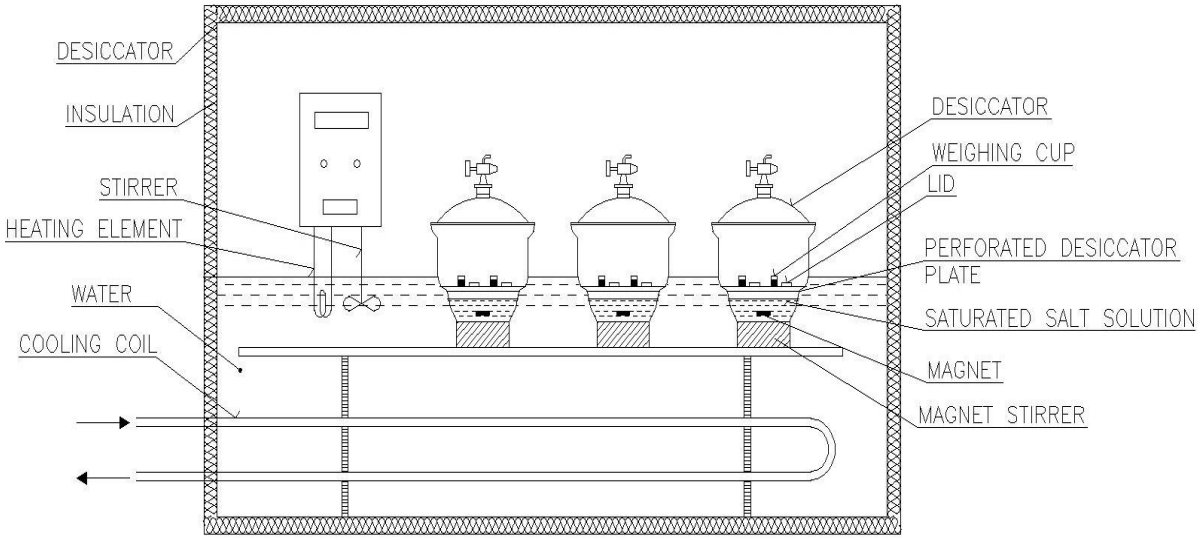

Figure 50: Vertical section of the constant-temperature chamber with placement of the desiccators in the water, including the saturated salt solution and the wood samples. Stirrer help the heating and cooling element keep the desired conditions in the chamber [author]

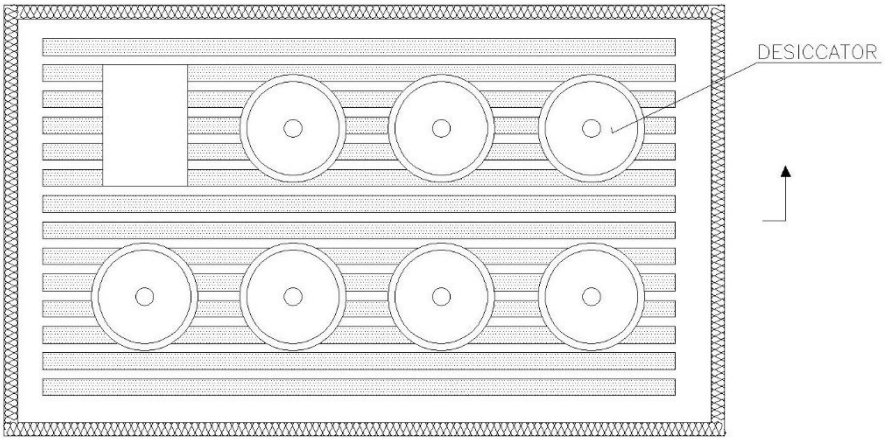

Figure 51: Horizontal section of the constant-temperature chamber [author]

Accuracy of measurement

The error in the moisture content can be established by using Equation (7.3):

$$\frac{\Delta u}{u} = \pm 0.0002 \frac{m_0}{m - m_0} \quad [-] \qquad (7.3)$$

where u moisture content mass by mass;
m mass of test specimen [g];
m_0 mass of dried test specimen [g].

In Figure 52 the author is placing the desiccators with wood samples into the constant-temperature chamber.

Figure 52: Constant-temperature chamber (left), author is placing the desiccators into constant-temperature chamber (right) [photos author]

Control of environmental conditions in desiccators

Reference sorption curves shall be established at T of 23 ±0.5 °C.

The relative humidity within the weighing cup is determined by the saturated solution used in the desiccators. The temperature in the constant-temperature chamber was carefully monitored with calibrated instruments and regularly logged.

Calculation and expression of results

The moisture content mass by mass, is calculated by Equation (1.10) for each specimen. For the adsorption curve or for the desorption curve, the mean of the calculated moisture content for a various specimens at each relative humidity is taken.

7.2.3 Results

After calculating the mean moisture content of the various test specimens at each relative humidity, the adsorption curve could be drawn by joining the data points with straight lines (Figure 53).

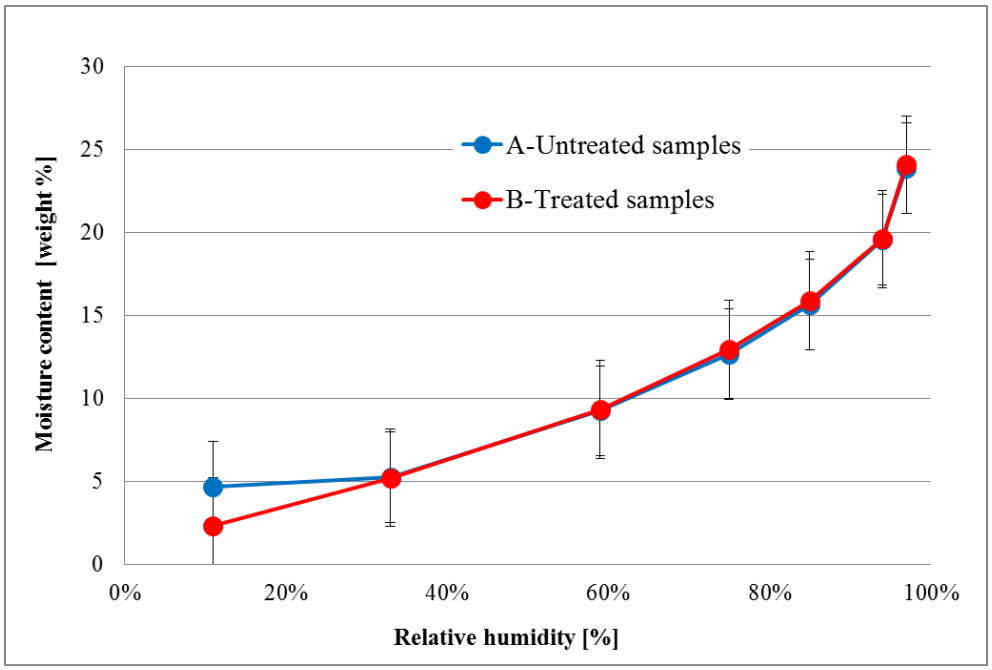

Figure 53: Sorption isotherms for A-untreated spruce samples (blue) and B-treated spruce samples (red)

7.2.4 Conclusions and discussions

The sorption curve for natural A spruce samples and impregnated B samples was established at a series of increasing equilibrium relative humidity. These curves establish a relationship between the moisture content of a material at equilibrium with the environment and the relative humidity of the ambient air at a specified temperature.

The results obtained clearly correspond to theoretical knowledge of sorption isotherm, as shown in Figure 12 and Figure 14.

There were no differences found between the isotherms for properties of natural spruce wood and impregnated spruce using supercritical CO_2. The differences found between the samples H ± placed in the desiccator with 11 % RH can be caused due to incautious placement of the samples in to the desiccator, thereby disturbing the equilibrium with the lowest relative humidity of ambient air.

7.3 Determination of water vapour diffusion resistance factor

The following determination of water vapour transmission properties of spruce is based on the author's experiments within the framework of this thesis. The presented results describe the water vapour diffusion resistance factor of Untreated and Treated spruce.

The experiment was performed according to [43] which specifies a method based on a cup test to determine the water vapour permeability of building materials under isothermal conditions. It applies to all hygroscopic building materials and results obtained by its method can be suitable for design purposes.

The aim of the experiment is to measure diffusion coefficients of spruce samples for comparison to the theoretical diffusion coefficient. Since timber is an orthotropic material, the diffusion varies, amongst other things, in radial, tangential and longitudinal direction. The material directions of interest for this experiment are tangential.

The test conditions for the "Dry cup" test give information about the performance of materials at low humidity when moisture transfer is dominated by vapour diffusion. The "Wet cup" test gives guidance on the performance of materials under high humidity conditions. At higher humidity, the material's pores start to fill with liquid water; this increases the transport of liquid water and reduces vapour transport. Tests in this area therefore give some information about liquid water transport within materials. [44] The relations between permeability and relative humidity are shown in a graph in Figure 54.

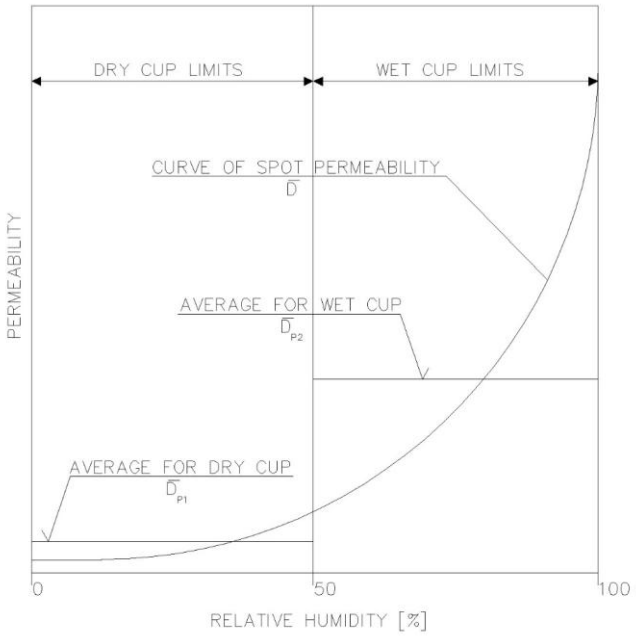

Figure 54: Relations between permeability and relative humidity [30]

7.3.1 Materials

The test specimens are representative of the product and were cut so that the parallel faces were normal to the direction of vapour flow of the product in use.

The six matched controlled samples of each Untreated (-) and Treated (+) spruce were collected in the laboratory and cut in a tangential direction in a circle shape. Such cut wood samples were put into Plexiglas rings, with the space between being sealed with the epoxy mixture of Component A and Component B from the company Condor® to ensure the airtight connection for the cup test (Figure 55). The diameter of a circular specimen of wood without the Plexiglas ring and epoxy was on average 0.08 mm and the average thickness of all specimens was 11.2 mm. The upper and lower free surface areas did not differ by more than 3 % of the mean in the case of homogeneous material.

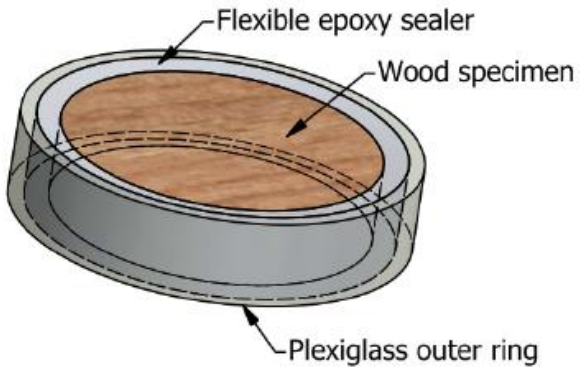

Figure 55: Wood specimen assembly: fixed in the Plexiglas outer ring and sealed in airtight connection by flexible epoxy sealer [44]

The numbering of the samples of Untreated (-) and Treated (+) spruce as well as the numbering of the cups used in the cup test experiment are described in Table 19.

Table 19: Numbering the samples of Untreated (-) and Treated (+) spruce for the Cup test

	Untreated spruce (-)			**Treated spruce (+)**		
Cup No.	Cup 1	Cup 2	Cup 3	Cup 4	Cup 5	Cup 6
Sample	B1-	B2-	B3-	B2+	B3+	B4+
Cup No.	Cup 7	Cup 8	Cup 9	Cup 10	Cup 11	Cup 12
Sample	C1-	C3-	C4-	C1+	C3+	C4+

After the specimens were assembled and the sealer had cured, the test specimens were stored at 23 °C, 65 % RH (Figure 56) for a couple of weeks until they were in equilibrium with surrounding conditions.

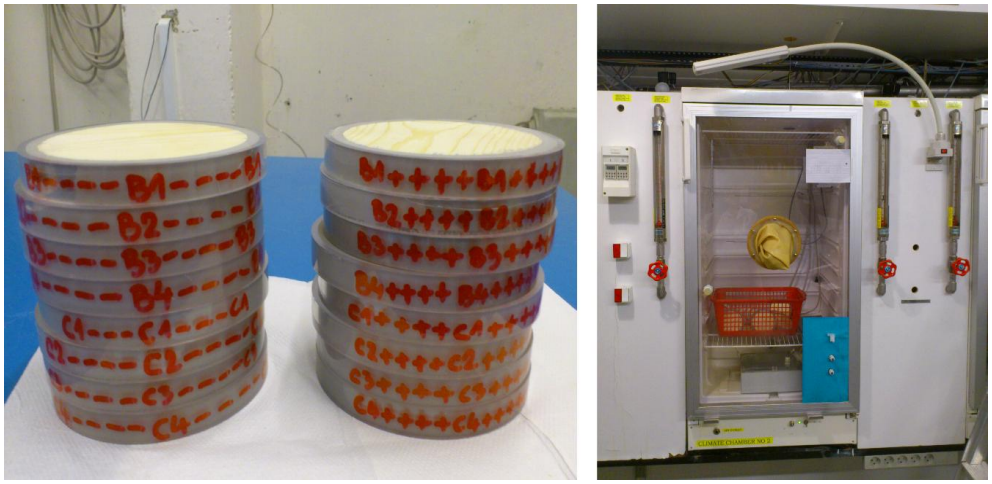

Figure 56: Total number of wood samples of Treated (+) and Untreated (-) spruce prepared for the cup test method (left); Conditioning the samples for wet cup test in the climate chamber (right) [photos author]

The specimen to be tested was placed in a sealed cup with one side of the specimen exposed to climatic conditions inside the cup and the other side exposed to the conditions outside the cup. The inside of the cup is partially filled with a desiccant (dry cup) or an aqueous saturated solution (wet cup) creating the desired RH. The procedure of positioning the airtight sealing on the lower and upper side of the wood specimen with the epoxy ring is shown in Figure 57.

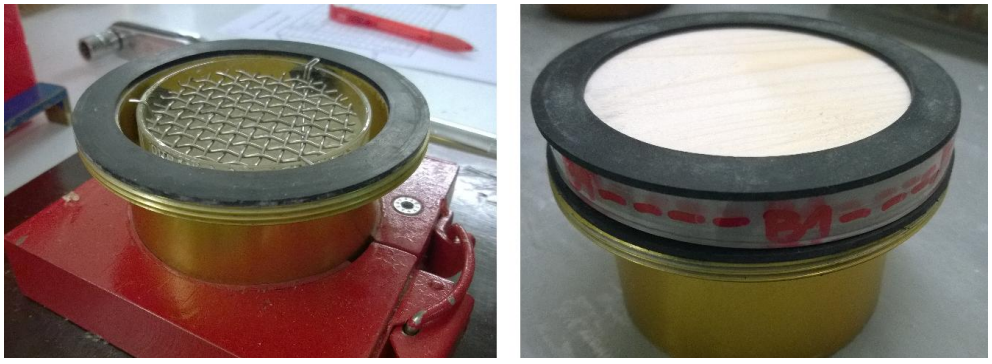

Figure 57: Placing the salt solution on the lower part of the wood sample (left), position of sealing on the wood sample in tangential cut (right) [photos author]

Two cup conditions were used in this experiment:

- dry cup filled with desiccant (Silicate gel) which absorbs moisture making an RH of 0 %;
- wet cup filled with Potassium nitrate KNO_3 producing a RH of 93 % inside the cup.

A regular check was made to ensure that the saturated solution remained a mixture of liquid with a large amount of undissolved substance.

The final assembly of the cups used in the experiment (see Figure 58) are of circular construction and made of metal. Their purpose is to seal the specimen in between the two different environments and house the cup environment (wet or dry).

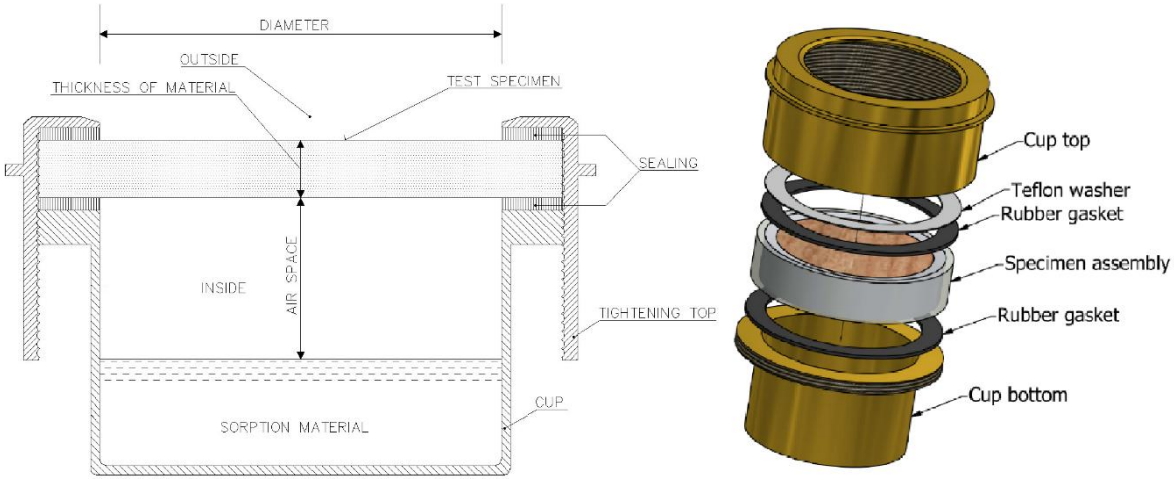

Figure 58: Designations of materials in the Cup assembly [author (left), 44 (right)]

The aqueous solution inside the wet cups must not come in contact with the surface of the specimen as this would influence the moisture flow across it. To combat this, a net is placed between the solution and the specimen, acting as a splashguard for when it is moved around.

The cup assembly (Figure 58) of all 12 samples was then placed in a temperature and humidity controlled test chamber set to 23 °C and 50 % RH (Figure 59).

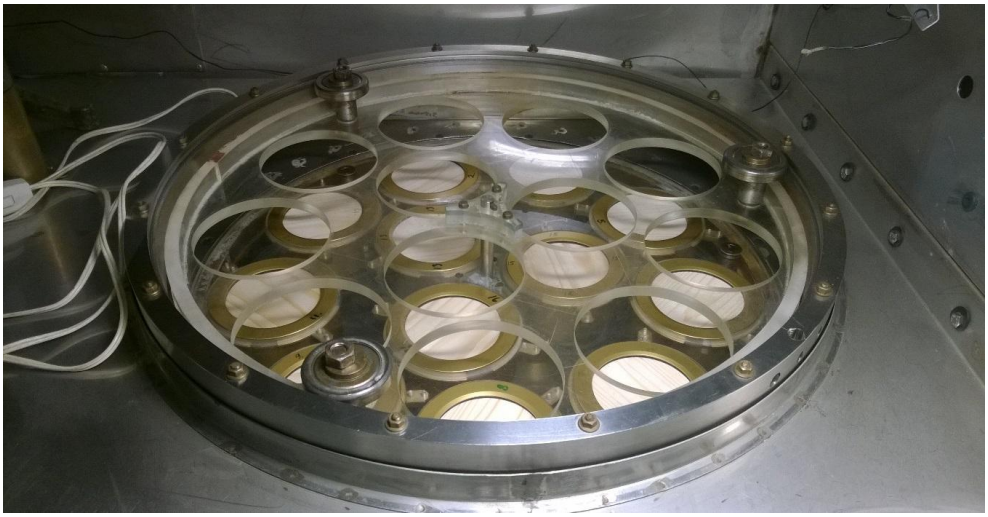

Figure 59: Total view on placed wood samples in the test chamber [author]

This creates a pressure gradient across the specimen due to the different partial vapour pressures between the test cup and the chamber. A one

dimensional vapour flow occurs through the permeable specimen, which reached a steady state within several days. The cup assembly, including the specimen, was weighed periodically and logged. The standard specifies that the experiment must continue until five successive determinations of change in mass per weighing interval for each test specimen are constant within ±5 % of the mean value for this specimen.

7.3.2 Method

The test apparatus is drawn in Figure 60 and Figure 61 and shall include:

- weighing cups;
- analytical balance, capable of weighing the test assembly with the repeatability needed for the required accuracy;
- constant temperature, constant humidity chamber, capable of being maintained within ±3 % relative humidity around the set point relative humidity and ±0.5 K around the set point temperature. In order to ensure uniform conditions throughout the chamber, the air shall be stirred so as to obtain velocities between 0.2 $m \cdot s^{-1}$ and 0.3 $m \cdot s^{-1}$;
- suitable sensors and a logging system to continuously record the temperature, relative humidity and, if necessary, the barometric pressure within the test chamber. The sensors shall be calibrated at regular intervals;
- sealant, which is impermeable to water vapour, does not undergo physical or chemical changes during the test and does not cause physical or chemical changes to the specimen.

Figure 60: Test chamber with the wood samples and connected PC to log the data [author]

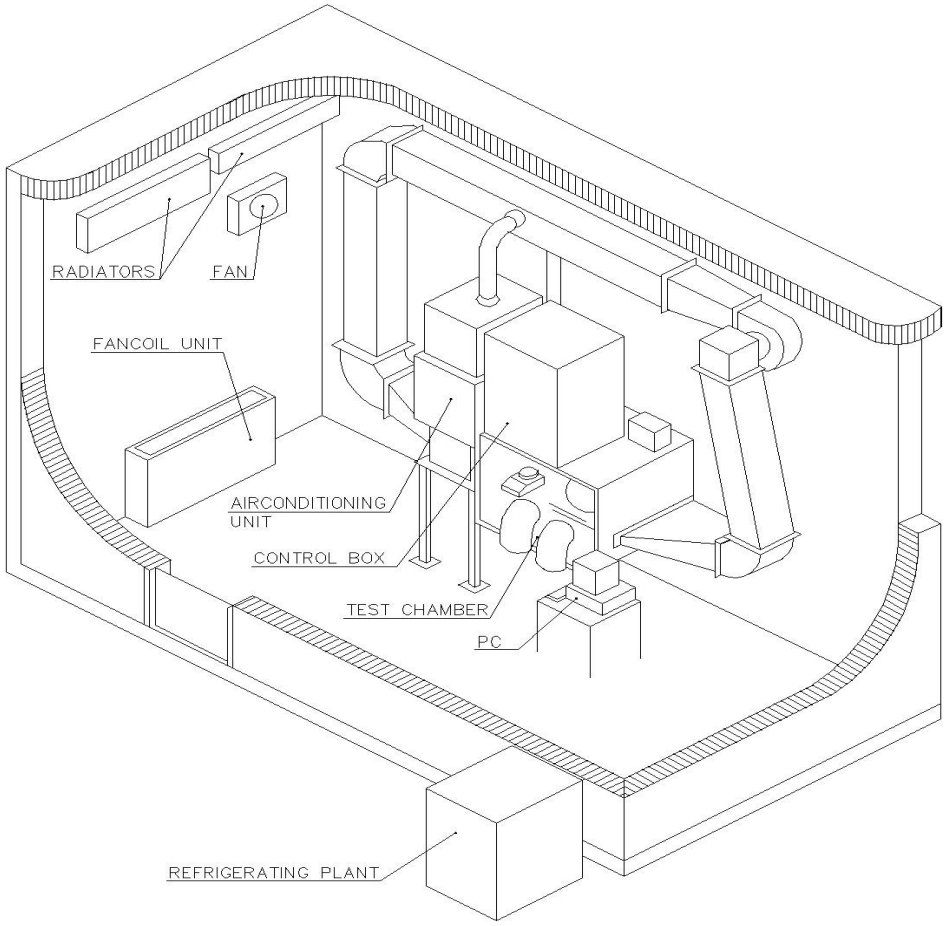

Figure 61: Equipment for the cup test method [author]

The climate chamber (Figure 60, Figure 61) that makes up the environment outside the cups must be able to maintain ±3 % relative humidity and ±0.5 °C temperature. To ensure uniform conditions, the air is stirred with velocities between 0.2 $m \cdot s^{-1}$ - 0.3 $m \cdot s^{-1}$. The chambers temperature and humidity were continuously recorded and logged.

Mass change rate

In the cup test, the parameter that is measured for each set of successive weightings of the specimens, calculates the mass change rate per time for a single determination "Δm_{12}" using:

$$\Delta \dot{m}_{12} = \frac{m_2 - m_1}{t_2 - t_1} \qquad [kg \cdot s^{-1}] \qquad (7.4)$$

where m_1 mass of the test assembly at time t_1 [kg];
m_2 mass of the test assembly at time t_2 [kg];
t_1 and t_2 successive times of weightings [s].

Throughout the experiment, a mass change is plotted and a regression line is fitted to the data once the flow has reached a steady state. The slope of that regression line is denoted as q.

The **water vapour permeance** "W" is given by:

$$W = \frac{q}{A_{sp} \cdot \Delta p_v} \qquad [\mathrm{kg \cdot s^{-1}}] \qquad (7.5)$$

where q the slope of the mass/time regression line;
A_{sp} exposed area (arithmetic mean of the free upper and free lower surface areas) of the test specimen [m^2];
Δp_v difference in water vapour pressure across the specimen [Pa].

The value of Δp_v shall be calculated from the mean of the measures temperature and relative humidity over the course of the test. This can be accounted from on either side of the sample using:

$$p_{sat} = \varphi \cdot 610.5 \cdot e^{\frac{17.269-\theta}{237.3+\theta}} \qquad [\mathrm{Pa}] \qquad (7.6)$$

If highly permeable materials or thin membranes, with $s_d < 0.2$ m, are being tested, the resistance of the air gap between the base of the sample and the desiccant or saturated solution shall be taken into account in the calculation of water vapour premeance W. [43]

The mass time history throughout the experiment along with the fitted steady state solution and error estimate of the mass change rate for the last five consecutive weightings for individual specimens were monitored.

7.3.3 Results

Averaged results for each untreated and treated specimen are shown for dry conditions (0-50 %) in Figure 62; the average μ value for A-untreated spruce samples was set to be 146.85 [-] and for B-treated spruce 142.49 [-]. For wet condition (50-100 %) are the averaged results for each untreated and treated specimen shown in Figure 63; the average μ value for A-untreated spruce samples was set to be 32.96 [-] and for B-treated spruce 35.58 [-]. The comparison of wet and dry cup for both kinds of wood is shown in Figure 64.

The average value for water vapour resistance factor from previous studies [44] was proved that the radial cut has a higher rate of diffusion then the tangential ones, especially in the wet condition.

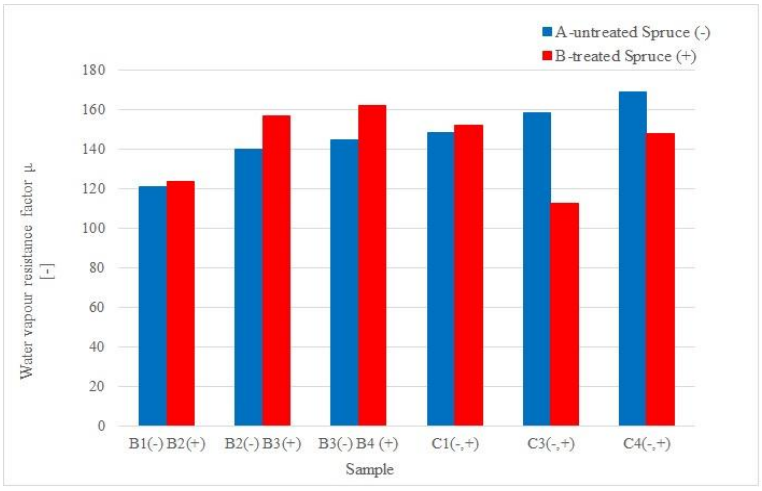

Figure 62: Water vapour resistance factor for each A and B spruce samples in dry (0 %) cup test; the average μ value for A samples was set to be 146.85 [-] and for B samples 142.49 [-]

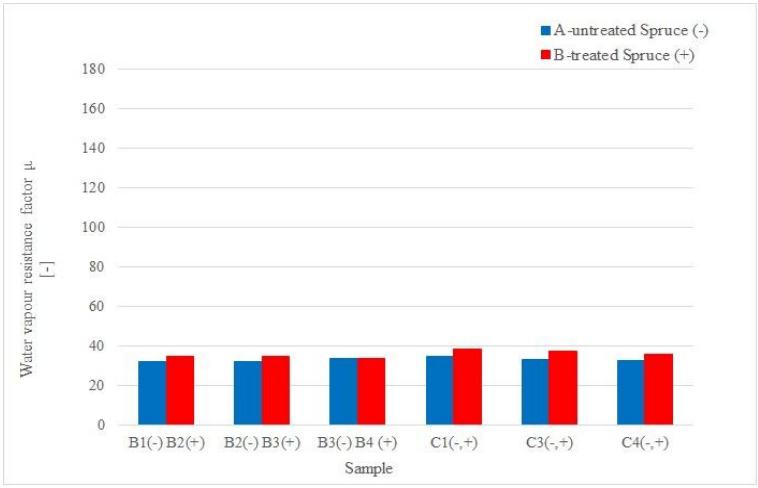

Figure 63: Water vapour resistance factor for each A and B spruce samples in wet (93 %) cup test; the average μ value for A samples was set to be 32.96 [-] and for B samples 35.58 [-]

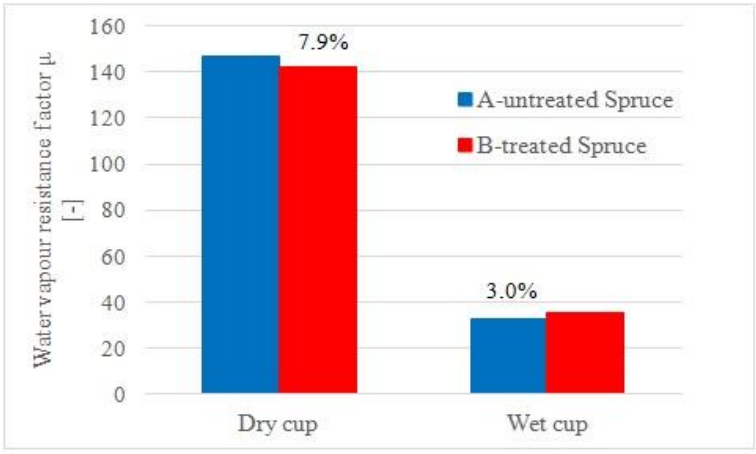

Figure 64: Mean water vapour resistance factor μ [-] for each A and B samples in dry and wet cup test; the wet cup resistance is about 3-4 times lower than dry cup, which corresponds to the statement that μ decreases for increasing RH.

7.3.4 Conclusions and discussions

Average value for water vapour diffusion resistance factor μ of B-treated samples is 7.9 % lower than A-untreated samples in the dry cup test. On the other hand, the wet cup test showed 3.0 % higher value of water vapour resistance μ for B-treated spruce samples than A-untreated spruce samples, always referenced to an A-untreated value. The dry cup C3+ appears to have an error during the measurement, because the decreased value of μ does not correspond to other cups in the wet experiment, which could then rapidly influence the result.

However, measurements of μ which were performed at different levels of relative humidity (dry-cup and wet-cup) may, according to [59], result in different values for one and the same material. This is due to surface diffusion which becomes noticeable at higher humidity levels but would be more properly treated as liquid transport. This additional moisture transport is usually not separated out in the analysis of the measurements and is lumped together with vapour diffusion, reducing the apparent diffusion resistance, resulting in a lower μ-value. In these cases, it is more appropriate to use a constant μ-value and to adjust the liquid transport coefficients to include surface diffusion. [59]

In the HAM simulation programme Delphin, is standardly used μ-value for spruce with fibres across the grain 236.224 [-] as the dry cup value, and such μ -values were used in the numerical calculations in Chapter 9.2.

8. MECHANICAL EXPERIMENTS ON SPRUCE

8.1 Determination of bending and shearing

The following determination of bending and shearing creep of spruce is based on the author's experiments within the framework of this thesis. The presented results describe the creep properties in longitudinal direction during long-term tests for bending and shearing of Untreated and Treated spruce.

The experiments were performed according to [9]. This issue and results were presented at the conference and published in [23].

8.1.1 Materials

The samples of A-untreated spruce and B-treated spruce were purchased from standard distribution of lumber and used in the study. Six samples were used in the failure load test with the dimensions of 25 × 25 × 400 mm and another twelve samples in the creep test with the dimensions of 25 × 25 × 700 mm (W × H × L). All of the samples were chosen without any knots with the purpose to get the most homogenous material and decrease the amount of uncertainties.

Table 20 shows the naming of all test specimens used for both long-term creep test, such as bending and shear tests.

Table 20: Naming the specimen for each series of test [23]

	Bending test		**Shear test**	
	A-untreated	**B-treated**	**A-untreated**	**B-treated**
Failure load test	A 1-3	B 1-3	A 4-6	B 4-6
Creep test	AL 1-3	BL 1-3	AL L4-6	BL 4-6

The samples had longitudinal direction of the fibres along the wooden beams, and the force applied to them was done in the case of 2, 3 B-treated samples for the bending test in tangential direction (Figure 65) and in the rest of the cases in radial direction of the wood (Figure 66). [23]

Figure 65: Radial and tangential (2, 3 B-samples for bending) grain orientations of the beams for bending test. The load was applied in the horizontal plane of the picture [23]

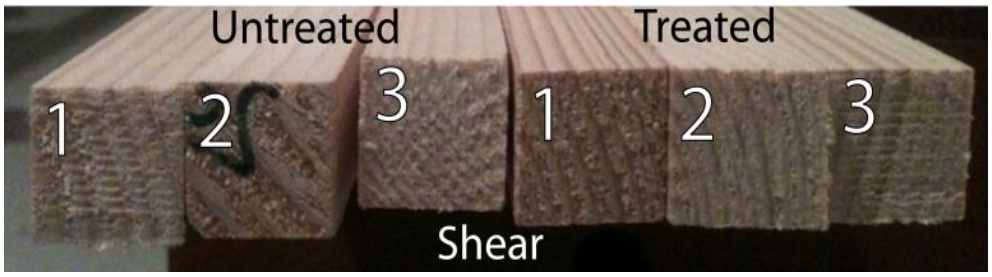

Figure 66: Radial and tangential (2, 3 B-samples for bending) grain orientations of the beams for shear test. The load was applied in the horizontal plane of the picture [23]

The shearing test was also conducted simultaneously with the creep test by means of 9 mm of deep cuts applied on, with a distance of 78 mm between them [9], as shown in Figure 67.

Figure 67: Samples for shearing test were cut 9mm deep on opposite sides [23]

The atmospheric test condition in the laboratory were regularly controlled and defined with a T of 20 ±1 °C and RH of 47 ±2 %.

8.1.2 Method

The samples were loaded with 30 % of the failure load to avoid any fail during the test period. The commercial three-point bending machine Stenhøj was used for determining the failure load of the individual species, as can be seen in Figure 68. For each test and wood type, three measurements (in a total of 12) were completed in order to obtain an average failure load.

The mass of the creeping-load m_{CL} for the tests was calculated by means of the following method on the basis of the sketch diagram and the photo of the test set-up, shown in Figure 69.

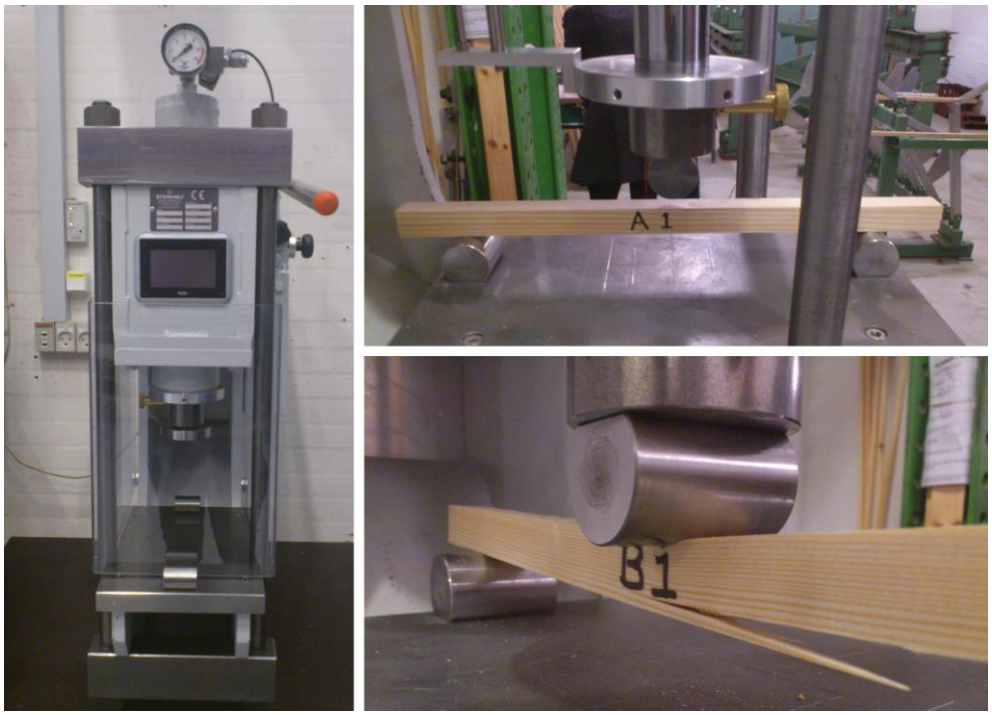

Figure 68: Three point bending machine Stenhøj (left), A-untreated spruce sample is prepared for determining the failure load (top right), B-treated spruce sample reaching load bearing capacity (bottom right) [author, and 23 (bottom right)]

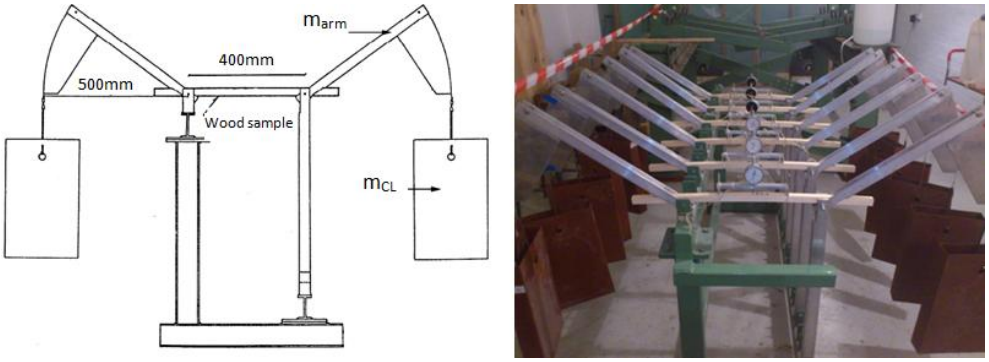

Figure 69: The test setup for bending and shearing test: Sketch diagram (left) and the test setup for the creeping test (right) [23]

The bending moment "M_u" for this load was calculated:

$$M_u = \frac{P_u \cdot L}{4} \qquad [\mathrm{N \cdot mm^{-1}}] \qquad (8.1)$$

where P_u failure load of the Stenhøj machine [N], see also Figure 69;
L beam span [mm], defined as 300 mm as commonly used in the literature and which also corresponds to the machine set-up of the supports.

In the creeping test, the bending moment applied on the samples is 30 % of the bending capacity, respectively the failure load M_u.

The mass of the bending moment "m" can then be calculated:

$$m = \frac{M_{30\%}}{g \cdot L} \quad [\text{kg}] \qquad (8.2)$$

where $M_{30\%}$ bending moment applied on each sample [$N \cdot mm^{-1}$];
g acceleration due to gravidity = 9.81[$m \cdot s^{-2}$];
L moment arm [mm].

In the calculation, it is assumed that the force is applied on a location that is 500 mm from the rotation axis and is perpendicular to the beam.

Then the mass of the creeping-load m_{CL} is calculated by subtracting the mass of the arm (0.437 kg) from the mass of the bending moment. So gained mass of the creeping-load m_{CL} was applied on both sides of the wood samples (Figure 70, left) and the degree of the deflection was regularly measured at the centre of the beam as a function of time, as can be seen in Figure 70, right. [23]

Figure 70: The set up for shearing test (left), The deflection measured on the A-untreated spruce sample in the shear test the 9mm deep cuts were applied on each sample, with a distance of 78 mm between each other (right) [author]

8.1.3 Results and discussions

The observations found in the failure load test P_u and equivalent mass of the bending moment, m, can be seen in Table 21. These equivalent masses of the creep-loads were then used for the weight applied on both sides of the wood samples in creeping tests.

For both the bending and shear tests, the failure load for the B-treated spruce is higher than for the A-untreated spruce samples. It can be explained that B-treated spruce has a higher density as a function of the treatment, and thereby should the mechanical properties differ from A-untreated spruce.

Table 21: Average load failures and the equivalent mass of the creeping-load m_{CL} obtained from failure load test on Stenhøj machine [23]

	Bending test		**Shear test**	
	A-untreated	**B-treated**	**A-untreated**	**B-treated**
$P_{u,average}$ [N]	1483	1708	905	1183
Equiv. mass of the creeping load[kg]	6.36	7.39	3.71	4.98

Bending test

The observations regarding the normalized deflection for the bending test – in the first hour are shown in Figure 71 and in the time of the test duration, respectively 7 days, in Figure 72.

Each of the test samples showed a unique variation for the case of tests applied for A-untreated such that: the deflections observed for samples 1 and 2 were found to be lower than sample 3. In the first hour of the test, samples 1 and 2 showed a slight deflection i.e. for the case of the sample 1 a steady deflection was observed of around 5–20 minutes, and in the case of sample 2 for around 15–36 minutes. The orientation of the radial/tangential direction was 45˚ for 1, 2, 3 of the A-untreated samples, as can be seen in Figure 71 and Figure 72, so the grain orientation could not explain the difference in deflection.

All three B-treated samples were also not behaving the same in comparison to each other. Samples 2 and 3 did not deflect as much as sample 1. The load was applied in the tangential direction for samples 2 and 3, and in the radial direction for sample 1, so the discrepancy between the samples could not be explained by a difference in fibre orientation. It was also interesting that the treated sample 3 did not deflect from the initial deflection in the first 16 minutes. [23]

According to the mechanical theory described in [9] it was expected that the biggest increase in deflection takes part in the first hour of the test, followed by a decrease in the increment rate. Only sample 1 for A-untreated and sample 3 for B-treated were observed with such increments in question. Looking at Figure 72, it is visible that the deflection decreases over time. There is also a probable measurement error, as the deflection of three samples for the B-treated sample has decreased after 2500 minutes, which was not expected to be observed. The creep behaviour was hence found to show no difference between A-untreated and B-treated samples, but the variations of the curves differ significantly. [23]

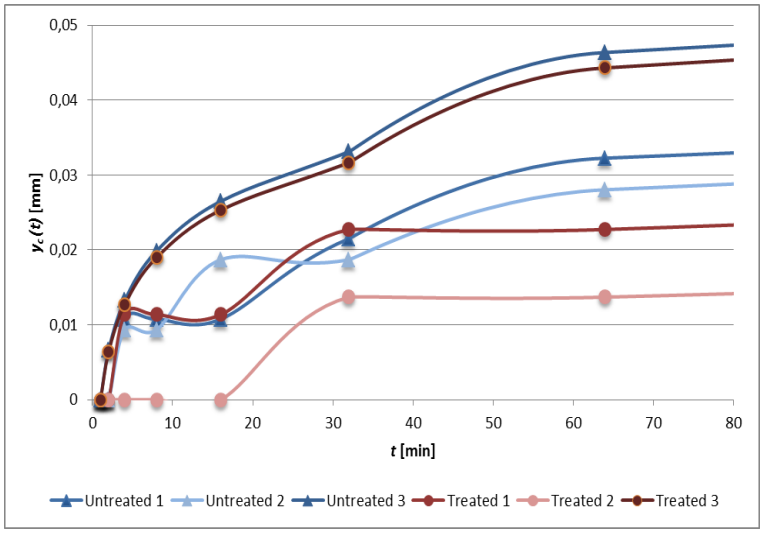

Figure 71: Deflection for the bending test – in the first hour [23]

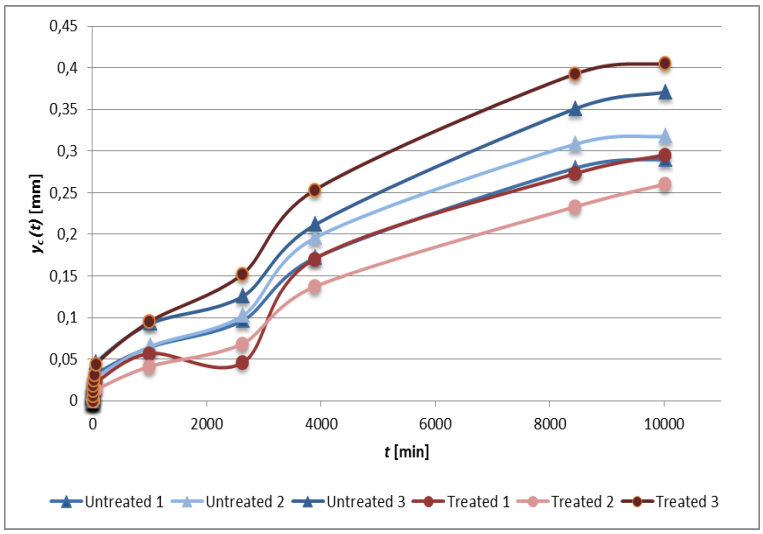

Figure 72: Deflection for the bending test – in the test period of 7 days [23]

Shear test

The observations regarding the normalized deflection for the bending test in the first hour are shown in Figure 73 and in the time of the test duration, respectively 7 days in Figure 74.

The variation of the results found for all samples in the shear test shows similar variations despite unique normalized deflection values found for each. As an example, sample 1 of A-untreated shows no deflection for an entire day, see Figure 73 and Figure 74, and the normalized deflection at the end of the test of the untreated sample 2 was almost double that of the untreated sample 1. Again, the direction of the load in relation to the fibre orientation of the beams does not agree with the difference observed for the deflection. [23]

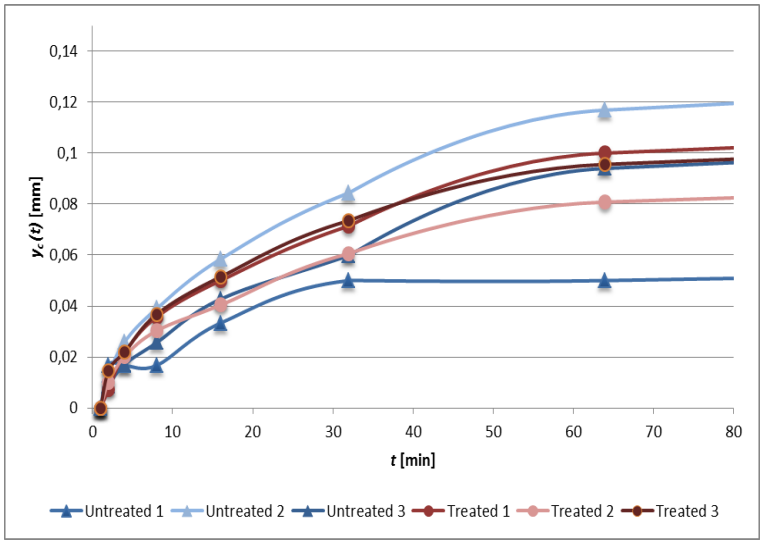

Figure 73: Shear test normalized deflection – in the first hour [23]

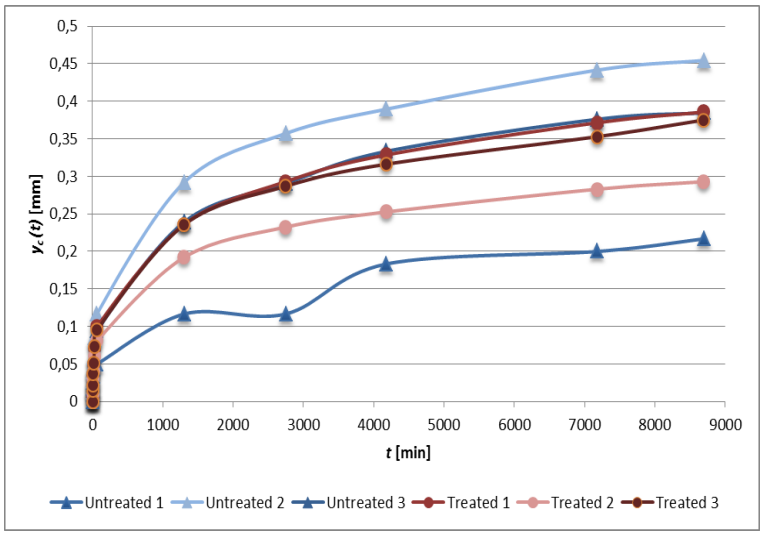

Figure 74: Shear test normalized deflection – in test period of 6 days [23]

8.1.4 Conclusions

The failure load for the Treated spruce is higher in both bending and shearing tests, for bending about 15 % and for shearing about 31 % respectively, compared to the reference values of A-untreated spruce.

In accordance with the observations with respect to creep tests, a slight change was observed between A-untreated and B-treated spruce. It is not expected that it is the case, as the Treated spruce is treated against biological decay and not treated in a way to try and increase the stiffness. In the pressure treatment process it gets a slightly higher density but nothing in the scale that it is possible to conclude that it could be the reason for the results.

Nevertheless, the creep behaviour seems to be the same for both types of spruce.

9. THERMAL AND HYGROTHERMAL NUMERICAL CALCULATIONS

9.1 Influence of using treated wood on heat losses of wooden building

The following numerical calculations are based on the author's experiments in Chapter 6.1 within the framework of this thesis. The presented results compare the thermal transmittance coefficient (Ψ) of chosen wall to floor junction with Untreated and Treated spruce used as a bottom plate with dried wood (0 weight-%) and wood with increased (35 weight-%) MC.

The calculations were performed according to [47, 55]. This issue and results were presented at the conference and published in [54].

9.1.1 Construction for simulations

The interpretation of the measurement results (Chapter 6.1) were used on the wall and the floor compositions on the basis of example in Andersen (2008), standardly used in Denmark [34]. The basic material properties used for the thermal simulations in detail were taken from commercial software for heat transfer in two dimensions – Heat 2 (Blomberg et al. 2000). The wooden bottom plate was a main subject of this study, so the thermal conductivity of this beam varied according to the results. Figure 75 shows the detail of the simulated parts of the wall to floor junction. [54]

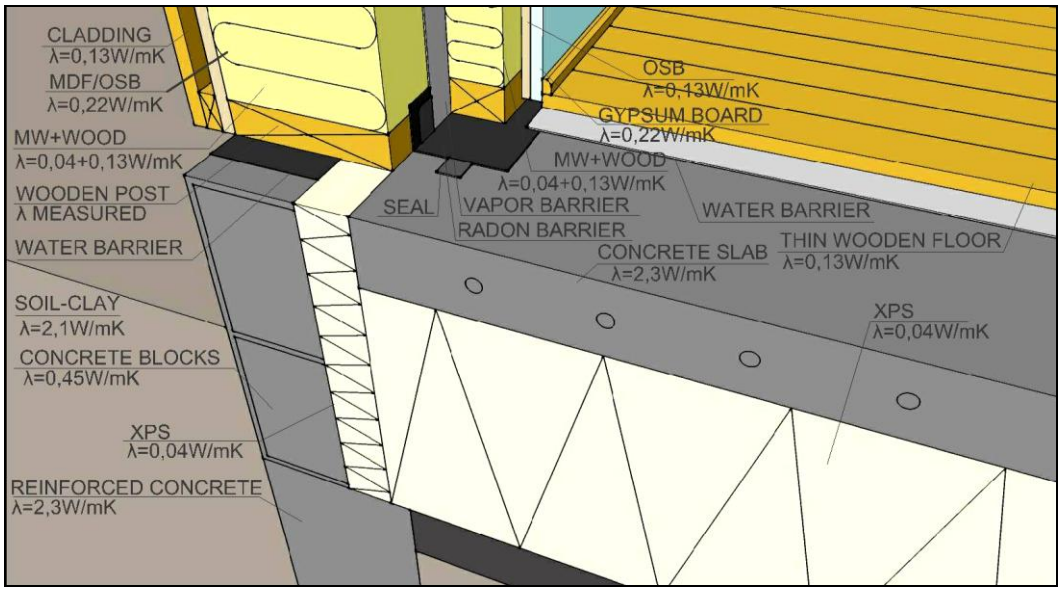

Figure 75: Illustration of the studied wall and floor joint with thermal conductivity parameters. The thermal conductivity of the bottom plate was the subject of this study [34, 54]

The thermal conductivity values affected by the moisture content were assigned only to a foundation wood element (bottom plate) which is in direct contact with the foundation and water barrier (see Figure 75). This means that wood contained in a wall structure, such as a wooden post 220 x 70 mm per 600mm and lathing for the inside wall 75 x 45 mm per 600 mm, had the standard thermal conductivity value of 0.13 $W \cdot m^{-1} \cdot K^{-1}$.

The highest and lowest values for both A-untreated and B-treated spruce samples were then subjected to further study for determining the difference in heat loss through the basement of the modelled wooden wall.

For better understanding of the influence of the moisture content to the thermal conductivity and heat losses, 1 m^2 of wooden wall was also modelled. The vertical wooden posts and posts for the inside wall were subjected to analysed conditions. [54]

9.1.2 Methods

The heat transfer investigation was performed in two dimensional (2D) commercial software of Heat 2, version 8.1 (Blomberg et al. 2000).

The method for calculation of the heat loss from the building to the ground was based on the simplified Danish method in [47] applicable for design proposes. The method is in agreement with the basic principles of the European standards; however it deviates from the method given in EN ISO 13370 as it defines linear thermal transmittance Ψ in a different way.

The method divides the heat loss stringently into a 1- and a 2-dimensional numerical transient contribution. Hereby the heat loss through the floor slab is considered as being 1D corresponding to the heat flow at the centre of the building and all 2D effects are considered as the thermal bridge effects for the wall/floor junction.

The detail was subjected to sinusoidal temperature variations in order to include the inertia of the soil volume, and to obtain a satisfactory level of accuracy on results [47, 55].

9.1.3 Geometry and simulation model

To ensure applicability of an adiabatic boundary for this detail 4 m of the floor slab and 1.5 m of the wall was modelled. For the soil 20 m is modelled both in a horizontal and vertical direction, according to EN ISO 10211-1.1997 [36]. Figure 76 shows the set-up for calculating heat loss with the position of the reference point. The mean temperature in the reference point during the heating season was used for calculating the 1D heat loss through the floor slab, as is described by Equation 1.23.

The reference point is located below the floor construction (see Figure 76) – the contact point of XPS and soil. Temperature at the reference point was measured in the middle of each month for the last simulated year. [54]

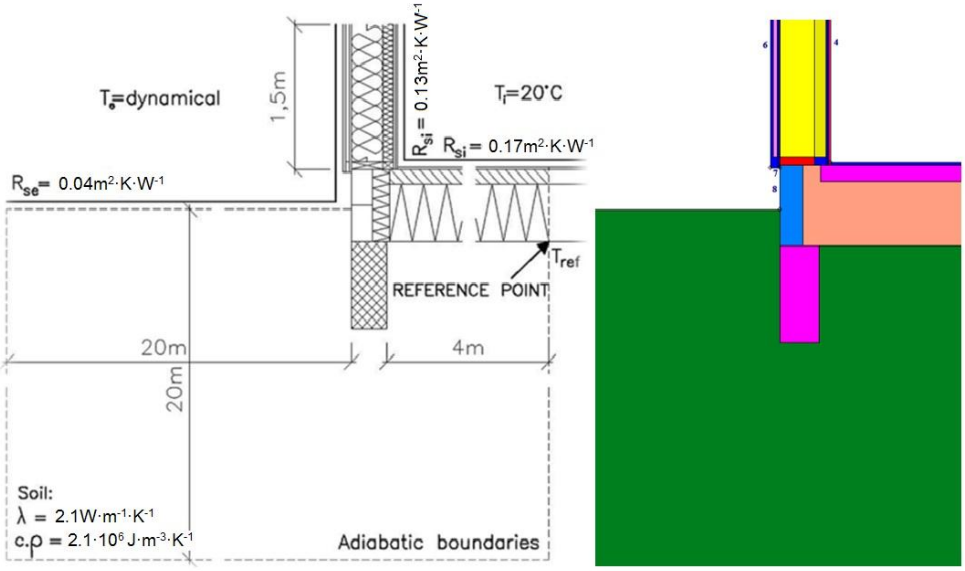

Figure 76: The set up for the calculation of the heat loss through the foundation (left), simulation model in 2D HAM programme HEAT2 (right) [author with 48, 54]

9.1.4 Boundary and initial conditions

The interior climate was described by boundary conditions with a constant air temperature of 20 °C and 50 % RH.

Standard surface heat transfer resistances were set as vertical heat transfers of 0.17 $m^2 \cdot K \cdot W^{-1}$, and as horizontal heat transfers of 0.13 $m^2 \cdot K \cdot W^{-1}$ and of 0.04 $m^2 \cdot K \cdot W^{-1}$, respectively for interior and exterior.

The exterior climate varies according to the following formula in accordance with EN ISO 13370. The weather-data were used for Denmark.

$$T_e = 8.0 + 8.5 \cdot \sin(2\pi \cdot \frac{M-4}{12}) \qquad [-] \qquad (9.1)$$

where M time of year [months] expressed as e.g. the 15th January meaning 0.5. This sinusoidal function (9.1) approximates the Danish Test Reference Year (TRY) [47].

The period of the temperature variation is 12 months (8760 hours), however to ensure that the calculation has become stable the calculation was run for 10 years.

The mean external temperature for the heating season was determined as 5.80 °C [47] for the period from September to May. The monthly mean temperatures for calculating the heat loss through the wall are given in

Table 22. ΔT for Equation (1.22) was used according to TRY [K]. [54]

The heat loss through the floor slab is calculated using a temperature difference at the reference point according to:

$$\Delta T = T_i - T_{mean,ref} \quad [K] \quad (9.2)$$

where T_i internal air temperature (20 °C) [°C];

$T_{mean,ref}$ average temperature measured in the reference point for selected month (calculated based on recorded results from Heat 2) [°C].

Table 22: Monthly mean external temperatures used for calculating the heat loss through the wall, Danish Test Reference Year, the heating period is from September to May, both months included [47, 54]

Month [-]	Outside temperature [°C]
January	-0.2
February	-0.2
March	2.0
April	5.8
May	10.2
June	14.0
July	16.2
August	16.2
September	14.0
November	5.8
December	2.0

Calculation of the linear transmittance was done on the basis of the principle; its expression is shown in Equation (1.22).

The 1D heat flows through the wall and floor were calculated by simple calculations based on the height of the wall and width of the floor slab according to a model (Figure 76) and Equation (1.23).

9.1.5 Results

The U-value for calculating 1D heat loss for the floor slab is given in Table 23.

Table 23: U-value for the floor construction [54]

	d[m]	λ[W·m^{-1}·K^{-1}]	R[m^2·K·W^{-1}]
$R_{internal}$	-	-	0.17
Thin wooden floor	0.015	0.13	0.12
Reinforced concrete	0.1	2.3	0.04
Insulation	0.4	0.04	10.00
		ΣR=	10.33
		U=1/ΣR=	0.10 W·m^{-2}·K^{-1}

For the studied wooden wall with 70 mm post per 600 mm percentage of wood in one section is 11.7 % (Equation 1.19). And λ will increase to 0.051 $W \cdot m^{-1} \cdot K^{-1}$. For internal lathing of 45 mm wide, the percentage of wood is 7.5 % and λ is then 0.047 $W \cdot m^{-1} \cdot K^{-1}$, in both cases compared to standard values, which are $\lambda_{insulation}$ = 0.04 $W \cdot m^{-1} \cdot K^{-1}$ and λ_{wood} = 0.13 $W \cdot m^{-1} \cdot K^{-1}$ with fibres across the grain. The U-value for calculating 1D heat loss for the wall construction is given in Table 24. [54]

Table 24: U-value for the wall construction [54]

	d[m]	λ[$W \cdot m^{-1} \cdot K^{-1}$]	R[$m^2 \cdot K \cdot W^{-1}$]
$R_{external}$	-	-	0.04
Cladding	0.02	0.13	0.15
Lathing+air gap	0.025	0.138	0.18
MDF/OSB	0.015	0.13	0.12
Wood+insulation	0.22	0.051	4.36
Lathing+insulation	0.075	0.047	1.60
OSB	0.015	0.13	0.12
Plasterboard	0.0125	0.22	0.06
$R_{internal}$	-	-	0.13
		ΣR=	6.74
		U=1/ΣR=	0.15 $W \cdot m^{-2} \cdot K^{-1}$

The influence of MC of the wood on the heat loss was also calculated for a wooden wall sizing of 1 m^2. The measured λ_{mat} was parachuted to vertical wooden posts of the walls. The results for U-value with a %-difference of the conditioned and dry values of the material are shown in Figure 77. The increase in the average heat loss is proportional to the increase in the U-value. [54]

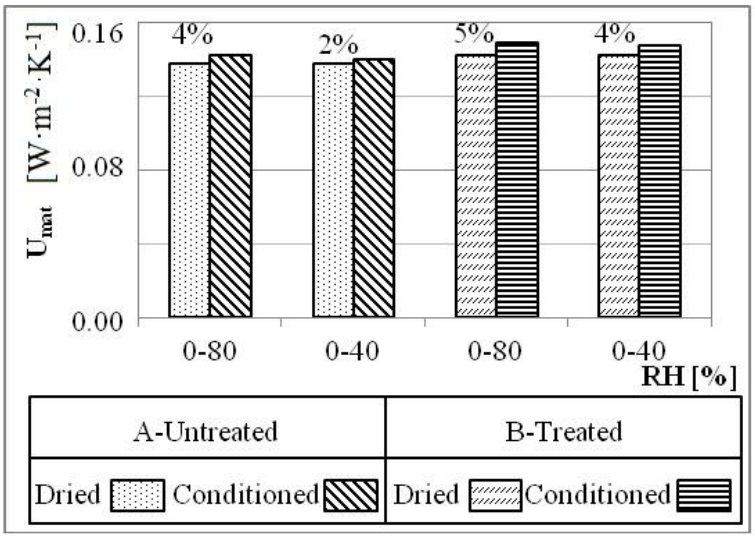

Figure 77: Increase of U-value of 1 m^2 modelled wooden wall with respect to different conditions such as 0 %, 40 % and 80 % RH [54]

The mean monthly line losses were determined for both A and B foundation beam in 0 % and 80 % RH, because of the highest result of λ-value gained from the previous measurement (Chapter 6.1). All calculations were performed for a transient external temperature.

The $\Psi_{connection}$ was calculated according to Equation (1.22) for the heating season by the mean temperature difference between inside and outside air. The comparison of $\Psi_{connection}$ between using conditioned bottom plate of A and B wood with 0 % and 20 % MC is described by Figure 78. [54]

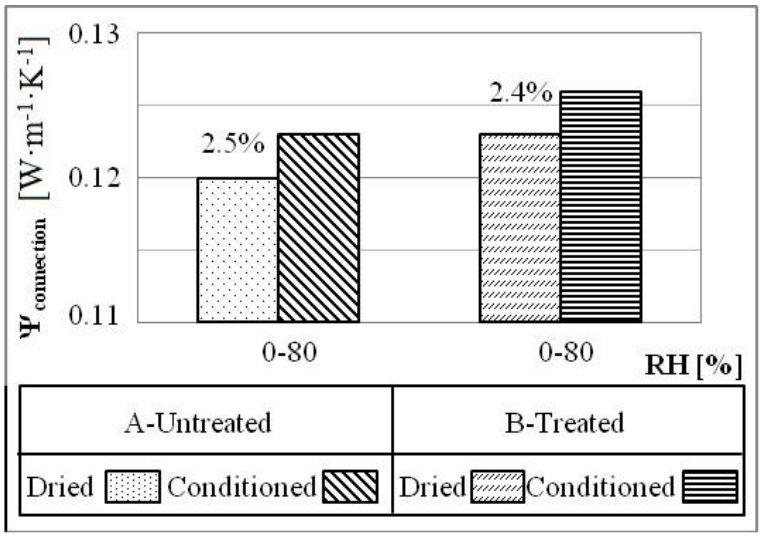

Figure 78: Linear thermal transmittance for the simulated detail using A-untreated and B-treated bottom plate in 0 % and 80 % RH [54]

The results gained from the measurement and transient simulations of the detail are expressed in Table 25 for clarity. T at a reference point and heat flows were read at the middle of each month for the last simulated year.

Table 25: Summary of the measured and calculated values for cases using A-untreated and B-treated wood [54]

	RH	ρ_{mat}	λ_{mat}	$C_{p,mat}$	q_{10y}	$\Psi_{connection}$
	[%]	[kg·m^{-3}]	[W·m^{-1}·K^{-1}]	[MJ·m^{-3}·K^{-1}]	[W·m^{-1}]	[W·m^{-1}]
A	80	368	0.110	0.541	10.223	0.123
	0	345	0.089	0.380	10.171	0.120
	40	385	0.103	0.477	10.207	-
	0	369	0.091	0.356	10.176	-
B	80	496	0.133	0.520	10.271	0.126
	0	477	0.110	0.465	10.222	0.123
	40	497	0.125	0.614	10.254	-
	0	476	0.106	0.490	10.212	-

Figure 79 shows the increase of the heat flow at the 10th simulated year for both kinds of material used for the bottom plate.

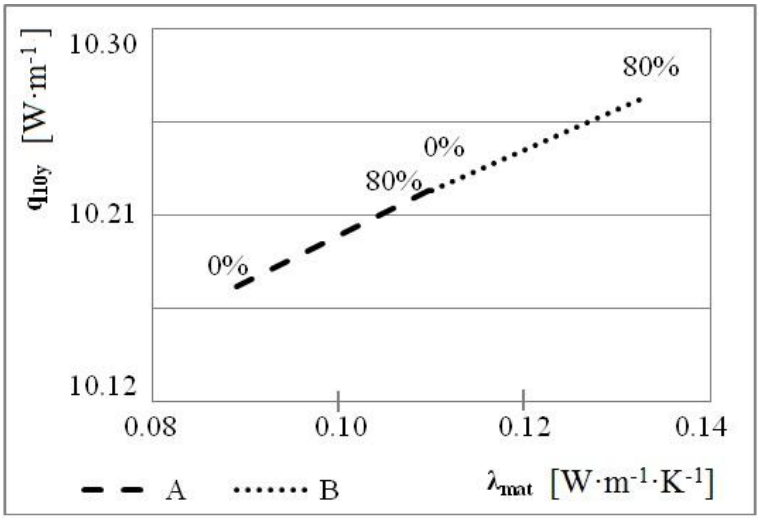

Figure 79: 2D heat flow through the section at 10th simulated year for the studied detail using A-untreated and B-treated bottom plate conditioned at 0 % and 80 % RH [54]

For better understanding of decomposition of T, Figure 80 presents the temperature field with isotherms at the beginning of the 1st simulated year. The minimal surface temperature in the corner was calculated as of 17.95 °C for the bottom plate assigned with λ of wood 0.11 $W \cdot m^{-1} \cdot K^{-1}$ for A-untreated spruce and as of 17.90 °C with thermal conductivity of wood 0.13 $W \cdot m^{-1} \cdot K^{-1}$ for B-treated spruce (both values correspond to the wood with 20 % MC, respectively conditioned at 80 % RH, see Table 25).

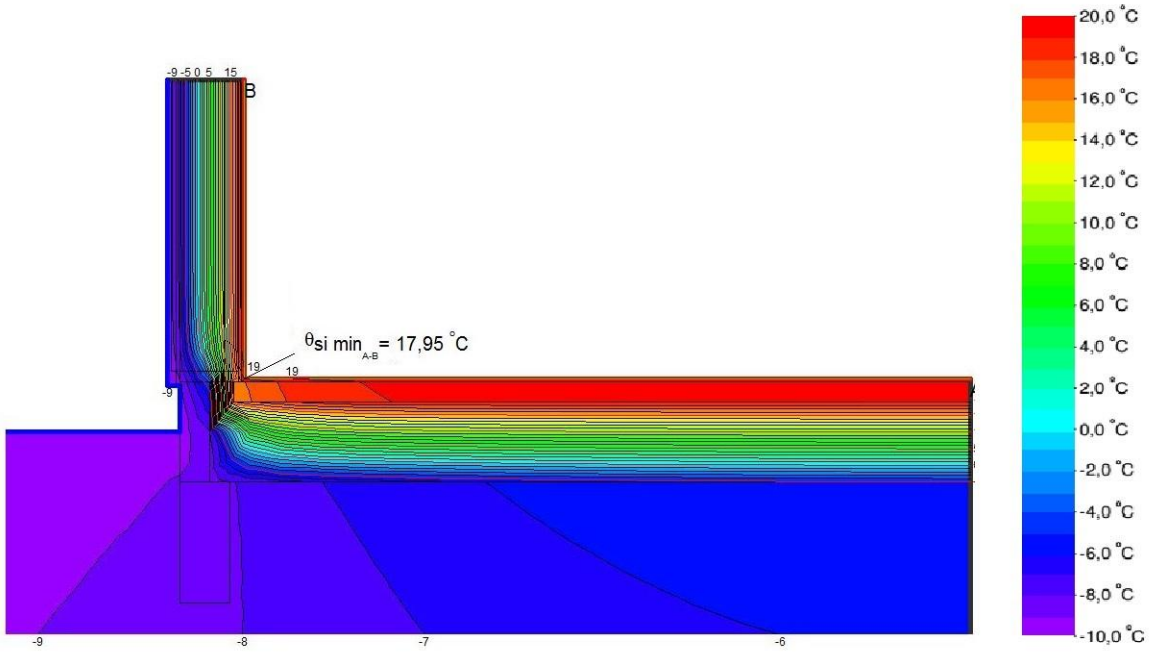

Figure 80: Temperature field of the simulated wall/floor junction at the beginning of the simulated year, the minimal surface temperature in the corner with bottom plate assigned with the thermal conductivity of wood 0.11 $W \cdot m^{-1} \cdot K^{-1}$ was calculated as of 17.95 °C [author with 65]

9.1.6 Conclusions and discussion

An increase of the U-value of a 1 m^2 wooden wall with applying the thermal conductivity λ_{wood} influenced by moisture content in the case of conditioning at 80 % RH was 4 % for A-untreated and 5 % for B-treated spruce samples and in the case of conditioning at 40 % RH the increase of the U-value was 2 % for A-samples and 4 % for B-samples. Both comparisons were related to a dry material with MC 0 %.

Other results were related to a modelled wooden wall and concrete slab. The linear thermal transmittance $\Psi_{connection}$ was calculated for the highest thermal conductivity value for both A-untreated and B-treated wood (such as the case of conditioning at 80 % RH), which was applied on the main beam in direct contact with a water barrier on the foundation and so the thermal transmittance has increased about 2.5 % for A-untreated and 2.4 % for B-treated wood. The influence of the clearly increased thermal conductivity for increasing moisture content of the wood thus results, however, only to a marginal increase in the heat loss of the studied construction detail.

Based on the results obtained for the thermal transmittance $\Psi_{connection}$ and minimal surface temperature in the wall to floor junction it is hard to determine a big difference in the thermal performance between treated and untreated wood used as a bottom plate. There is a slight tendency towards the statement, that Untreated spruce has better thermal properties then Treated spruce with increasing moisture content but nothing conclusive.

The Treated spruce is treated against biological decay and in the process it gets a slight higher density then Untreated spruce but nothing in the scale that makes it possible to conclude that it could be the reason for the results.

Usage of this simplified calculation method should be applicable for any other country as well, if the weather–related data is changed to weather-data for that particular country. [47]

9.2 Influence of construction design on moisture damage of wooden buildings

The following numerical calculations are based on the author‘s on site measurements of the MC of bottom plate, within the framework of this thesis (Chapter 3.2.3). The average value was settled to 35 weight-%. The presented results compare the influence of two construction solutions on the hygrothermal performance in order to estimate the durability of the constructions with respect to the risks of mould growth. The analysis was performed on two wooden buildings with different construction solutions and thus potential of dry out the moisture, described in Chapter 4, CS1 and CS2.

For the mould growth analysis the Viitanen model, described in Chapter 1.6.2, was applied. For analysis of mass loss due to the decay fungi, empirical model described also in Chapter 1.6.2 was used.

This issue and results were presented at the conference and published in [55].

9.2.1 Construction for simulations

A study of the hygrothermal condition was carried out using numerical calculations on two modern wooden structures - CS1 and CS 2, commonly used in the Czech Republic and Denmark, described in Chapter 4,

Nevertheless, in order to be able to compare the performance of the two details as well as possible, the insulation thickness of wall and floor was altered in CS1 to obtain the same U-value of the floor and wall constructions as in CS2, as shown in Figure 81.

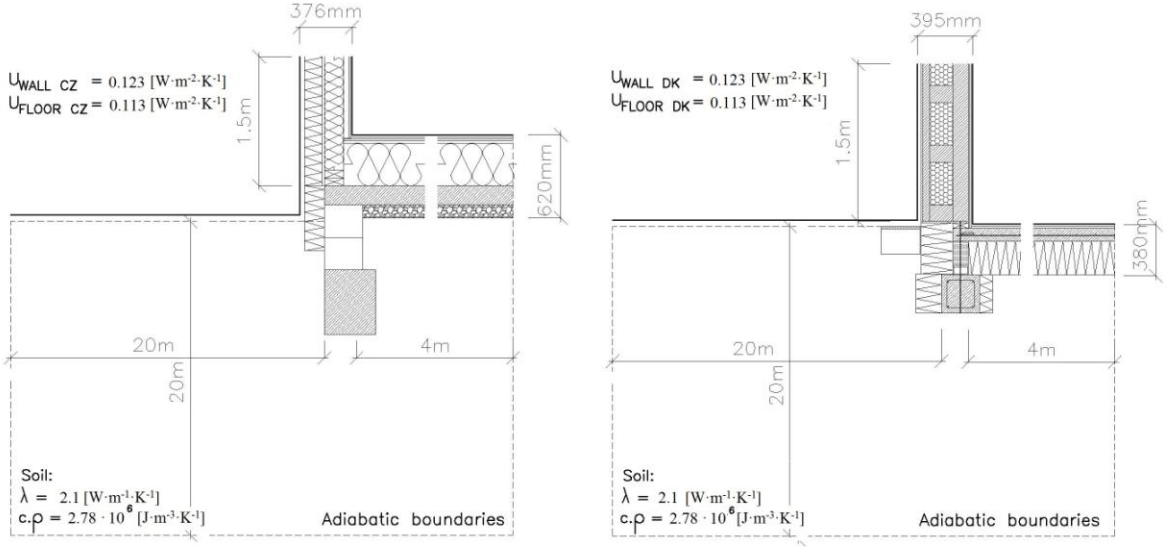

Figure 81: Simulation set up models with total thicknesses of wall and floor insulation – Case study 1 (left), Case study 2 (right) [55]

The insulation layer of the floor construction in Case study 1 was increased from the normally used 120 mm to 330 mm in order to get the U-value of 0.113 $W \cdot m^{-2} \cdot K^{-1}$. The main reason for the difference in total thickness is the use of stone as capillary breaking layer in diffusion closed Case study 1, whereas Case study 2 - diffusion opened construction uses the EPS insulation as capillary breaking layer. In addition, a thicker concrete slab is used in Case study 1. [55]

As for wall construction, Case study 1 is characterised by having a layer of EPS closed cell foam insulation as the external insulation layer, and mineral wool as insulation between the wooden posts, while Case study 2 uses cellulose insulation throughout. In order to achieve the same U-value, the thickness of the EPS insulation in Case study 1 was increased from the typical 100 mm to 155 mm to achieve a U-value of 0.123 $W \cdot m^{-2} \cdot K^{-1}$. The diffusion opened Case study 2 was completed on the outside with an air gap and wooden cladding, which was not included in the numerical simulation model. [55]

For visual comparison, the temperature fields of the original and optimized wall to floor junction of diffusion closed Case study 1 are shown in Figure 82.

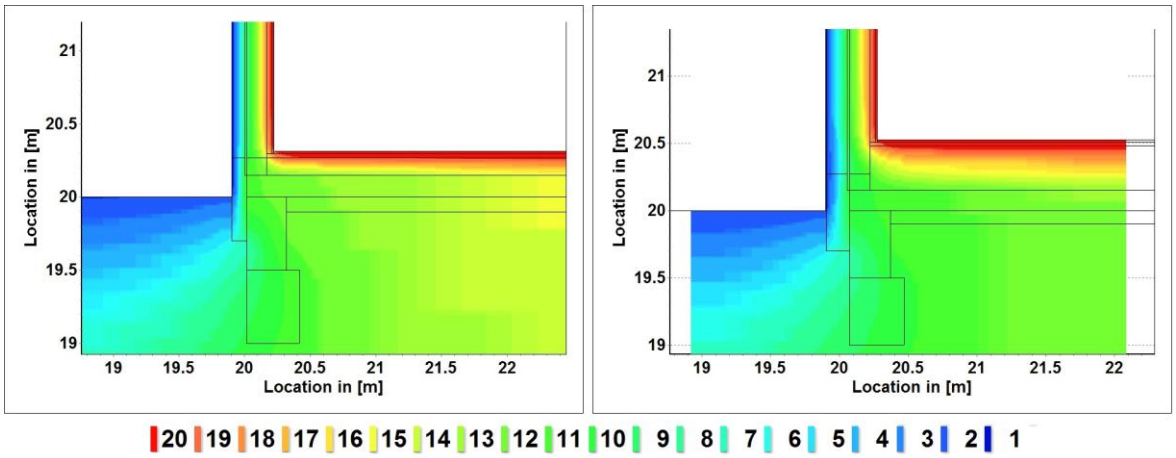

Figure 82:Temperature field of the original wall/floor junction of the diffusion closed Case study 1(left); temperature field of the optimized wall/floor junction of the diffusion closed Case study 1 for more accurate comparison with Case study 2 (right) [author with 51]

The compositions of both cases of floor and wall constructions are described in Table 26 and 27, respectively. [55]

The vapour barrier behind the wooden post on the internal side of the diffusion closed external wall in Case study 1 was modelled as a contact resistance between the layers with equivalent air-layer thickness of s_d = 98.3m. There is no vapour barrier in the diffusion opened Case study 2.

Table 26: U-values for floor constructions for simulated details in Case study 1 (left) and in Case study 2 (right) [55]

CS1	d [m]	λ [W·m^{-1}·K^{-1}]	R [m^2·K·W^{-1}]
$R_{internal}$	-	-	0.17
Wooden floor	0.01	0.13	0.078
2x OSB	0.03	0.13	0.23
Mineral wool	0.330	0.04	8.25
Concrete slab	0.150	2.1	0.071
Stone	0.100	2.43	0.041
Σd=	0.620	ΣR=	8.84
		U=1/ΣR=	0.113 W·m^{-2}·K^{-1}

CS2	d [m]	λ [W·m^{-1}·K^{-1}]	R [m^2·K·W^{-1}]
$R_{internal}$	-	-	0.17
Wooden floor	0.015	0.13	0.115
Concrete screed	0.100	2.1	0.048
EPS	0.265	0.031	8.549
Σd=	0.380	ΣR=	8.88
		U=1/ΣR=	0.113 W·m^{-2}·K^{-1}

Table 27: Material layers and calculation of U-values for wall constructions for simulated details in Case study 1 (left) and in Case study 2 (right) [55]

CS1	d [m]	λ [W·m^{-1}·K^{-1}]	R [m^2·K·W^{-1}]
$R_{internal}$	-	-	0.13
Gypsum board	0.013	0.2	0.065
Mineral wool	0.04	0.056	0.714
Post, MW	0.15	0.047	3.19
OSB	0.015	0.13	0.115
EPS	0.155	0.04	3.875
Plaster	0.003	0.595	-
$R_{external}$	-	-	0.04
Σd=	0.376	ΣR=	8.13
		U=1/ΣR=	0.123 W·m^{-2}·K^{-1}

CS2	d [m]	λ [W·m^{-1}·K^{-1}]	R [m^2·K·W^{-1}]
$R_{internal}$	-	-	0.13
Gypsum board	0.013	0.2	0.065
OSB	0.012	0.13	0.09
Post, cellulose	0.36	0.048	7.5
Wood fireboard	0.01	0.05	0.2
Air gap	0.025	-	-
Cladding	0.025	-	-
$R_{external=internal}$	-	-	0.13
Σd=	0.395	ΣR=	8.12
		U=1/ΣR=	0.123 W·m^{-2}·K^{-1}

The corresponding basic material properties used for the heat and moisture numerical calculation in Delphin programme are listed in Table 28 and 29.

Table 28: Material parameters for hygrothermal simulation, part 1 (IBK library version 3.9.1.) [51, 55]

Material parameters	Mineral wool	EPS CS1	Soil, clay	OSB	Climate plaster	Gypsum board
Thickness [mm]	-	155	-	15	3	12.5
Density [kg·m^{-3}]	30	34	2650	630	1291	850
Heat capacity [J·kg^{-1}·K^{-1}]	840	1300	1050	1880	1000	850
Thermal conductivity [W·m^{-1}·K^{-1}]	0.056	0.04	2.1	0.13	0.595	0.2
Open porosity [m^3·m^{-3}]	0.92	0.94	0.43	0.4	0.51	0.65
Eff. Water saturation [m^3·m^{-3}]	0.9	0.935	0.427	0.35	0.32	0.551
Water absorption coefficient [kg·m^{-2}s$^{-0,5}$]	-	-	0	0.0019	0.0514	0.277
Vapour diffusion resistance [-]	1	30	10	280	17.7	10

Table 29: Material parameters for hygrothermal simulation, part 2 (IBK library version 3.9.1.) [51, 55]

Material parameter	Bottom plate, spruce	Concrete C20/25	Stone	Light weight concrete	Wood fireboard	Cellulose DK	EPS CS2
Thickness [mm]	-	400	100	300	10	365	265
Density [kg·m^{-3}]	528	2320	1939	1250	300	55	34
Heat capacity [J·kg^{-1}·K^{-1}]	2000	850	831	1050	1180	2544	1300
Thermal conductivity [W·m^{-1}·K^{-1}]	0.13	2.1	2.43	0.18	0.05	0.04	0.031
Open porosity [m³·m^{-3}]	0.7	0.14	0.27	0.42	0.42	0.93	0.94
Eff. Water saturation [m³·m^{-3}]	0.695	0.143	0.23	0.4	0.4	0.7	0.935
Water absorption coefficient [kg·m^{-2}s$^{-0,5}$]	0.0582	0.02	0.07	0.01	0.0674	0.53	-
Vapour diffusion resistance [-]	236.2	110	19.3	10	5	2	30

The dimensions of the bottom plate in Case study 1 were 150/120 mm (W/H) and in Case study 2 were 120/45 mm (W/H).

9.2.2 Methods

For this investigation, the coupled heat and moisture calculations were performed with the 2D hygrothermal simulation tool Delphin version 5.6.8. It is a simulation programme for the calculation of coupled heat, moisture air pollutant and salt transport in porous building materials. A screenshot from the programme with the modelled CS1 in the original stage is shown in Figure 83. The material properties were taken from Delphin material library (IBK library version 3.9.1) and are listed above in Table 28 and 29. [55]

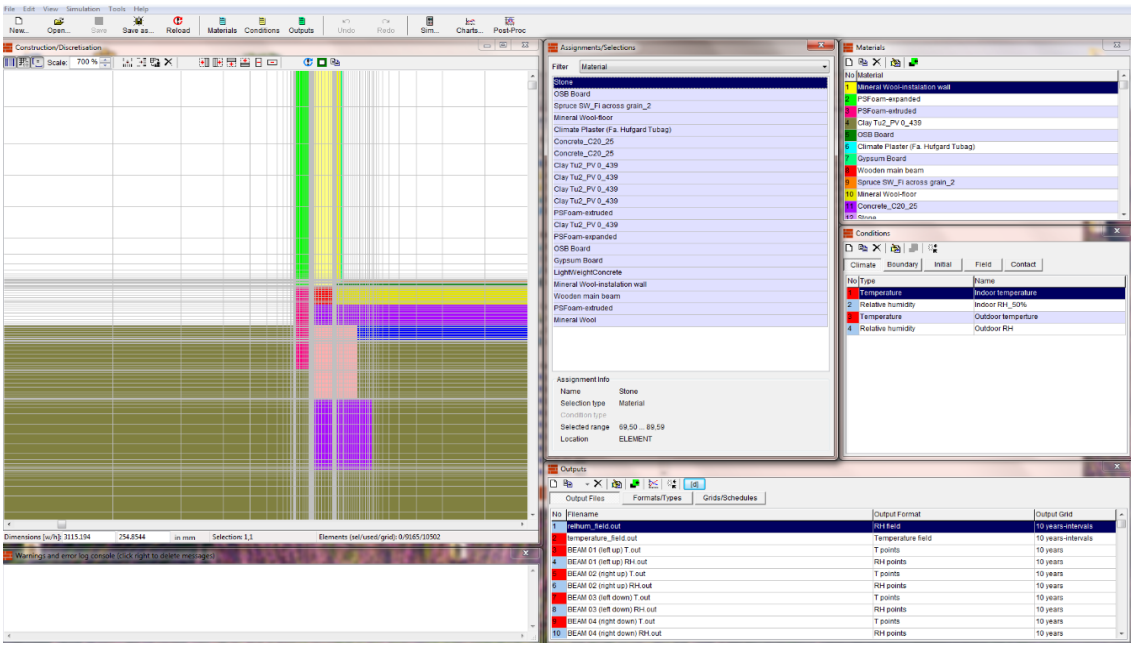

Figure 83: Screenshot from the hygrothermal simulation programme Delphin version 5.6.8 with modelled diffusion closed Case study 1 in original stage [author with 51]

9.2.3 Geometry of simulation models

To ensure applicability of an adiabatic boundary for this detail 4 m of the floor slab and 1.5 m of the wall was modelled. For the soil 20 m is modelled both in horizontal and vertical directions (EN ISO 10211-1 1997) [36] Figure 81 and Figure 84 applies this model in the Delphin programme.

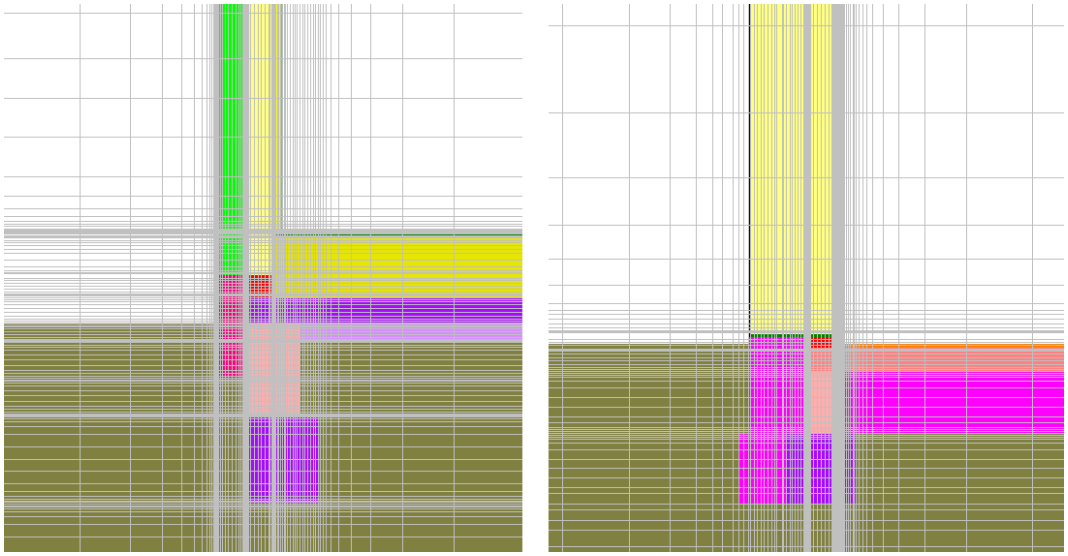

Figure 84: Simulation set up models in Delphin – Case study 1 (left), Case study 2 (right) [author with 51]

9.2.4 Boundary and initial conditions

Simplified interior and exterior climates were described by boundary conditions with a sinusoidal varying air temperature with a sinusoidal varying relative humidity according to WTA (2006) [50] as described in Table 30.

Table 30: Sinusoidal varying interior and exterior boundary conditions (WTA Merkblatt 6-2-01/D) [50, 55]

Boundary conditions	Interior		Exterior	
	T	RH	T	RH
Mean value [°C], [%]	21	50	9	80
Amplitude [K]	1	10	9	8
Period [year]	1	1	1	1
Phase shift with maximum in	June	August	July	December
Heat exchange coefficient [$W \cdot m^{-2} \cdot K^{-1}$]	8		17	
Vapour diffusion exchange coefficient [$kg \cdot m^{-2} \cdot s^{-1} \cdot Pa^{-1}$]	25.10^{-9}		75.10^{-9}	

Two sets of calculations were carried out: a “Dry” and a “Wet” set. The initial conditions for the “Dry” hygrothermal simulations were set to temperature of 20 °C and 80 % RH. In order to illustrate the possible effect of very wet initial conditions and especially the drying capacity of the different

solutions, the bottom plate was assigned to have an initial moisture content equivalent to 35 weight-% MC in the "Wet" set of simulations. Simulations for all cases were performed over 10 years.

9.2.5 Risk of mould growth and decay of the bottom plate

The hygrothermal performance of the studied wooden constructions is assessed by calculating the risk of mould growth around and the risk of decay of the bottom plate. Photos of the bottom plate in CS1 and CS 2 are shown on Figure 85.

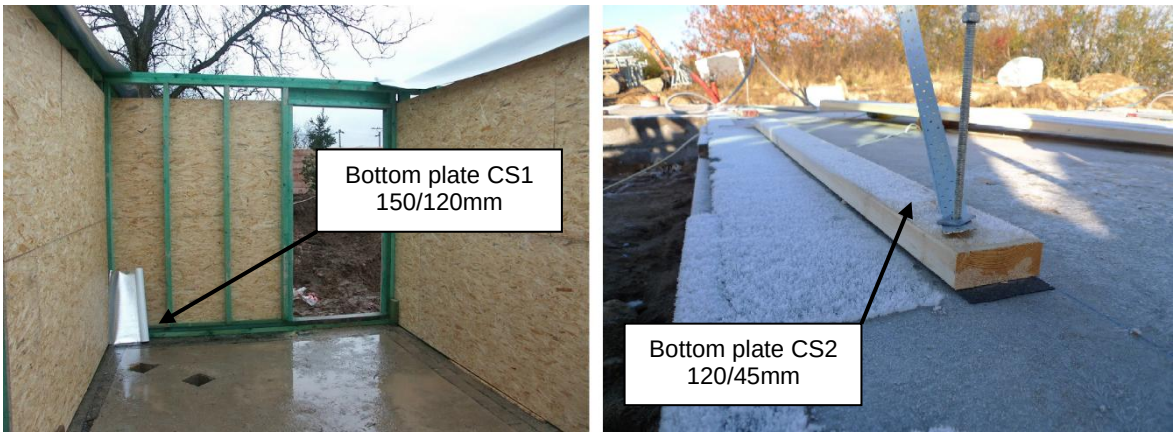

Figure 85: Total view on the wet wall of CS1 (left) Photo © Karel Šuhajda; The bottom plate under weather conditions in CS2 (right) Photo © Ruut Peuhkuri [55]

Both case studies were subjected to have the same position and dimensions of simulating registration points on the bottom plate, such as 16/16mm (W/H). The simulation mesh was settled in four positions point as shown on Figure 86. From the simulation results, T and RH at registration points at bottom plate were post-processed. The Viitanen model [49] was used as a risk model for mould growth and for the decay of wooden construction, a model described in [27, 55], both models are also described in Chapter 1.6.2.

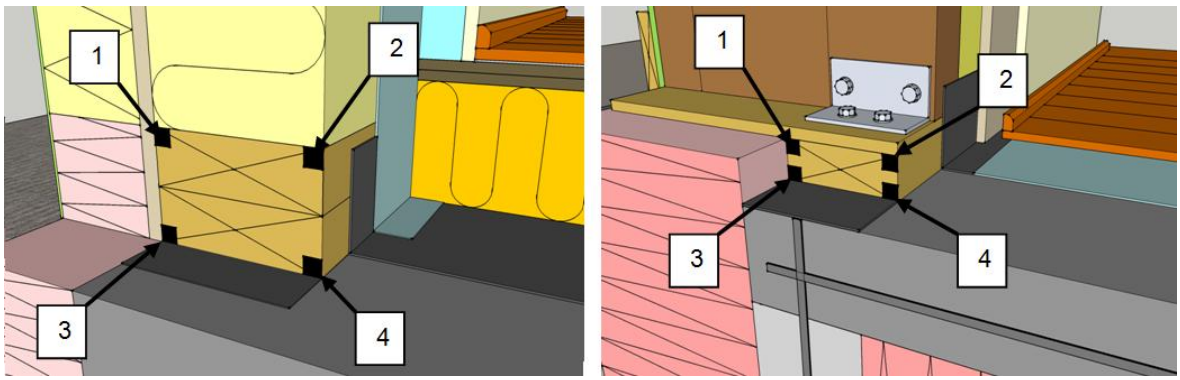

Figure 86: Registration points on bottom plate: diffusion closed Case study 1 (left) and diffusion opened Case study 2 (right) [55]

9.2.6 Results

Relative humidity at registration points

Initial conditions (T and RH) for mould growth index calculation at the registration points 01, 02, 03 and 04 in "Dry stage" for bottom plate of simulated detail of both variants are expressed by graphs in Figure 87and in "Wet stage" by graphs in Figure 88.

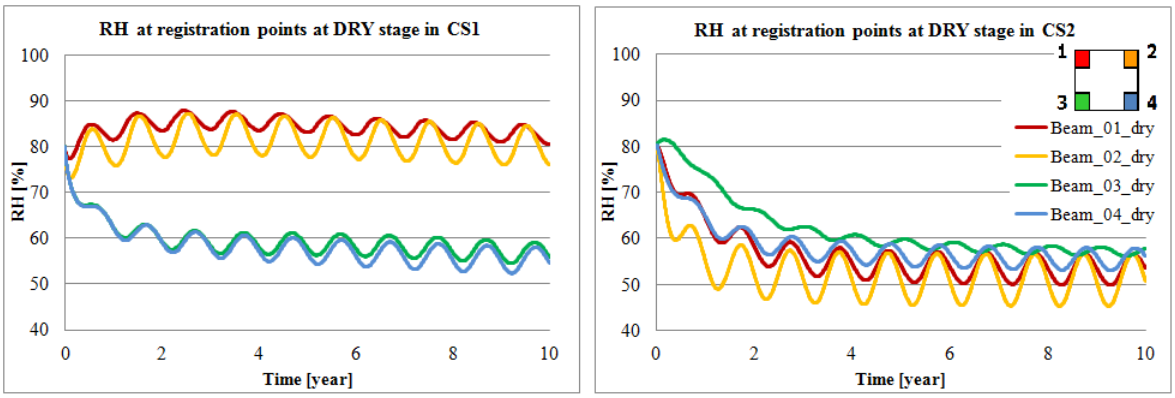

Figure 87: Comparison of RH at the "DRY stage" at the registration points of diffusion closed Case study 1 (left) and diffusion opened Case study 2 (right) [55]

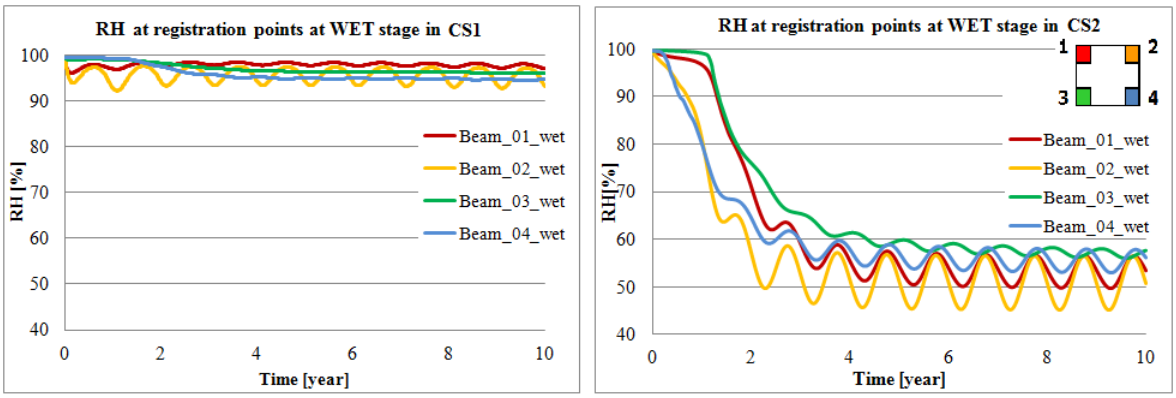

Figure 88: Comparison of RH at the "WET stage" at the registration points of diffusion closed Case study 1 (left) and diffusion opened Case study 2 (right) [55]

RH of all registration points in diffusion closed Case study 1 in the "Wet stage" are for the whole simulation period of 10 years in a dangerous range above 90 %. Even the relative humidity of initially dry wood near the interior side, respectively in registration points 02 and 03, is oscillating between 75-85 %. The usage of relatively vapour tight, respectively vapour retarding diffusion material on the exterior side (EPS) is causing minimal drying potential of the wood, conditioned at 35 weight-%. Similar behaviour is visible on the bottom of the dry bottom plate, such as registration points 03 and 04, there the relative humidity oscillates between 55-65 %.

On the other hand, the relative humidity of all registration points on the dry and wet bottom plate of the diffusion opened Case study 2 will decrease within a few months to two years to less than 60 %. Initially wet wood will dry out from all registration points in about 2 years. [55]

Calculated mould growth and wood decay risk

The calculated mould growth risks for the points of Case study 1 and Case study 2 at registration points are given in Figure 89 and Figure 90.

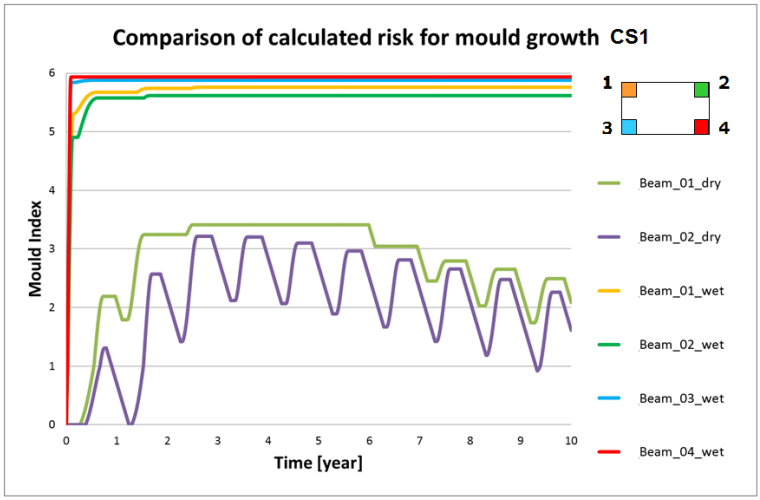

Figure 89: Comparison of the calculated risk of mould growth for registration points for diffusion closed Case study1.Results showing no risk (Mould index = 0) are omitted [55]

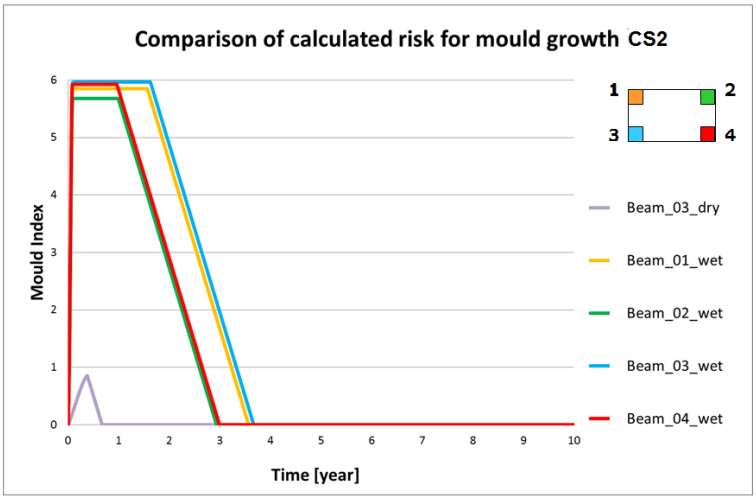

Figure 90: Comparison of the calculated risk of mould growth for registration points for diffusion opened Case study 2. Results showing no risk (Mould index = 0) are omitted [55]

Figure 91 shows the calculated risk for mass loss of wooden construction for 10 simulated years as a consequence of decay fungi. Figure 92 then detailed part for 2 years. The calculated mass loss above 100 % makes no

physical sense but is an expression of the continuing risk. Only cases with initial high moisture content (35 weight-%) showed a risk for decay.

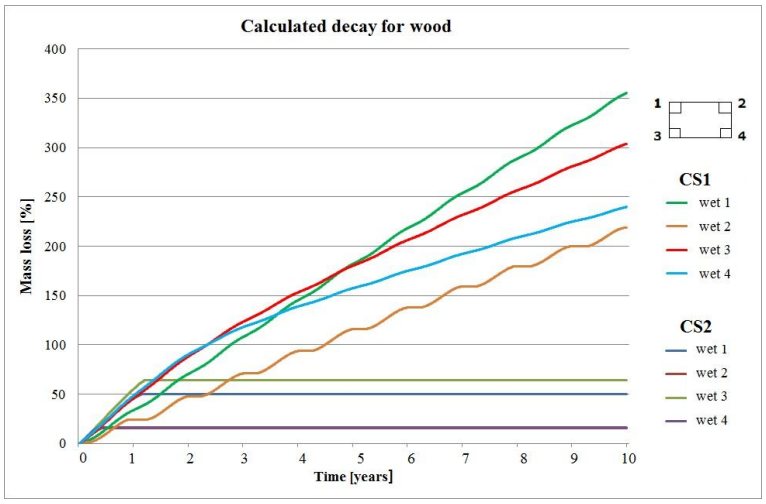

Figure 91: Comparison of Case study 1 and Case study 2 with typical results for the calculated risk of decay fungi (Mass loss): for 10 simulated years [55]

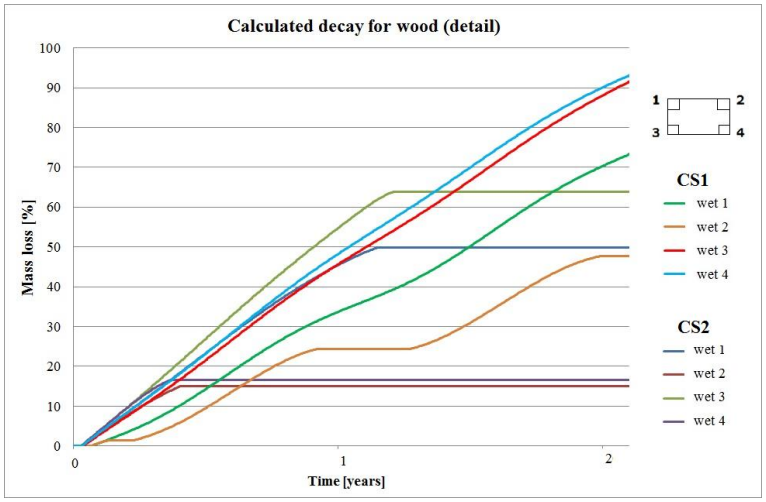

Figure 92: Comparison of Case study 1 and Case study 2 with typical results for the calculated risk of decay fungi (Mass loss): detailed for 2 years [55]

The comparison of the drying potential of diffusion closed and opened structures (CS1 and CS2) express also the outputs of the condensate mass from Delphin programme. The bottom plate with increased initial moisture content of 185 $kg \cdot m^{-3}$ (which corresponds to 35 weight-%) "Wet stage" causes in the optimized Case study 1 wall/floor junction detail at the end of the 1st simulated year the condensate mass behind the OSB and at the bottom plate about 0.06 $m^3 \cdot m^{-3}$ (Figure 93, left), after 10 years the condensate stays in the area behind the OSB and insulation in the mass of about 0.04 $m^3 \cdot m^{-3}$ (Figure 93, right).

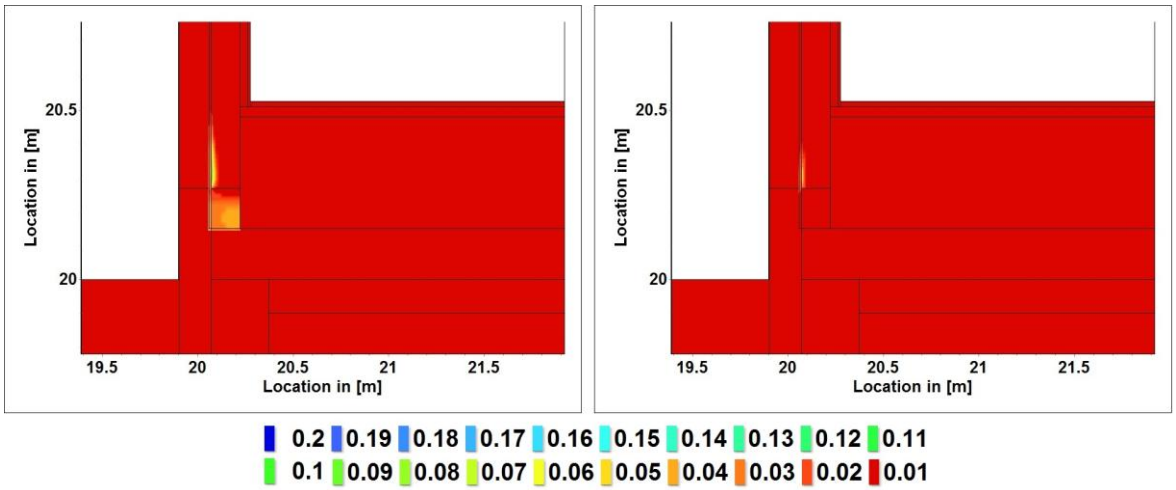

Figure 93: Condensate mass [$m^3 \cdot m^{-3}$] in the optimized diffusion closed Case study 1 of wall/floor junction detail in "WET stage" (bottom plate assigned with 35 weight-%): at the end of the 1st simulated year (left) and at the end of 10th simulated year (right) [author with 51]

The situation in the diffusion closed CS1 wall/floor junction in optimized and original variant is very similar (Figure 94, right). It is caused by using of insulation material on external side with very high diffusion resistance. The built-in moisture does not have a possibility to fully dry out even after 10 years. The condensate still remains behind the OSBs (Figure 94, right).

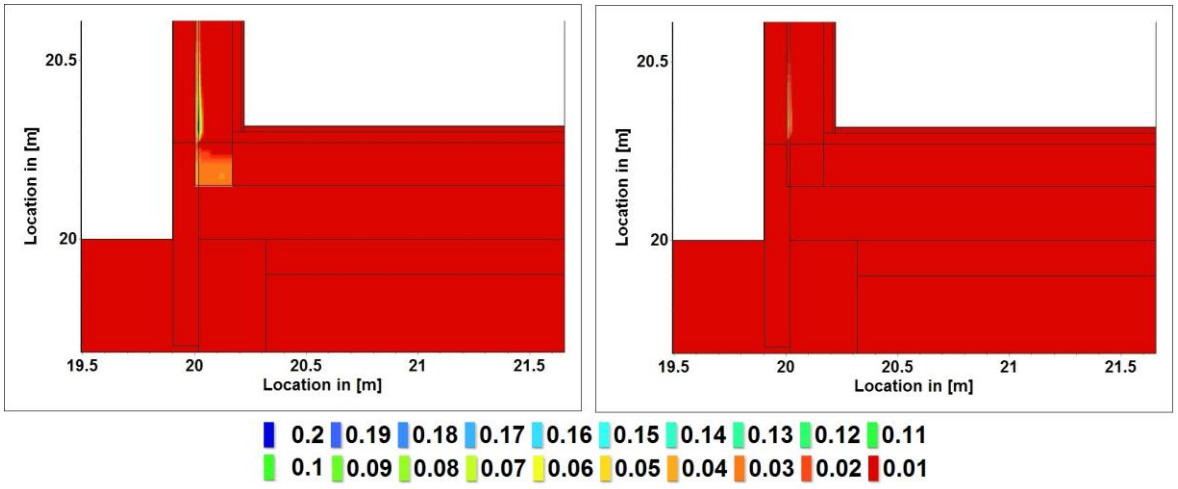

Figure 94: Condensate mass [$m^3 \cdot m^{-3}$] in the original diffusion closed Case study 1 of wall/floor junction detail in "WET stage" (bottom plate assigned with 35 weight-%): at the end of the 1st simulated year (left) and at the end of 10th simulated year (right) [author with 51]

On the other hand the increased initial moisture content of the bottom plate in diffusion opened CS2 had the possibility to dry out within first 8 months so at the end of the 1st simulated year the simulation did not show any condensate mass within the structures and therefore the figures are omitted.

9.2.7 Discussion

Risk of mould growth and wood decay fungi

The hygrothermal performance of the studied constructions was also assessed with numerical models estimating the risk for both mould and decay fungi [49, 60]. The results in Figure 89 and Figure 90 show clearly how the hygrothermal conditions in the initially wet bottom plate are very favourable for initiating biological growth. The better drying potential of diffusion opened Case study 2 is seen as the drop in the mould growth risk over approximately 2 years. The risk of mould growth in the initially dry diffusion closed Case study 1 is either not existing or relatively low. A mould growth index below 3 corresponds to growth that is not visible to naked eye (see Table 7).

In Figure 92 typical cases are presented for the initially wet constructions. The initially dry constructions do not have any risk for decay. While the mass loss of diffusion opened Case study 2 stops at a stage when the construction is dried enough, the mass loss of the diffusion closed Case study 1 seems to go on. The initially dry diffusion opened construction does not have any mould growth or risk of decay.

The investigated bottom plate is a part of the load-bearing structure and not in direct contact with interior air. Therefore it can be discussed if calculating the mould index makes any sense for the assessment. However, the mould growth can be seen as the first sign of moisture related failure, even before more severe damage happens with rot and decay.

When using these models for the assessment, it must be kept in mind that the mould growth index and mass loss due to decay fungi only describe how risky the hygrothermal conditions are, not the actual mould growth or decay. These methods work best as a comparison of different solutions or parameter variations and not as absolute values. [55]

9.2.8 Conclusions

Hygrothermal assessment with risk of mould growth and decay fungi highlighted the importance of the correct design of this connection of wooden wall and the foundation that ensures drying potential. Also the necessity of ensuring the usage of construction wood which does not have excessive initial moisture content was clearly pointed out. This last observation also supports the guidelines that require sheltering of the construction site from rain. [55]

10. CONCLUSIONS OF DISSERTATION

The issues of critical detail of wooden wall to floor structures on the building's foundation as well as different treatment solutions for mould protection of wood addressed in this thesis are very topical, especially with regard to the increasing number of built wooden structures and the associated presence of numerous thermal and moisture deformations in these critical areas.

10.1 Established scientific findings

The findings look at the influence of increased moisture content of wood on heat losses and the influence of construction design on moisture damages with determination of the differences between natural spruce and spruce impregnated with carbon dioxide as a possible treatment of wood.

10.1.1 Determination of differences between natural and impregnated spruce

Following findings were collected from author's experiments in laboratory and presents differences between natural spruce and spruce impregnated supercritical carbon dioxide method. This impregnation method was chosen as a newest impregnation method to protect wood against biotic attack and thus, not itself, could be a solution of limited protection of build in wooden elements with increased moisture content.

Anatomic structure

"*The supercritical impregnation procedure is theoretically simple; it is difficult to control in practical use. Because of the relatively high pressures involved during the treatment, there is a risk of developing excessive pressure gradients in the wood that caused fatal aftermaths to the anatomic structure*", Kjellow mentioned in his Dissertation (2010) [2], presented in Chapter 5 This was confirmed by visible differences in the shape in radial direction of the cell wall of Treated spruce. In the longitudinal direction there are not any visible perceptible differences in the anatomic structure.

This statement was also confirmed by Scanning Electron Microscopy pictures results. In radial direction, there is a visible difference in the shape of the cell wall of Treated spruce (Figure 34 and Figure 35). The cell walls look to be slightly damaged; a high-pressure during the impregnation process could explain it. In the longitudinal direction there are not any visible perceptible differences in the anatomic structure (Figure 36).

Thermal conductivity

Increased moisture content of the wood clearly affects thermal conductivity of the wood, presented in Chapter 6. Nevertheless, the thermal behaviour of Untreated and Treated spruce seems to be the same for dry and conditioned stage.

The standard increase of thermal conductivity in dependency of increased moisture content of the Untreated and Treated wood and dry density is similar what is mentioned in standard literature, such as maximal increase of 33 % (Koch 1950) [58].

Capillary suction

The water absorption of wood is an extremely variable property accounted for the huge natural variation. The results, presented in Chapter 7.1 shows that the Treated spruce has a higher value of mass gain Δm_t over the time and also a higher water absorption coefficient W_w than Untreated spruce. Out of the three test conditions the Hot water condition with temperature, around 30 °C had a higher influence on the water absorption coefficient W_w and an increase of mass gain for both Untreated and Treated samples.

The contact of wood with liquid water can cause dramatic changes in MC through a variety of mechanisms, such as capillary action. Liquid water sorption can raise the MC above the FSP and up to the maximum moisture content where all lumens are filled with water. Rainwater on wooden elements can influence the MC time history, and thereby the moisture induced deformation.

Sorption isotherms

Obtained results, presented in Chapter 7.2 clearly correspond to theoretical typical shape of adsorption isotherm for wood. There were not found any differences between the isotherms for properties of Untreated and Treated spruce.

The protection requirement for wood and/or wood-based materials is mentioned in technical standard CSN 730540 and such structures must be designed with suitable structural measures to protect the organic materials from the adverse effects of moisture and a long-lasting protection of these materials at least for the 2^{nd} class of risk, which means the method of application preservative is arbitrary if there is no limitation in the test certificate for the device (vacuum-pressure impregnation, vacuum impregnation, impregnation coating, spraying, immersing and soaking etc).

Water vapour permeability

According to the results, obtained in Chapter 7.3, an average value for water vapour diffusion resistance factor μ of B-treated samples is 7.9 % higher than A-untreated samples in the dry cup test. On the other hand, the wet cup test showed 3 % higher value of water vapour resistance μ for A-untreated spruce samples than B-treated spruce samples, always referenced to an A-untreated value.

Nevertheless, the water vapour resistance factor seems to be the same for both types of spruce, even a slight change was observed between Untreated and Treated spruces. The results clearly confirmed spruce as an airtight but not water and vapour tight material.

Long term bending and shearing

According to the results obtained in Chapter 8 the failure load for the treated spruce is in both bending and shearing test higher, compared to the reference values of Untreated spruce.

The creep behaviour seems to be the same for both types of spruce, even a slight change was observed between Untreated and Treated spruces.

The presented conclusions of all monitored properties pointed out the differences between non-impregnated and carbon dioxide impregnated spruce. On the other hand the presented conclusions could not unanimously answer the question: if the supercritical carbon dioxide impregnation fatally changes the structure of the wood and so can influence the thermal and hygrothermal behaviour of spruce. Further tests with higher amount of specimen are required for a certain conclusion.

10.1.2 Influence of moisture content on heat losses

Determination of thermal conductivity of Untreated and Treated spruce described in Chapter 9.1, were carried out on the specimens with different density and moisture contents (0 and 35 weight-%). Data obtained from these laboratory experiments were used for modelling the detail of the connection of outer wooden wall on monolithic foundation standardly used in Denmark.

The thermal behaviour seems to correlate for both Treated and Untreated spruce. Therefore the influence of the increased moisture content of the wood is for this well insulated detail insignificant.

Based on the results obtained for the thermal transmittance $\Psi_{connection}$ it is hard to determine a difference in the thermal performance between, Treated and Untreated wood used as bottom plate, which is in direct contact with concrete screed, respectively with the waterproofing layer. There is a slight

tendency towards the statement, that Untreated spruce has better thermal properties than Treated spruce with increasing moisture content but nothing conclusive.

10.1.3 Influence of construction design on moisture damage

A hygrothermal performance, presented in Chapter 9.2, of two well-insulated wooden structures with increased initial MC to 35 weight-% of wooden plate clearly showed how the hygrothermal conditions in the initially wet bottom plate are very favourable for initiating biological growth.

The better drying potential of diffusion opened construction (Case study 2) is seen as the drop in the mould growth risk over approximately 2 years. The risk of mould growth in the initially dry diffusion closed construction (Case study 1) is either not existing or relatively low. A mould growth index below 3 corresponds to growth that is not visible to the naked eye (see Table 7).

Only cases with initial high moisture content (35 weight-%) of diffusion opened and closed construction showed a risk for decay. This corresponds also to the experience of laboratories in the Czech Republic, that the effect of decaying fungi causes the most damages to wood built-in risk class 2nd (humid, closed and not air-conditioned space in the interiors of buildings). [20]

10.2 Utilization of examined issues in the field of structural engineering

The hygrothermal assessment with risk of mould growth and decay fungi highlighted the importance of the correct design of this connection of wooden wall and the foundation that ensures drying potential.

The observation also supports the guidelines that require sheltering of the construction site from rain. The reality on construction sites may be that the constructions are not protected well enough from precipitation and other excessive exposure to moisture, and thus the choice of constructions that are robust to failures during the process should be promoted. The type of insulation and its position in relation to the moisture sensible wood-based construction members may be crucial in this respect.

The impregnation of the wood itself cannot ensure durable construction. According to the presented conclusions, the durable and long service-life wooden construction and its layers can be reached with the following building and user assumption:

1. Usage of the construction timber with recommended value of initial moisture content, such as between 15-22 %;
2. Protection of the construction site against the climatic conditions (rain, freeze). If possible use the hall mounted and prefabricated wooden walls;
3. Controlled moisture content of wood within the layers;
4. Determination of the right type and position of the insulation layer in the wall and floor construction;
5. Avoiding of puncturing and/or ensuring the airtight connection between the air retarding layers.

Control of the moisture content in the construction wood should be constantly monitored in practice, especially when using the vapour tight materials on the outer layer of the peripheral wall.

This topic has been currently solved by experts from the University Centre for Energy Efficient Buildings in Prague who developed a system for continuous moisture and humidity monitoring, called "Moisture guard" [52]. It is a control unit which generates visual and/or acoustic alarms in case of increased critical humidity or moisture detection. The sensitive sensors are applied on the wooden elements (see Figure 95).

Figure 95: The model of wall/floor junction (top left), application of Moisture Guard sensors: on the OSB from the internal side (bottom left), on the wooden post (top right), on the bottom plate (bottom right) [52], Photos © Jan Včelák

10.3 Assumption of the further experimental work

In further theoretical and experimental activities it would be useful to expand gained experience and knowledge, in order to promote the correct process with the following points:

- a handbook with a functioning technological process useful for professionals, highlighting:
  - the importance of proper protection of the wooden structures against precipitation and other excessive exposure to moisture, and thus the choice of constructions that are robust to failures during the process;
  - the type of insulation and its position in relation to the moisture sensible wood-based construction members;
  - possibilities to monitor the humidity and moisture directly in the structure of the building construction.
- to monitor the realistic relative humidity indoors in the period of time under specific conditions to ensure the realistic condition for simulation models.

References

[1] Dalehaug, A. et al. 2013. Laboratory investigation of drying of build-in moisture in wood frame walls at passive house level, Proceedings of 2nd CESBP Building Physics, Austria, 979s, pp 291-298.

[2] Kjellow, A. W. 2010. Supercritical Wood Impregnation, PhD dissertation, University of Copenhagen, Faculty of Life Science.

[3] Kjellow, A. W. Henriksen O. 2009. Supercritical wood impregnation, The Journal of Supercritical Fluids, Issue 50, pp 297-304.

[4] Iversen, S. B. Larsen, T. Heriksen, O. Felsvang, K. 2003. The World´s First Commercial Supercritical Wood Treatment Plant, The International Society for Advancement of Supercritical Fluids, 6th International Symposium on Supercritical Fluids, Versailles, France.

[5] Havířová, Z. 2012. Konstrukční ochrana dřeva zabudovaná ve stavbách. Stavební partner No.1.

[6] Gaare, M. Løtveit, K. 2012. Kritiske fuktforhold ved lukking av høyisolerte konstruksjoner i bindingsverk av tre, Master Thesis, Norwegian University of Science and Technology, Department of Civil and Transport Engineering

[7] Wood and growth rings. Retrieved at http://en.wikipedia.org/wiki/Latewood#Growth_rings on 10.5.2015

[8] Butterfield, B.G. 1997. Microfibril angle in wood, International association of wood anatomic, The proceedings of the IAWA/IUFRO, Westport, New Zealand.

[9] Svensson, S. 2012. Wood science and technology, Denmark Technical University, Department of Civil Engineering. Lyngby.

[10] Larsen, F. Olesen, J. F. Ormarsson, S. 2013 Thermal/moisture-related stresses and fracture behaviour in solid wood members during forced drying. PhD thesis, Denmark Technical University, Lyngby.

[11] Šuhajda, K. 2006. Sanace vlhkého zdiva staveb, Využití tyčové antény při mikrovlnném ysoušení zdiva, Disertační práce, Vysoké učení technické v Brně, Fakulta stavební, PhD thesis, Brno.

[12] Kožíšek, O. 2011. Hydrofobizace povrchu dřeva smrku ztepilého (Picea abies). Diplomová práce, Mendelova universita v Brně, Lesnická a dřevařská fakulta, Ústav nauky o dřevě, Brno.

[13] Capillary action. Retrieved at Wikipedia.org: https://en.wikipedia.org/wiki/Capillary_action on 10.5.2015

[14] Staube, J. 2006. Building Science corporation 138 Moisture and materials. Retrieved at Buildingscience.com: http://buildingscience.com/documents/digests/bsd-138-moisture-and-materials on 20.7.2015

[15] Nauka o dřevě. Retrieved at Ped.muni.cz: www.ped.muni.cz/wtech/03_studium/mtdr/nauka_o_dreve.doc on 15.7.2015

[16] Treacy, M. Evrtsen, J. Dhubháin, Á. N. 2000. A comparison of mechanical and physical wood properties of a range of Sitka spruce provenances, COFORD. p 4 – 5.

[17] Lourenço, P. B. Feio, A. O. Machado, J. S. 2007. Chestnut wood in compression perpendicular to the grain: Non-destructive correlations for test results in new and old wood, Construction and Building Materials, 21, (8), pp 1617 – 1627.

[18] Aghayere, A. Vigil J. 2007. Structural Wood Deign: A Practice-Oriented Approach using the ASD method. John Wiley & Sons, Inc., Haboken, New Jersey, pp 16 – 17.

[19] Zásady chemické ochrany dřeva. Retrieved at drevari.humlak.cz/data_web/Data_skola/HUdreva/6.pdf on 23.6.2015

[20] Přirozená odolnost a trvanlivost dřeva. Retrieved at drevari.humlak.cz/data_web/Data.../HUdreva/7.pdf on 10.6.2015

[21] Superwood manual. Retrieved at Superwood.dk: superwood.dk/en/ on 5.5.2013

[22] Základy vztahu mezi dřevem a vodou. Retrieved at Mendelu.cz: https://is.mendelu.cz/eknihovna/opory/zobraz_cast.pl?cast=9176;lang=cz on 10.6.2015

[23] Vahalová, E. Hlavsa, P. Šuhajda, K. Novotný, M. Škramlík, J. 2013. Analysis of Long Term Bending and Shear Test of Treated and Untreated spruce. Global Journal on Advances Pure and Applied Sciences, roč. 2013, č. 1, s. 516-522. ISSN: 2301- 2706.

[24] Otáhal, A., Využití vakua v dřevařském průmyslu. Retrieved at. umel.feec.vutbr.cz/~bousek/vak/SUSENI/DREVO_OTAHAL.pdf on 10.6.2015.

[25] Viitanen, H. Toratti, T. Makkonen, L. Peuhkuri, R. Ojanen, T. Ruokolainen, L. Räisänen, J. 2010. Towards modelling of decay risk of wooden materials. European Journal of Wood and Wood Products. Vol. 68 (2010) No: 3, 303 – 313

[26] Zidler, A. 2012 Lexikon dřeva. Český zemědělská univeersita v Praze. Fakulta lesnická a dřevařská.

[27] Viitanen, H. 1997. Modelling The Time Factor in the Development of Brown Rot Decay in Pine and spruce Sapwood – The Effect if Critical Humidity and Temperature Conditions, Holzforschung 51, No.2, 99-106.

[28] Tepelné mosty v dřevostavbě. Retrieved at http://www.woodsystem.cz/cs/tepelne-mosty-v-drevostavbe, on 10.9.2015

[29] Vahalová, E., Posouzení navrhnutých skladeb obvodových stěn experimentální dřevostavby, Brno: Fakulta stavební, Sborník anotací konference JUNIORSTAV 2011, 13. Odborná konference doktorského studia, únor 2011, 4 s. ISBN 978-80-214-4232-0

[30] Rode, C. Peuhkuri, R.H. 2012. Heat and mass transfer in building, Denmark Technical University, Department of Civil Engineering. Lyngby.

[31] Šubrt, R. Volf, M. 2002. Stavební detaily – Tepelné mosty. Praha. Grada Publishing, spol. s r.o., 148s

[32] ČSN 730540-2 Tepelná ochrana budov- Část 2: Požadavky. Praha: Český normalizační institut, 2011. 56s.

[33] ČSN 730540-3 Tepelná ochrana budov – Část 3: Návrhové hodnoty veličin. Praha. Český normalizační institut, 2011. 56s

[34] Munch-Andersen, J. 2008, Træsklethuse, Træ 56. Lyngby: TræinFformation.

[35] Vaverka, J., a kol., Stavební tepelná technika a energetika budov. VUT v Brně. 2006. 647s. ISBN 80-214-2910-0

[36] EN ISO 10211-1.1997. Thermal bridges in building construction – Heat flows and surface temperatures – Part 1: General calculation methods.

[37] Staněk, K. 2010. Šíření vodní páry a povrchová teplota. České vysoké učení technické v Praze.

[38] Staněk, K. 2010. Šíření vodní páry a kondenzace v konstrukci. České vysoké učení technické v Praze.

[39] Staněk, K. 2012. Sanace obvodové stěny dřevostavby (dynamický výpočet ve WUFI). České vysoké učení technické v Praze.

[40] Peuhkuri, R. 2003. Moisture dynamic in building envelopes. PhD Thesis. Denmark technical University, Department of Civil engineering, Lyngby. ISSN 1601-2917. 239s.

[41] DS/EN ISO 15148. 2003. Hygrothermal performance of building materials and products / determination of water absorption coefficient by partial immersion.

[42] ISO 12571 Hygrothermal performance of building materials and products – Determination of hydroscopic sorption properties, First edition 2000-03-15

[43] EN ISO 12572 Hygrothermal performance of building materials and products – Determination of water vapor transmission properties, First edition 2001-07-16

[44] Óskar V. Gíslason, Moisture transport and monture induced deformations in wooden beams, Master's Thesis, DTU Lyngby, August 2014.

[45] Ahmet, K. Dai, G. Tomlin, R. Kaczmar, P. Riddiough, S. 2000. The equilibrium moisture content of common U.K. species at three conditions of temperature and relative humidity, Forest Products Journal, 50 (6), pp 64 – 68.

[46] Salin, J. 2011. Inclusion of the Sorption Hysteresis Phenomenon in Future Drying Models. Some Basic Considerations, Maderas. Ciencia y Tecnologia, 13 (2), pp 173 – 182.

[47] Rose, J. 2004. A method for calculating heat loss from building to the ground, Technical University of Denmark.

[48] Blomberg, T. 2000. Heat2: A PC-program for heat transfer in two dimensions. Version 5.0. Lund University.

[49] Ojanen, T. Viitanen, H. Peuhkuri, R. Lähdesmäki, K. Vinha, J. Salminen, K. 2010. Mould growth modelling of building structures using sensitivity classes of materials. Proceedings to Performance of Exterior Envelopes of Whole Buildings XI, Clearwater, Dec 2010. Florida.

[50] WTA 6-2-01/D Simulation wärme- und feuchte technischer Prozesse (Simulation of Heat and Moisture Transfer), Frauhofer IRB Verlag, 2006, ISBN 978-3-8167-6826-5, 20s.

[51] Nicolai, A. Grunewald, J. Numerical simulation program Delphin 5, 2005-2006. User Manual and Program references, Version 5.2. with IBK library

[52] Včelák, J. Moisture guard system for continuous moisture and humidity monitoring, University centre of energy efficient buildings of Czech technical university in Prague, www.uceeb.cz, jan.vcelak@uceeb.cz

[53] Vahalová, E. Hlavsa, P. 2013. Monitoring of Capillary Suction of spruce in Three Different Conditions. In Young Scientist 2013, Kosice: Technical University of Kosice, Faculty of Civil Engineering. s. 1-9. ISBN: 978-80-553-1305- 4.

[54] Vahalová, E. Peuhkuri, R. Šuhajda, K. Influence of using treated wood on thermal properties and heat losses in basements of wooden buildings. 2013. Proceedings of the 2nd Central European Symposium on Building Physics (CESBP 2013), Contributions to Building Physics. Vienna, Austria: RSA. s. 847-854. ISBN: 978-3-85437-321- 6.

[55] Vahalová, E. Peuhkuri, R. Rode, C. Šuhajda, K. 2014. Influence of construction design on moisture damage of wooden buildings. 10th Nordic Symposium on Building Physics, NSB 2014. 1. Lund, Sweden: Lund University. s. 1077-1084. ISBN: 978-91-88722-53- 9.

[56] Vahalová, E. 2012. Optimalizace návrhu moderních nízkoenergetických dřevostaveb – Pojednání k disertační práci, VUT v Brně, Fakulta stavební.

[57] Ottinger, O. 2014. Moisture transport in porus material. Passive Hosue Institute presentation

[58] Koch, B. 1950. Grundlagen des Wärmeaustausches (Stoffwerte). BeuckeDissen T. W.

[59] Water vapour diffusion resistance factor, μ-value. Retrieved at http://www.wufi-wiki.com/mediawiki/index.php5/Details:WaterVaporDiffusion, on 14.10.2015

[60] Viitanen, H., Vinha, J., Peuhkuri, R., Ojanen, T., Lähdesmäki, K., Salminen, K. Development of an improved model for mould growth: Modelling. Retrieved at: http://web.byv.kth.se/bphys/copenhagen/pdf/223-3.pdf, on 4.1.2016

[61] Sedlbauer, K. 2001. Prediction of mould fungus formation on the surface of/and inside building components. Dissertation, University of Stuttgart

[62] Leicester, R.H.,Wang, C-H., Ngyen, M.N., Thornton, J.D., Johnson, G., Gardner, D., Foliente, G.C., MacKenzie, C. 2003. An engineering modelfor the decay in timber in ground contact. Document No IRGWP 03-20260. International Research Group on Wood Protection, Stockholm

[63] Brischke, C., Rapp, A.O. 2008. Dose-response relationships between wood moisture content, wood temperature and fungal decay determined for 23 European field test sites.Wood Sci Technol 42:507– 518

[64] Carll, C.G., Highley, T.L. 1999. Decay of wood-based products above ground in buildings. J Test Eval 27(2):150–158

[65] Heat flow software Flixo Pro 7, infomind.ch, Switzerland.

Author's publications

2016

ARNAUTU, D; VAHALOVÁ, E.; STEIGER, J. Overall refurbishment plan for step-by-step retrofits to EnerPHit standard. Young Researchers Conference: Energy Efficiency & Biomass, The framework of the "World Sustainable Energy Days", Wels, Austria. 2016

2015

VAHALOVÁ, E.; BASTIAN, Z. Practical implementation of step-by-step EnerPHit retrofits carried out on selected case studies across Europe. In 7PHN SUSTAINABLE CITIES AND BUILDINGS, ISBN 978-87-78774-23-1, Passivhus.dk, Copenhagen, 2015

2014

VAHALOVÁ, E.; PEUHKURI, R.; RODE, C.; ŠUHAJDA, K. Influence of construction design on moisture damage of wooden buildings. In 10th Nordic Symposium on Building Physics, NSB 2014. Lund, Sweden: Lund University, 2014. s. 1077-1084. ISBN: 978-91-88722-53- 9.

OTTINGER, O.; VAHALOVÁ, E.; BRÄUNLICH, K.; KAUFMANN, B. Vier Innendämmsysteme im Vergleich – Messungen und hygrothermische Simulationen. In 18. Internationale Passivhaustagung 2014. Aachen, Germany: Passive House Institute, 2014. s. 367-372. ISBN: 978-3-00-045215- 4.

OTTINGER, O.; VAHALOVÁ, E.; BRÄUNLICH, K.; KAUFMANN, B. Comparison of in- situ measurements and hygrothermal simulations of four different interior insulation systems. In 18th International Passive House Conference. Aachen, Germany: Passive House Institute, 2014. s. 357-362. ISBN: 978-3-00-045216- 1.

VAHALOVÁ, E.; MATYŠCÁK, O.; VAHALA, J.; ARNAUTU, D. Pressure test on Treated and Untreated spruce. In JUNIORSTAV 2014 - 16. odborná konference doktorského studia. Brno: Vysoké učení technické v Brně, Fakulta stavební, Veveří 331/95, 602 00 Brno, 2014. s. 312-312. ISBN: 978-80-214-4851- 3.

ARNAUTU, D.; THEUMER, S.; STEIGER, J.; VAHALOVÁ, E. PHPP Interface Certification. In 18th International Passive House Conference 2014. Aachen, Germany: Passive House Institute, 2014. s. 605-608. ISBN: 978-3-00-045216- 1.

MATYŠČÁK, O.; VAHALOVÁ, E. Nedestruktivní možnosti odsolování a odvlhčování. In JUNIORSTAV 2014 - 16. odborná konference doktorského studia. 2014. ISBN: 978-80-214-4851- 3.

2013

VAHALOVÁ, E.; HLAVSA, P.; ŠUHAJDA, K.; NOVOTNÝ, M.; ŠKRAMLIK, J. Analysis of Long Term Bending and Shear Test of Treated and Untreated spruce. Global Journal on Advances Pure and Applied Sciences, 2013, roč. 2013, č. 1, s. 516-522. ISSN: 2301- 2706.

VAHALOVÁ, E.; PEUHKURI, R.; ŠUHAJDA, K. Influence of using treated wood on thermal properties and heat losses in basements of wooden buildings. In Proceedings of the 2nd Central European Symposium on Building Physics (CESBP 2013), Contributions to Building Physics. Vienna, Austria: RSA, Vienna, Austria, 2013. s. 847-854. ISBN: 978-3-85437-321- 6.

HLAVSA, P.; VAHALOVÁ, E.; AUTRATOVÁ, L. Building Energy Performance Certificate – Assesment of existing constructions according to the Energy Management act. In Proceedings of the International Scientific Conference Innovative Trends in Construction and Real Estate sector (ITCRES 2013). 1. 2013. s. 1-12. ISBN: 978-80-227-3932- 0.

HLAVSA, P.; VAHALOVÁ, E.; AUTRATOVÁ, L. Building Energy Performance Certificate - Assessment of Existing Constructions According to the Energy Management Act. Book of Abstracts of the International Scientific Conference Innovative Trends in Construction and Real Estate sector (ITCRES 2013). 1. Bratislava: Slovak University of Technology in Bratislava, 2013. s. 33-34. ISBN: 978-80-227-3931- 3.

VAHALOVÁ, E.; HLAVSA, P. Monitoring of Capillary Suction of spruce in Three Different Conditions. In Young Scientist 2013 - The 5th PhD. Student Conference of Civil Engineering and Architecture. Kosice: Technical University of Kosice, Faculty of Civil Engineering, 2013. s. 1-9. ISBN: 978-80-553-1305- 4.

HLAVSA, P.; VAHALOVÁ, E.; AUTRATOVÁ, L. Building energy performance certificate, energy management act and existing buildings – assessment and actual situation in the Czech Republic. Nehnuteľnosti a bývanie, 2013, roč. 2013, č. 2, s. 54-64. ISSN: 1336- 944X.

2012

VAHALOVÁ, E. Problematika nástaveb v bytových domech. In Juniorstav 2012 - 14. odborná konference doktorského studia - Sborník anotací (+ CD s plným zněním příspěvků). Brno: VUT v Brně, Fakulta stavební, 2012. s. 67-67. ISBN: 978-80-214-4393-8.

2011

VAHALOVÁ, E. Posouzení navrhnutých skladeb obvodových stěn experimentální dřevostavby. In Juniorstav 2011 - 13. odborná konference doktorského studia - Sborník anotací (+CD s plným zněním příspěvků). Brno: Akademické nakladatelství CERM, s.r.o. Brno, Purkyňova 95a, 612 00 Brno, 2011. s. 51-51. ISBN: 978-80-214-4232- 0.

List of Figures

List of Tables

Nomenclature

Latin alphabet

Symbol	Unit	Description
A	$[m^2]$	area of flow, initial face area
a_d	$[m^3]$	amount of absorbed gas
c	$[m^2 \cdot s^{-1} \cdot Pa^{-1}]$	permeability coefficient
C	$[m^2]$	coefficient of specific permeability
c_1, c_2	[-]	constants
d	[m]	thickness of the material
D	$[m \cdot s^{-2}]$	diffusion coefficients
f_{Rsi}	[-]	factor of minimal surface temperature on internal side, risk of mould growth
$f_{Rsi,cr}$	[-]	critical factor of minimal surface temperature on internal side
$f_{Rsi,N}$	[-]	required value of minimal surface temperature on internal side
G	[J]	free enthalpy
g	$[kg \cdot m^{-2} \cdot s^{-1}]$	density of water vapour flow rate
g	$[m \cdot s^{-2}]$	acceleration due to gravidity = 9.81
h	[m]	height the liquid
H_v	$[m^3]$	level of the hydrophobization
k_1, k_2	[-]	coefficients expressing the delay in early and late stages of growth
L	[m]	length of element, beam span, moment arm
L_{wall}	[m]	length of the composite wall for one section
$L_{wall/floor}$	[m]	length of the modelled wall (floor)
L_{wood}	[m]	length of the wood used in the wall
m	[kg]	mass of test specimen
m_0	[g]	mass of dried test specimen
m_1	[kg]	mass of the test assembly at time t_1
m_2	[kg]	mass of the test assembly at time t_2
$M_{30\%}$	$[N \cdot mm^{-1}]$	bending moment applied on each sample
$M_{c,a}$	$[kg \cdot m^{-2} \cdot year^{-1}]$	amount of condensed water vapour
$M_{ev,a}$	$[kg \cdot m^{-2} \cdot year^{-1}]$	Amount of evaporated water vapour
MH	[%]	moisture on hydroscopicity level
ML	[%]	mass loss
m_i	[kg]	initial mass of specimen or substance

m_t	[g]	mass of specimen after time t
M_u	[N·mm^{-1}]	bending moment
m_w	[kg]	mass of water
N	[-]	number of capillary in area unit
NV	[%]	mass absorption, resp. moisture content
NV_f	[%]	water absorptions under the cold conditions with the forced submersion
NV_v	[%]	volumetric absorption
NV_{ws}	[%]	water absorptions boiling on the water surface
NV_{ws}	[%]	absorption due to the boiling on the water surface of the non-hydrophobic matter
$NV_{ws,f}$	[%]	under boiling with the forced submersion
$NV_{ws,h}$	[%]	absorption due to the boiling on the water surface of the hydrophobic matter
p	[Pa]	pressure
p	[%]	porosity
p_1, p_2	[Pa]	partial water vapour pressures of air of outside and inside surface of the construction
P_{sat}	[Pa]	saturated vapour pressure 2584.1634 Pa
P_u	[N]	failure load of the Stenhøj machine
P_v	[Pa]	ratio of the partial water vapour pressure
$P_{v,sat}$	[Pa]	partial pressure of saturated water vapour
$p_{ws,h}$	[Pa]	pressure of gas
Q	[m^3·s^{-1}]	volume flow
q_{floor}	[W·m^{-1}]	1D heat flow through the floor slab
q_{mt}	[kg·m^{-2}·s^{-1}]	overall density mass flow of liquid eater by transmission
$q_{mt,1}$	[kg·m^{-2}·s^{-1}]	density of a mass flow of liquid water by transmission
$q_{mt,2}$	[kg·m^{-2}·s^{-1}]	density mass flow of liquid water by transmission
q_{total}	[W·m^{-1}]	2D heat flow through section for transient mean external temperatures (Heat2)
q_{wall}	[W·m^{-1}]	1D heat flow through the adjacent wall segments for transient mean external temperatures
r	[m]	radius of the capillary
Re	[-]	Reynolds number
R_{si}	[m^2·K·W^{-1}]	heat transfer resistance on internal side
R_{se}	[m^2·K·W^{-1}]	heat transfer resistance on external side
s_d	[m]	water vapour diffusion-equivalent air layer thickness
T	[K]	thermodynamic temperature, temperature of ambient air
t	[s, months]	time flow

t_1 and t_2	[s]	successive times of weightings
T_e	[°C]	temperature of external air
t_f	[h]	duration of the test
T_i	[°C]	internal air temperature
$T_{ref,mean}$	[°C]	average temperature measured in the reference point for selected month
U	[$W \cdot m^{-2} \cdot K^{-1}$]	heat transfer coefficient
u	[%]	moisture content mass by mass
U_N	[$W \cdot m^{-2} \cdot K^{-1}$]	required heat transfer coefficient
$U_{wall/floor}$	[$W \cdot m^{-2} \cdot K^{-1}$]	thermal transmittance of the wall or floor
V	[m^3]	volume of the extruded liquid
V_s	[m^3]	volume of solids
V_v	[m^3]	volume of void space
w	[%]	water (moisture) content
w_d	[kg]	mass of a sample after drying up
w_{max}	[%]	maximal moisture
w_{mc}	[%]	mass equilibrium moisture content
w_w	[kg]	mass of a sample before drying up
W	[-]	wood species (0=pine and 1=spruce)
W_w	[$g \cdot cm^{-2} \cdot h^{-0.5}$]	water absorption coefficient
$\Delta m'_{tf}$	[$g \cdot cm^{-2}$]	value of Δm on the straight line at time t_f
Δm_{12}	[$kg \cdot s^{-1}$]	mass change rate per time for a single determination
Δm_t	[$g \cdot cm^{-2}$]	mass gain per face area after time t
Δp	[Pa]	pressure difference at the end of test specimen
ΔT	[K]	mean temperature difference between inside and outside air for heating season

Greek alphabet

Symbol	Unit	Description
θ_ω	[°C]	dew point according to ČSN 730540-3
θ_{ai}	[°C]	designed temperature of indoor air
θ_{ex}	[°C]	designed temperature of environment connected to the external side of construction in winter phase
θ_{gr}	[°C]	designed temperature of soil
γ	[$N \cdot m^{-1]}$]	liquid-air surface tension
δ	[$kg \cdot m^{-1} \cdot s^{-1} \cdot Pa^{-1}$]	water vapour resistance permeability
δ_a	[Pa]	water vapour permeability of stagnant air

δ_{ekv}	[kg·m^{-2}·s^{-1}]	equivalent water vapour resistance permeability
η	[-]	dynamic viscosity of the fluid
θ	[°]	contact angle
κ_m	[m^2·s^{-1}]	coefficient of moisture conductivity
κ_t	[K^{-1}]	coefficient of moisture conductivity during the temperature gradient
λ_{ISO}	[W·m^{-1}·K^{-1}]	thermal conductivity of insulation
λ_{wall}	[W·m^{-1}·K^{-1}]	expression of total thermal conductivity of the composite wooden wall
μ	[-]	water vapour resistance factor
μ_{ekv}	C	equivalent resistance factor of non-homogeneous material layers
μ_u	[J.kg^{-1}]	chemical potential of the moisture
ρ	[kg·m^{-3}]	density of the liquid
ρ_0	[kg·m^{-3}]	density of absolutely dry sample
ρ_d	[kg·m^{-3}]	volumetric mass density of dried sample
ρ_s	[kg·m^{-3}]	volumetric mass density of material in dried state
ρ_w	[kg·m^{-3}]	volumetric mass density of the water
τ	[s]	time
φ	[%]	relative humidity of air
φ_i	[%]	relative humidity of inside air
$\varphi_{i,r}$	[%]	relative humidity of indoor
χ_N	[W·K^{-1}]	required value of the point thermal transmittance
ψ	W·m^{-1}·K^{-1}]	linear thermal transmittance
$\Psi_{connection}$	[W·m^{-1}·K^{-1}]	thermal transmittance of wall/floor connection
ψ_N	[W·m^{-1}·K^{-1}]	required value of the linear thermal transmittance

General notations

Symbol	Unit	Description
$\frac{du}{dx}$	[m^{-1}]	moisture gradient
$\frac{dt}{dx}$	[s·m^{-1}]	temperature gradient
dp(x)/dx	[Pa·m^{-1}]	gradient of partial water vapour pressure in the air in the construction in the x-direction
∂H_{Rh}		difference in relative humidity across the specimen
∂MC		difference in moisture content across the specimen

Abbreviations

Symbol	Unit	Description
A, (-), -		Untreated, natural, non-impregnated spruce
AF		Untreated spruce in Cold conditions
AH		Untreated spruce in Hot conditions
AR		Untreated spruce in Room conditions
B, (+), +		Treated, impregnated spruce using supercritical CO_2
BF		Treated spruce in Cold conditions
BH		Treated spruce in Hot conditions
BR		Treated spruce in Room conditions
EPS		expand polystyrene
FSP		fibre saturation point
H		height
L		length
M	[months]	time of year
MC	[%]	weight-% moisture content
MW		mineral wool
OSB		oriented strand board
RH	[%]	relative humidity
SEM		Scanning Electron Microscopy
SQ		surface quality from the drying process
T	[°C]	temperature
TRY		Danish test reference year
CS1		Case study 1 – diffusion closed wall system of the wooden building built in the Czech Republic
CS2		Case study 2 – diffusion opened wall system of the wooden building built in Denmark
VTT		Viitanen's model
W		width
XPS		extruded polystyrene